Y 3.AT 7:
36/11-2

Important!
READER SURVEY—
see page iii

REACTOR AND FUEL-PROCESSING TECHNOLOGY

A Quarterly Technical Progress Review

Prepared for DIVISION OF TECHNICAL INFORMATION, U. S. ATOMIC ENERGY COMMISSION,
by ARGONNE NATIONAL LABORATORY

ARGONNE STATE LIBRARY
JUL 30 1968

Spring 1968

● VOLUME 11

● NUMBER 2

TECHNICAL PROGRESS REVIEWS

The United States Atomic Energy Commission publishes the Technical Progress Reviews to meet the needs of industry and government for concise summaries of current nuclear developments. Each journal digests and evaluates the latest findings in a specific area of nuclear technology and science. *Nuclear Safety* is a bimonthly journal; the other three are quarterly journals.

Isotopes and Radiation Technology
P. S. Baker, A. F. Rupp, and Associates
Isotopes Information Center, Oak Ridge National Laboratory

Nuclear Safety
Wm. B. Cottrell, W. H. Jordan, J. P. Blakely, and Associates
Nuclear Safety Information Center, Oak Ridge National Laboratory

Reactor and Fuel-Processing Technology
Argonne National Laboratory

Reactor Materials
E. M. Simons and Associates
Battelle Memorial Institute

All are available from the U. S. Government Printing Office. See the back cover for ordering instructions.

The views expressed in this publication do not necessarily represent those of the United States Atomic Energy Commission, its divisions or offices, or of any Commission advisory committee or contractor.

Availability of Reports Cited in This Review

United States Atomic Energy Commission (USAEC) reports are available at USAEC depository libraries and are sold by the Clearinghouse for Federal Scientific and Technical Information (CFSTI), National Bureau of Standards, U. S. Department of Commerce, 5285 Port Royal Road, Springfield, Va. 22151. All reports sold by CFSTI are $3.00 for printed copy and $0.65 for microfiche. Each separately bound part of a report is priced as a separate report. Some reports may not be available because of their preliminary nature; however, the information contained in them will generally be found in later progress or topical reports on the subject.

Other U. S. Government agency reports identified in this journal generally are available from CFSTI.

Private-organization reports should be requested from the originator.

United Kingdom Atomic Energy Authority (UKAEA) and Atomic Energy of Canada Limited (AECL) reports are available at USAEC depository libraries. UKAEA reports are sold by Her Majesty's Stationery Office, London; AECL reports are sold by the Scientific Document Distribution Office, Atomic Energy of Canada Limited, Chalk River, Ontario, Canada. UKAEA and AECL reports issued after March 1, 1967, are sold by CFSTI to purchasers in the United States and its territories.

Contents

Reactor and Fuel-Processing Technology
Vol. 11, No. 2, Spring 1968

PHYSICS

Predictions of Fuel Burnup for Thermal Reactors
B. I. Spinrad 69

Pulsed Neutron Experiments in Nonmoderating Systems
Friedrich H. Helm 72

REACTOR SAFETY

Superheating of Liquid Metals in Relation to Fast Reactor Safety
Hans K. Fauske 84

DESIGN AND CONSTRUCTION PRACTICE

Letters to the Editor:
Realistic Analysis of Fuel Elements 89

FLUID AND THERMAL TECHNOLOGY

Letter to the Editor:
Shippingport Hot-Channel Factors 90

AQUEOUS PROCESSING

Research and Development on Aqueous Processing
C. E. Stevenson and D. M. Paige 91

NONAQUEOUS PROCESSING

Compact Pyrochemical Processes
W. E. Miller and R. K. Steunenberg 96

Volatility Processes
G. J. Vogel and J. J. Barghusen 101

WASTE DISPOSAL

Progress in Waste-Disposal Research and Development
Phillip Fineman 107

See the Reader Survey on page iii

Superintendent of Documents, U. S. Government Printing Office, Washington, D. C. 20402, $2.50 per year.

Reactor and Fuel-Processing Technology

is a quarterly review of developments in reactor and reactor fuel technology. As such, this journal reports and interprets progress in the reactor field in terms of its significance to the reactor designer, operator, and fuel-cycle specialist. Articles either summarize and critically evaluate recently reported developments or review the "state of the art" of a particular topic. Both types of articles reference reports and publications that merit study; readers are urged to consult the references for additional information and the judgments of the original authors. If a reader has information that causes his evaluation to reinforce, modify, or contradict the opinions of our reviewers, he is encouraged to write to the Editor.

The scope of the journal encompasses:

CONCEPTS and APPLICATIONS: Progress in evaluating the applicability and economics of various reactor types and systems (including unconventional approaches), as well as of fuel resources and cycles, for utility central-station generation of electricity, auxiliary power, process radiation and heat, desalting, and propulsion — and for terrestrial, undersea, aerospace, and other advanced uses.

ANALYSIS and EXPERIMENTATION: Advancements in the techniques of reactor physics, fluid and thermal technology, energy conversion, fuel elements, materials, mechanics, control and dynamics, and reactor safety.

SYSTEMS and COMPONENTS: Experience as reflected in design and construction practice, components, systems technology, and operating performance of various specific types of reactors — including pressurized- and boiling-water reactors, molten-salt, organic-, gas-, and liquid-metal-cooled reactors, as well as generally applicable aspects of research and test reactors.

FUEL PROCESSING: Recent research and development on fuel aqueous processing, nonaqueous processing, waste disposal, and processing safety.

This journal is prepared by Argonne National Laboratory at the request of the Division of Technical Information of the U. S. Atomic Energy Commission. At Argonne, the Reactor Engineering Division (L. J. Koch, Director) and the Chemical Engineering Division (R. C. Vogel, Director) have the principal responsibility for the preparation of *Reactor and Fuel-Processing Technology*, with the regular assistance of the Reactor Physics Division (R. A. Avery, Director) and the Idaho Division (M. Novick, Director) and the occasional assistance of other divisions (Metallurgy, Chemistry, and Reactor Operations). Thus, unless noted otherwise, the reviewers and authors of articles are Laboratory staff members. The editors welcome interpretive review articles contributed by authors outside the Laboratory.

Editor, *James J. Dutton*
Advisory Editor, *David H. Lennox*
Managing Editor, *Karl K. Brown*
Co-Editor (Fuel Processing), *Joseph Royal*
Associate Editor (Physics), *Raymond Gold*
Assistant Editor, *Paul H. Gregory*

Argonne National Laboratory

Issued quarterly by the U. S. Atomic Energy Commission. Use of funds for printing this publication approved by the Director of the Bureau of the Budget on July 8, 1966.

Y 3.AT 7:
36/.11-2

READER SURVEY

The USAEC Division of Technical Information wishes to evaluate and affirm the usefulness and viability of this journal. Your answers to the following questions are important to the future course of the journal and would be appreciated.

1. Is *Reactor and Fuel-Processing Technology* useful to you? Yes ____ No ____

Fold

2. As described in the foreword, which of the following areas are of most interest? (Indicate order by 1, 2, 3, 4, 0)

   Fuel Processing ____

   Systems and Components ____

   Analysis and Experimentation ____

   Concepts and Applications ____

3. Should this journal be continued? Yes ____ No ____

   Comments: _____

   _____

4. Suggestions for improving this journal: _____

   _____

   _____

   _____

Fold _____

5. Reader's occupation: _____

   _____

6. Optional—reader's name and address: _____

   _____

   _____

   _____

Please fold, staple, and mail. Postpaid. Thanks.

Cut along this line

From:

Postage and Fees Paid
U. S. Atomic Energy Commission

Division of Technical Information
U. S. Atomic Energy Commission
Washington, D. C. 20545

Staple here

Predictions of Fuel Burnup for Thermal Reactors

By B. I. Spinrad, International Atomic Energy Agency

From Apr. 10 to Apr. 14, 1967, a panel was convened in Vienna under the sponsorship of the International Atomic Energy Agency to discuss Fuel Burnup Predictions in Thermal Reactors. The report of this panel has recently been issued.[1]

The proceedings consist of a number of topical papers presented to the panel and a summary of discussions and conclusions. The reader is referred to the proceedings volume for detailed information.

The panel was able to reach agreement concerning the current state of the art, the targets of burnup physics, and recommended topics for further work and/or international collaboration. These items are summarized below.

Status and Goals of Burnup Physics

The requirements on burnup are:

- To determine actual reactor flux well enough so that design tolerances are not set by the error in reactor-physics models.
- To determine local and total isotope production, power distribution, and reactivity well enough to provide a reasonable basis for operating decisions.
- To predict isotope depletion and buildup well enough to provide a reasonable ceiling for errors in materials accounting.

It is quite clear that critical experiments, other integral experiments, and careful measurements of properties of operating reactors all improve our general understanding.

There was much debate on the absolute magnitude of the error in current predictions. Major differences do exist between a carefully controlled, base-loaded power-reactor experiment and nuclear station operation on a utility grid under load-following conditions. In addition, the important differences between prediction of measured isotopic composition at a few selected points in a fuel element, where burnup also has been measured, and prediction in a global sense over the entire reactor were clarified. In the global case the precision of the predicted spatial distribution of burnup is much more important.

The following section treats flux and power distribution, reactivity, reactivity lifetime, isotopic buildup and depletion, and power and reactivity coefficients. The panel, after assessing the state of the art, developed goals for reactor physics that would preclude strong physics contributions to design error (bearing in mind that many engineering uncertainties are probably irreducible).

FLUX AND POWER DISTRIBUTION

In estimates of many burnup quantities, precision is severely limited by knowledge of the absolute thermal power level of a reactor. Typically process instrumentation was cited as uncertain to about 4% of total plant thermal output and this uncertainty may be even larger for a small power reactor. In-core instrumentation is characterized by an accuracy of about ±5%.

For graphite and heavy-water reactors, power reactors with clean lattices, prediction and measurement agree within the accuracy of measurement. For configurations involving mixed fuels, empty fuel channels, and so forth, measurements have shown rms deviations of about 5%; however, the flux maps have indicated high-flux points that are considerably poorer—10% deviations are not uncommon. More detailed theoretical modeling seems appropriate.

For light-water reactors (rarely as "clean" as graphite- and D_2O-moderated reactors), some rms deviations of 3 to 5% are reported, but a 10% error range describes the flux map more accurately. Flux errors up to ±20% have been reported for low-flux regions, and systematic trends with region and with exposure have been noted; these are likewise attributed to inadequate theoretical modeling of the reactor, both as to spatial resolution and physical description.

Goal. The goal of the reactor physicist must be to reduce uncertainty in burnup analysis to a value that is small compared with the error introduced by the thermal-power uncertainty. The practical aim is to locate hot spots and predict their heat output well

within the tolerances required for manufacture. A target precision is 5% error in prediction of local heat generation rate at all sensitive locations.

REACTIVITY

Initial reactivity for most reactors of proven type can be predicted to better than 1% and often to 0.5%. This ability derives from the large number of suitable experiments analyzed by theoretical models that can be extrapolated to power-reactor conditions. For more speculative reactors for thorium fuel cycles, recycled plutonium, etc., reactivity is only slightly less predictable because available critical experiments already cover the field fairly well.

Once a reactor has been loaded and brought to power, its reactivity is, of course, known. Reactivity change becomes the important parameter. Errors of ±0.2% in k_{eff} or ±10% in δk_{eff} (whichever is larger) characterize initial predictive ability at desirable burnup levels. Later loadings can be predicted at least twice as accurately as the first loading, if the first loading is carefully monitored.

Reactors that are to be continuously fueled pass from an initial reactivity to some steady-state reactivity. The same ±10% error characterizes this reactivity change.

Goals. Initial reactivity, for systems that have even a crude resemblance to previous experiments, should be predictable to better than ±0.5% in k_{eff}. The important configuration is the control-free reactor, against which reactivity change is to be assessed.

For any reactor that is partially refueled at frequent intervals, the change in reactivity for such a refueling operation should be known to ~0.1% (k units) when the fueling cycle has been established. The difference in reactivity between the initial loading and the equilibrium loading for any reactor that is partially refueled at frequent intervals should be known within an error in δk_{eff} of ±0.1% (k units) for all charges after the first.

REACTIVITY LIFETIME

A 10% error in δk_{eff} due to burnup leads to a 10% error in reactivity life. Although 10% is typical, this may become worse if the control strength is not adequately represented because reactor control systems are usually designed to accommodate burnup.

Initial operation defines the strength of the control system, as built, and adds precision to estimates of burnup reactivity changes. Therefore later charges and derivative reactors may have their reactivity lifetimes predicted to ≤5%. With careful characterization the errors in heat output may become dominant.

Reactors of very high conversion, and reactors with fixed poisons that burn out significantly but not completely, have a very flat curve of reactivity vs. burnup, even though isotopic concentrations change considerably. Predictions of reactivity life for first-of-a-kind systems of this sort are prone to gross error. However, because of the flat reactivity curve, if the first charge of such a reactor is designed to be only slightly more reactive than required, it may virtually be guaranteed that reactivity life will not be the limiting factor on burnup.

For reactors that are shimmed by very frequent refueling, the 10% error quoted applies to the fuel burnup when steady state is achieved. Problems of fuel management incorporate additional errors during the transition period; thereafter, effects of small changes in initial fueling on burnup lifetime can be predicted to within ±1%.

Errors in power distribution lead to errors in isotope and in reactivity distribution and contribute strongly to errors in burnup reactivity changes.

Goals. The target precision for prediction of the burnup of spent fuel in a reactor (whether incrementally loaded at frequent intervals or not) should be 5% once a steady-state fueling has been achieved. In achieving a steady state, no fuel discharged should have a burnup disagreeing with its predicted value by more than 10%.

Fuel charges that can be considered as perturbations of the initial fuel should have lifetime *changes* predictable within 20% of the *difference* in lifetime when mixed with initial fuel and 10% of that difference when they reach steady state by themselves. (These errors should also be characteristic of burners with large amounts of removable control, burners incorporating burnable poison, and high-conversion near-breeders.)

ISOTOPIC BUILDUP AND DEPLETION

Errors in fissile-material content for reactors are of the order of 1 to 0.5%. However, there are many reservations. Errors are greatest for reactors (such as seed–blanket) where production and burnup are in separate regions and a large part of the produced fuel remains in the system for many burnup cycles. For such reactors, discrepancies of 3% in fissile content have been observed.

In general, the error in predicting the ratio of ^{239}Pu content to ^{235}U destruction is about 5% of its value. In some cases where considerable experience has been accumulated, the error is appreciably smaller; also, there are a few outstanding cases where the error is more severe.

The error in isotopic ratio of each higher plutonium isotope to its predecessor may be about 10%. It is reported that the corresponding ratios for uranium isotopes in the ^{235}U–Th cycle actually have smaller errors, provided that the errors in ^{233}Pa burnup are minimized.

Goals. Total fissile atom concentration for the reactor should be predictable within 1% of true value, and local concentration within 5%.

The ratio of total plutonium content of the reactor to ^{235}U depletion should be predictable within 1 to 0.5% of true value. For incrementally fueled reactors, a varying precision in the average value at discharge exposures is implied; a typical number might be ±2%.

The ratios $^{240}Pu/^{239}Pu$ and $^{241}Pu/^{240}Pu$ should be predictable within 5% of their values, if the extra uncertainties due to errors in estimating exposure are ignored.

POWER AND REACTIVITY COEFFICIENTS

Although the dynamic properties of a reactor are strongly dependent on design details that are sometimes outside the control of the physicist, certain types of reactivity coefficients should be covered by adequate physics predictions. These include moderator temperature coefficient, fuel temperature coefficient, void coefficients, and the effect of control configuration on these coefficients. Generally a requirement for greater predictive precision than 20% is associated with use of the parameter as a measure of special physics interest, rather than design interest.

It is particularly important to know the time constants of delayed dynamic effects to a precision of better than ±20%, especially when they are in such a range as possibly to resonate with control-rod dead bands, pump noise, coolant cycle times, etc. Although the time constants are more thermodynamic than reactor-physical parameters, it is important that the physics model not introduce additional errors.

Goals. In a particular reactor any one of many reactivity coefficients may dominate. A target for the dominant coefficient should be a precision of ±10%. Unfortunately no prediction of the accuracy of power coefficients can be made while insufficient knowledge exists about the burnup-dependent mechanical behavior of the fuel.

Recommendations

The panel believes that it has assessed current efforts and the status of burnup physics and makes the following recommendations.

- Although nuclear data are good, improvements are needed in fission-product resonance results, plutonium cross sections and η values. Better accuracy in fission-product yields (±3%) is desirable for certain fission products, e.g., ^{148}Nd, ^{140}La, and others that may be useful for burnup determination. Resonance data on ^{238}U may need reevaluation.
- The data from zero-power-reactor programs on nonuniform lattices (often adequate) and thorium lattices, and on temperature coefficients for all types of lattices, should be surveyed, and gaps in our knowledge filled by appropriate new programs.
- Improvements in theory and in mathematics are needed. We should (1) develop reliable procedures for testing the precision and convergence of alternate mathematical techniques, (2) improve the speed and stability of convergence of methods used to predict large, loosely coupled cores, (3) achieve some standards of characterization for heterogeneous codes, (4) develop improved general methods for dealing with fuel and absorber management problems, and (5) develop improved methods for dealing with operational problems paying due regard to the associated mathematical problems.
- Standard reactor configurations, including some for which the representation of details is important, are recommended as calibration standards on which the existing large variety of computing codes should be intercompared.
- More and better instrumentation is required if we are to obtain adequate operating data. Precise, detailed data on operating power reactors are needed; these data should be published in a coherent form, and it is particularly recommended that review articles, describing how these data interact with theory systems, be prepared. Associated data resulting from analysis of the irradiated fuel ought also to be published as a check of this interaction process.
- Reactor operators should be encouraged to measure and publish the burnup dependence of the power coefficient of operating reactors. This information is required to improve and test predictions.
- The goals for precision of burnup predictions are recommended as standards.

Reference

1. Proceedings of a Panel on Fuel Burnup Predictions in Thermal Reactors, Vienna, Apr. 10–14, 1967, International Atomic Energy Agency, 1968.

Pulsed Neutron Experiments in Nonmoderating Systems

By F. H. Helm*

In recent years pulsed neutron techniques have been used increasingly to measure parameters of fast-neutron systems when other techniques fail or are inaccurate and difficult. Most of these measurements can be divided into three categories:

- Macroscopic cross sections important in reactor design.
- Reactivity and related quantities in subcritical systems.
- Neutron spectra by the time-of-flight method.

The basic methods for many measurements have been derived from similar measurements on thermal systems performed successfully during the last decade.[1,2] However, to adapt pulsed neutron experiments to nonmoderating systems, considerable development has been necessary. For example, a timing accuracy of a few nanoseconds is required for most cross-section measurements. Further, for time-of-flight measurements on nonmultiplying systems, neutron production rates of at least the order of 10^{15} neutrons/sec are required during the pulse. The analysis of most experiments is complicated by the large spread in neutron energies.

This review describes the various pulsed neutron generators and also examines the status of theory and experiment; however, discussion focuses on those recent prompt decay measurements useful in cross-section determinations, on reactivity measurements, and on spectra measurements.

Pulsed Neutron Generators

Various types of pulsed neutron generators are being used in experiments on fast assemblies. All of these machines have the common feature that a pulsed beam of charged particles is directed onto a target where neutrons are produced by nuclear reactions. Requirements of specific experiments (mostly in terms of neutron production rate and neutron energy) determine the type of generator that is most suitable. Figures 1 to 3 show the most common design concepts for pulsed neutron sources.

DRIFT-TUBE GENERATORS

The drift-tube generator (Fig. 1) is very widely used, can produce an intensity of 10^{10} to 10^{12} neutrons/sec, and is one of the least-expensive neutron generators. (Generally $15,000 to $50,000.) In these

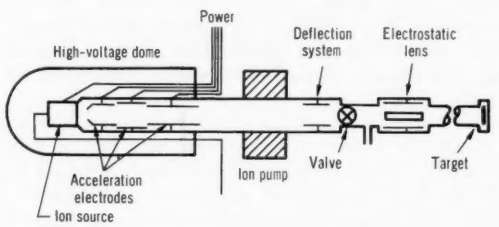

Fig. 1 Drift-tube generators produce 14-Mev neutrons from the $T(d,n)^4He$ reaction. Production is usually at a rate of 10^{10} to 10^{12} neutrons/sec during pulses; minimum pulse width is ~10^{-6} sec, which can be reduced by special devices to ~10^{-8} sec.

devices, deuterium ions are accelerated to 150 to 400 kv and impinge on a tritium target where 14-Mev neutrons are produced by the $T(d,n)^4He$ reaction. Usually the target is at ground potential and the ion source at positive high voltage. Vacuum in the accelerator is about 10^{-5} torr. The pressure differential between the accelerating space and the interior of the ion source is maintained by an oil diffusion pump or an ion pump.

Pulsed neutron output can be achieved by various methods; usually the ion beam is directed by deflec-

*Present address is Kernforschungszentrum, Karlsruhe, West Germany.

tion plates next to the beam path and downstream from the accelerating electrodes. In the pulse-off condition, the plates are biased by a d-c voltage so that the beam is deflected off the target. Then voltage pulses are applied to one of the deflection plates so that the beam is directed to the target for the duration of the pulse.

The pulse-to-background ratio of the neutron production rate achieved in this way is about 10^4. Post-acceleration deflection can be combined with preacceleration deflection or with ion-source pulsing to improve this ratio. For preacceleration pulsing a deflecting voltage is applied to an electrode near the ion-source extraction channel. Ion-source pulsing is done by pulsing the voltage, which produces the gaseous discharge in the ion source.

Minimum pulse width for most commercial post-acceleration deflection systems is about 1 μsec. It has been reduced into the nanosecond region using a cable-discharge pulser,[3] a simple network for discharging the capacity of an open-ended cable through a thyratron and guiding the resulting nanosecond voltage pulse along the drift tube with the approximate speed of the deuterons, using delay lines. A more elaborate method of reducing the pulse width is based on the well-known klystron bunching mechanism, which has the advantage that the intensity is increased as the pulse is shortened.

Drift-tube neutron generators are commercially available from a large number of companies in the United States and abroad, and detailed descriptions of individual machines are readily available from manufacturers. Laboratory-built generators of high intensity are described in Ref. 4.

Because of the limited intensity and the fixed energy of the neutrons, the use of drift-tube generators in fast reactor physics has been mostly restricted to prompt decay measurements in nearly critical systems. However, Paterson and others have shown that for high multiplications the intensity of 10^{12} neutrons/sec is sufficient for time-of-flight measurements.[5–8]

RELATED SYSTEMS

In a similar type of neutron generator that also produces neutrons by the $T(d,n)^4He$ reaction, the accelerating stretch is compressed to a few centimeters, and the drift tube is eliminated. With such a short beam path, the effects of scattering (on neutral gas) and of space charge (beam exploding) lose most of their significance, and the machines can be run at higher gas pressures and ion currents than the drift-tube accelerators. Neutron output is controlled by pulsing the ion-source voltage or ion-source and accelerating voltages. One such machine, which retains the differential pumping ("differential" refers to the pressure step between the ion source and the beam path) but goes to instantaneous currents of up to 500 ma, with a neutron production rate of 2×10^{13} neutrons/sec, is described by Eyrich and Schmidt.[9] However, most of the compact sources with short acceleration stretches have no pressure differential between ion source and target,[10] and many are of the sealed-tube type.[11–13] In the sealed tubes the problems of target depletion are minimized by using a filling gas mixture of deuterium and tritium. After an initial decay in neutron yield, a balance between target and filling gas is established, and the decline in output becomes very slow. Sealed-tube generators can reach instantaneous production rates of up to 10^{14} neutrons/sec; however, the pulse repetition rate and the minimum pulse width are more limited than for the drift-tube generators.

VAN DE GRAAFF GENERATORS

A Van de Graaff generator, although much bulkier and more expensive than the accelerators previously described, is practically indispensable for all pulsed neutron experiments in which the energy of the source neutrons must be well defined and adjustable. The big advantage of the Van de Graaff (Fig. 2) is the availability of accelerating voltages of up to several million electron volts. This allows production of approximately monoenergetic neutrons by endothermic threshold reactions of protons with various target materials (Table 1). The neutron energy and its spread are determined by the accelerating voltage

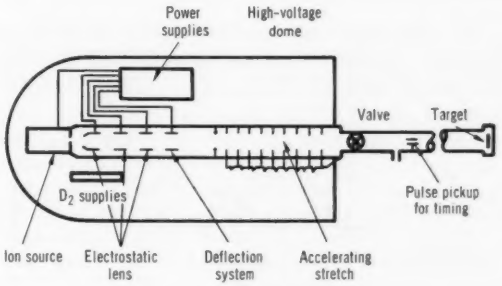

Fig. 2 Van de Graaff generators yield neutrons of various well-defined energies from endothermic threshold reactions between protons and selected targets. Minimum pulse width is ~10^{-9} sec.

Table 1 SOURCE REACTIONS FOR PULSED NEUTRON GENERATORS[14,15]

Reaction	Accelerating voltage	Useful neutron-energy range, kev
$^7Li(p,n)^7Be$	>1880	>30
$T(p,n)^3He$	>1020	>70
$^{51}V(p,n)^{51}Cr$	1560–2360	10–800
$^{45}Sc(p,n)^{45}Ti$	>2908	>5
$^{12}C(d,n)^{13}N$	400–3000	0.07–2.76

and by the spread in emission angle of the neutrons being utilized.[14,15]

Most of the operational principles are the same as for small drift-tube accelerators. Protons are extracted from an ion source and accelerated onto a target where neutrons are produced. The ion beam is pulsed by a beam deflection system, usually prior to acceleration, because the time-averaged current capacity of a Van de Graaff generator is quite limited.

The system shown in Fig. 2 is essentially that used by both Beghian and Salomaa[16] at MIT and Smith and Cox[17] at ANL. Protons are produced in a radio-frequency ion source (frequency about 100 Mc), extracted, and focused by an electrostatic lens onto a small aperture. An oscillator (frequency about 10 Mc) sweeps the beam across the aperture and thus produces pulses of a few nanoseconds' duration. (There is only 1 pulse per oscillator cycle; the pulse that would be caused by the return sweep is suppressed.) Beyond the pulsing aperture, the protons traverse the accelerating column and finally reach the target. Just before reaching the target, the protons pass through a copper tube; the pulse they induce provides a zero-time mark for time analysis.

LINEAR ACCELERATORS

The electron linear accelerator (Fig. 3) produces the greatest intensities of all accelerator-type pulsed neutron sources. Electrons are accelerated to energies between 15 and 50 Mev. The target is a block of heavy, often fissionable material. Bremsstrahlung caused as the electrons stop produces neutrons by (γ,n) and (γ,f) reactions with the heavy nuclei. (For neutron yields with various target materials, see Refs. 18 to 21). The neutron yield becomes significant at about 10 Mev and increases strongly with the electron energy up to about 40 Mev. Above 40 Mev the increase is very slow. The best neutron yields are obtained with elements of high Z. For approximately equal Z the yield for fissionable materials surpasses considerably that for nonfissionable materials due to neutron production by the (γ,f) reaction. The yield ratio is about 2.3 for natural uranium to lead.[18] The yield for a thick ^{238}U target at 30 Mev is $\sim 4 \times 10^{15}$ neutrons/(sec)(amp)(Mev). Most electron linear accelerators used as pulsed neutron sources have an energy between 15 and 50 Mev and a peak current between 200 and 800 ma. The neutron production rates are therefore between 10^{16} and 10^{17} neutrons/sec.

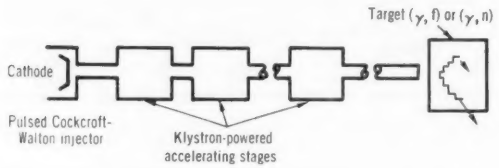

Fig. 3 Linear accelerators produce neutrons from (bremsstrahlung) (γ,n) and (γ,f) reactions in high-Z targets. Production rates are 10^{16} to 10^{17} neutrons/sec. Minimum pulse width is $\sim 10^{-9}$ sec.

At the injector end of the accelerator, electrons emitted by a hot cathode are electrostatically accelerated (electron gun) to ~100 kv. The beam can be switched on and off by modulating the voltage on a control grid or on the accelerating electrodes. It is possible to reach pulse widths of a few nanoseconds.

A survey of Linac facilities is given in Ref. 20. The Rensselaer Polytechnic Institute (RPI) Linac is described in detail in Ref. 19, and some operating experience is given in Ref. 22. The General Atomic (GA) Linac is described in Ref. 23.

Prompt Decay Measurements for Cross-Section Determinations

Diffusion coefficients, nonelastic-scattering cross sections, and capture cross sections in the Mev and kev range have been measured by observing the decay of the neutron flux after pulsing nonmultiplying or far-subcritical assemblies with monoenergetic neutron pulses of a few nanoseconds' duration.

CLASSIC METHOD

The classic method of deriving cross sections from neutron-decay measurements which has been used successfully in many experiments with thermal neutrons makes use of the equation

$$\lambda = v\Sigma_r + vDB_g^2 + CB_g^4 \qquad (1)$$

where λ is the decay constant of the asymptotic mode, v is the neutron velocity, and Σ_r is the combined cross section for all reactions that make the neutron undetectable for the detector. The geometrical buckling B_g^2 is calculated from the shape of the assembly, including an extrapolation length that is usually taken as $0.71\lambda_{tr}$. The coefficient C represents a transport correction to the diffusion approximation. (For fast systems it has a different physical significance than in thermal-neutron problems, where it is determined predominantly by the diffusion cooling effect.)

If λ is measured for a number of different bucklings, Σ_r can be determined from the intercept of the λ vs. B_g^2 curve with the ordinate axis; D is found from the derivative $d\lambda/dB_g^2$ for small bucklings, and C, from the shape of the curve at higher bucklings.

APPLICATION IN FAST SYSTEMS

The method was first used on a larger scale for nonmoderated systems by Beghian and others[24-27]

who measured removal cross sections and diffusion coefficients for lead and removal cross sections for uranium and iron at energies of ~1 Mev. In Beghian's basic setup, monoenergetic neutrons are produced by the $^{7}Li(p,n)^{7}Be$ reaction using a Van de Graaff generator with a lithium target. Pulse width was 3 nsec. The energy spread of the neutrons was ~50 kev due to the target thickness and to the angular spread of the neutrons intercepted by the assembly. The assembly was always placed about 30 cm from the target to reduce this angle; in some experiments a conical collimator made of lithium-loaded paraffin was placed between target and assembly. Plastic scintillators (Stilbene and Pilot B) were placed at the center of the assembly surface facing away from the neutron generator to detect the neutrons. The pulses were time sorted with a time-to-height converter and a 256-channel analyzer. Windows were selected to sort pulse heights.

Interpretation. Before an experiment of this type can be interpreted successfully, a number of problems must be resolved.

Decay Mode. Is there a fundamental decay mode which is identifiable and stable? Deconninck, D'Oultremont, and Stievenart[28] have shown experimentally and by Monte Carlo calculations that the measured decay constants of neutron fluxes in copper assemblies depend strongly on the detector position; the flux transmitted through an assembly decays much more slowly than the reflected flux. They suggest that during a large part of the decay time the flux in the assembly is much better described as a propagating wave than as a stationary decaying mode. According to their work a stationary decay is established only a relatively long time (50 nsec) after the pulse—too late for a meaningful measurement.

To clarify the situation, Beghian, Hofmann, and Wilensky[27] performed measurements on a lead slab with the detector in three different locations (center, edge, and intermediate position on the back surface of the assembly). They found that after about 15 nsec the decay is determined by an easily measurable decay constant that is the same for all three cases. So it appears that, even if the existence of a fundamental decay mode is not completely established, it is at least justified as a working hypothesis for the interpretation of the measurements.

Removal Cross Sections. Another important question concerns the definition of the removal cross section Σ_r. The detection probability for a neutron can be diminished or eliminated by inelastic scattering or elastic moderation to an energy of lower detector efficiency, by inelastic scattering below the detector threshold, or by capture. For some materials (e.g., lead), the detector can be biased in such a way that any collision of a neutron results either in its effective removal or does not significantly affect its detection probability. If the material has low nuclear energy levels (^{238}U), there will always be inelastic-scattering processes which will not remove neutrons but will reduce the efficiency of detection. One must then work with an effective cross section $\Sigma_{nel}(1-\xi)$, where ξ is the fraction of the detector efficiency remaining for the degraded neutron.

In addition, for intermediate-weight nuclei (e.g., iron[25,26]), the effect of elastic moderation must be considered. For this purpose the detector was biased in such a way that above the threshold the efficiency was a linear function of the neutron energy. The effect of elastic moderation can then be expressed as an approximately energy-independent pseudo cross section $\Sigma_p = b\overline{\Delta E}/\lambda_{tr}$, where $\overline{\Delta E}$ is the average energy loss per collision and b is a constant. For iron, where the lowest nuclear energy level is at 850 kev, Σ_p was measured at an incident neutron energy below this value (740 kev). The capture cross section is negligible. Once Σ_p is known the nonelastic-scattering cross sections at higher energies can be found as the difference between the total removal and the contribution of elastic moderation:

$$\Sigma_{nel} = \Sigma_r - \Sigma_p \qquad (2)$$

Buckling Limitations. Another point that is important for the interpretation of the measurements is the fact that λ as a function of B_g^2 can be measured only over a limited range of B_g^2. For too small assemblies there is too much uncertainty in the extrapolation length, whereas for very large assemblies the signal-to-noise ratio becomes too small and the costs of material in some instances become prohibitive. The range of bucklings for which decay measurements can be made is thus not always sufficient for a meaningful fit of three parameters (Σ_r, D, and C). Therefore Beghian fitted all three parameters only for lead; for uranium and for iron, the analysis was restricted to the evaluation of Σ_r.

MEASUREMENTS IN THE KEV REGION

Arai, Miessner, and Beckurts[29] used the fast pulsed method to measure effective capture and transport cross sections in uranium and lead in the low kev region. They used a 3-Mev Van de Graaff generator with pulse widths of 1 or 10 nsec. Neutrons of 30 kev were produced by the $^{7}Li(p,n)^{7}Be$ reaction near threshold, and neutrons of 7.5 kev, by the $^{45}Sc(p,n)^{45}Ti$ reaction at the lowest resonance of the (p,n) cross section. The detectors used were a ^{6}Li-loaded glass scintillator and a LiI crystal. Because these experiments were done in an energy region where the resonances are separated, the authors emphasize that they yield effective cross sections that include the effect of resonance self-shielding. These data are useful in reactor design work; however, for compari-

son with cross sections found by other methods, the values from the pulsed neutron experiments have to be divided by a calculated self-shielding factor.

In the low kev regions, the nonelastic-scattering cross sections are zero. The change in detector efficiency due to elastic moderation was assumed to have equal time dependence for all the neutrons in the pulse. It was taken in account by dividing the measured decay curve by a correction function $F(t)$. The measured removal cross section therefore is entirely due to capture.

RESULTS WITH PULSED TECHNIQUES

Table 2 shows a number of cross sections measured by the groups of Beghian and of Arai using the pulsed neutron technique and compares them with results found by other methods.[24–29] They generally agree within the experimental error.

Table 2 COMPARISON OF CROSS SECTIONS MEASURED BY PULSED SOURCE AND OTHER METHODS

Cross section	Ref.	Energy, kev	Cross section, barns: Pulsed source method	Other method*
σ_r(Pb)	24	820	0.125	<0.2
		1240	0.33 ± 0.05	0.3
D(Pb)	24	820	2.17 ± 0.13†	2.23†
		1240	2.28 ± 0.09	2.42
σ_r(U)	24	840	0.76 ± 0.08	0.6 ± 0.14
σ_{nel}(Fe)	25,26	930	0.087 ± 0.012‡	Good agreement with LASL data in same energy region
		1040	0.406 ± 0.044	
		1150	0.321 ± 0.037	
		1280	0.490 ± 0.013	
		1390	0.491 ± 0.013	
		1520	0.713 ± 0.018	
σ_{nel}(Pb)	27	2140	0.83	Good agreement with UCRL data in same energy region
		1740	0.65	
σ_{tr}(Pb)	29	30 ± 6	10.1	10.0
σ_a(^{238}U)	29	30 ± 6	0.54	0.38, 0.47, 0.50, 0.53
		7.5 ± 0.8	0.61	0.63, 0.64
σ_{tr}(^{238}U)	29	30 ± 6	15.1	13.6, 13.4, 13.7, 12.0
		7.5 ± 0.8	15.9	15.8, 15.3

*The derivation or the origin of the values given here may be found in detail in the references given.

†Diffusion coefficient in centimeters.

‡These cross sections contain a fractional reduction of detector efficiency for part of the inelastic scattering. They have therefore no absolute physical significance.

A number of studies were made of the agreement that can be reached when the pulse decay in a nonmoderating system is analyzed by the P_N transport theory.[30–32] Cockrell, Perez, and Dalton[30] showed that a P_1 approximation gives very good agreement with Beghian's decay data in lead. They also suggest that it is possible to determine the angular moments of the Legendre polynomial expansion of the scattering kernel from the pulsed neutron data. Beghian, apart from evaluating cross sections, studied the decay constants for successively thinner lead slabs down to a thickness of 2 in. and compared the results with various predictions of transport theory.[26] All calculated values predicted a faster decay than was measured. In Ref. 27 the series was continued to a lead-slab thickness of 1 in., and the results are compared to recent transport calculations by Paik, Travelli, and Kaplan.[31,32] The agreement between measurement and theory is improved; however, at thicknesses below 4 in., it becomes very difficult to determine a fundamental decay constant from the measured data, and the com ·ison is not very significant.

Reactivity Measurements

One of the most frequent applications of the pulsed source technique in fast as well as in thermal reactor physics is the measurement of negative reactivities. Basically two different approaches have been used to derive the reactivity $\rho = (k-1)/k$ from the measured data in a pulsed neutron experiment.

THE FUNDAMENTAL-DECAY-CONSTANT METHOD

One method, which was first described by Simmons and King,[33] is based on the observation of the fundamental decay constant α_0 of the prompt-neutron flux. This constant is given by the equation

$$\alpha_0 = \frac{\bar{\beta}}{\Lambda} - \frac{\rho}{\Lambda} \tag{3}$$

with definitions and nomenclature taken from Refs. 34 and 35.

Here the reactivity* is

$$\rho = \frac{[W,(-L+\chi P)\Phi]}{[W,\chi P\Phi]} \tag{4}$$

the delayed-neutron fraction is

$$\bar{\beta} = \sum_{i=1}^{n} \frac{[W,\beta_i \chi_i P\Phi]}{[W,\chi P\Phi]} \tag{5}$$

and the generation time is

$$\Lambda = \frac{[W,v^{-1}\Phi]}{[W,\chi P\Phi]} \tag{6}$$

where L, P = loss and production operators
χ, χ_i = operators describing fission spectra
Φ = real prompt flux
W = an arbitrary weighting function

*As shown in Ref. 36, this reactivity is equivalent to the static reactivity computed by most reactor codes if the weighting function W is chosen as the adjoint Φ_g^* of the static flux distribution.

The brackets indicate an integration over energy and space.

If a constant generation time is assumed,

$$-\frac{\rho}{\beta}=\frac{\alpha_0-\alpha_c}{\alpha_c} \tag{7}$$

where α_c is the prompt decay constant at critical as measured by a Rossi alpha experiment or as extrapolated from pulsed neutron measurements when the critical condition is approached. However, in most cases at subcriticalities of several percent, the neutron-generation time will change markedly, and a meaningful determination of reactivities by the Simmons and King method is possible only if these changes can be calculated with good accuracy.

AREA METHODS

The second type of reactivity measurement by the pulsed technique is the so-called modified or area method. These measurements require the ratio of the multiplications of the prompt neutrons (neutrons in the decay chain immediately following the source pulse without delayed intermediaries) to the total neutron population (including the delayed neutrons). This ratio is given by

$$R=\frac{A_P}{A_{\text{total}}}=\frac{\rho}{\rho-\beta} \tag{8}$$

The ratio of the multiplications is experimentally determined by measuring the ratio of the time integral of the prompt and the total flux. If the system is repetitively pulsed, the time analysis in general will show pulses sitting on an essentially constant background. The prompt flux integral is given by the area under the pulses (excluding the background), whereas the total flux integral is given by the sum of the areas under the prompt and delayed flux. In general, Eq. 8 is rewritten as

$$-\frac{\rho}{\beta}=\frac{A_P}{A_d} \tag{9}$$

which yields reactivity in dollars. A_d is the integral over the delayed background.

Difficulties. All reactivity measurements based on the area principle encounter the following difficulties:

- Because the source distribution from the pulsed generator is not similar to the source distribution of the fundamental-mode fission source (either in energy or in space), a large amount of higher spatial and energy modes will be excited by the pulse. The different reactivities associated with the higher modes will distort the result of the area evaluation.
- The other problem of the area method has become known as the kinetic distortion, which means the difference between the flux distributions of the prompt and delayed fundamental modes. This can be seen from the general neutron-balance equation,[35,37] which for any mode can be written in the form

$$\left[-L+\left(\chi-\sum_i \beta_i \chi_i \frac{\omega}{\lambda_i+\omega}\right)P-\frac{\omega}{v}\right]\Phi_\omega=0 \tag{10}$$

$1/\omega$ is the period of the flux, and λ_i is the decay constant of precursor group i. The largest (least negative) eigenvalue, ω_l, corresponds to the stable period of the reactor; a much more negative eigenvalue ω_p corresponds to the prompt period.

Comparing the balance in Eq. 10 for the solutions ω_l and ω_p, we find that in the prompt case a decrease in the production term is compensated by an increase of the (positive) term $-(\omega/v)\Phi_\omega$. This corresponds to the steady-state equation for a reactor with a smaller production in the core but less absorption throughout the whole reactor, so that the prompt mode in reflected systems is shifted somewhat toward the reflector. In terms of the area methods of determining reactivities, larger negative reactivities will be measured if one goes from the core toward the reflector.

More detailed analyses of the kinetic distortion and related effects are given in Refs. 35, 36, and 38 to 41.

Early Developments. The first area-ratio method for the determination of reactivities was developed by Sjöstrand.[42] He used pulse lengths which were long compared to the prompt period but short compared to all precursor decay times. The duty cycle was about 50% (pulse-on time ≈ pulse-off time). The reactivity is found directly by applying Eq. 9. The areas used for the evaluation of the Sjöstrand experiment contain all the higher modes in the prompt as well as in the delayed part, and for reflected systems the result naturally is also influenced by the kinetic distortion. However, as pointed out by Masters and Cady,[35] there is a tendency for the two effects to cancel, so that the radial variation of the Sjöstrand result becomes very small.

Gozani adapted the technique for shorter pulses and eliminated the higher harmonics from the prompt contribution by disregarding the initial part of the decay curve.[43] Instead the decay curve, measured after a certain waiting time (t_w) when the higher modes have decayed, is extrapolated back to the time of the source pulse. For the reactivity the following formula is obtained:

$$-\frac{\rho}{\beta}=\frac{C_1 x F}{\alpha_0 N_d} \tag{11}$$

where C_1 = extrapolated amplitude of the fundamental exponential at zero time
F = pulsing frequency
α_0 = fundamental decay constant
N_d = delayed background

COMBINED METHODS

Garelis and Russell have found a method that combines the two approaches described above.[44] This technique too avoids the necessity of making the reactor critical and also includes all modes based on a simple one-group diffusion model. The time dependence of the subcritical prompt and delayed fluxes is used to determine $k\beta/l = \alpha_c$ by the equation:

$$\int_0^\infty N_p e^{k\beta/l}\, dt - \int_0^\infty N_p\, dt = N_d/F \qquad (12)$$

which can be solved by iteration methods. (N_p is the time-dependent prompt flux. It is advantageous to perform the integration explicitly only over the first part of the curve and to assume a decay with the fundamental exponential when the flux approaches the background level.) Once α_c is found from Eq. 12, the reactivity is calculated from Eq. 7. In Ref. 45 Garelis shows how his method can be used even when the pulses from the source are of varying height and of a frequency comparable to or lower than the precursor decay constants. It is done by starting the time analyzer with the first source pulse, having it sweep at an integer multiple of the source frequency, and continuing the sweep for a few cycles after the pulsing has stopped.

For all area-ratio measurements, especially those made using drift-tube accelerators, the parasitic background should be eliminated. Ruby[46] suggests that the background be determined in the pulse-off condition after a pulsing run and that ample time be allowed so that the longest-lived precursor will decay.

The comments of several experts about the determination of negative reactivities by pulsed methods and its problems were given in a session of a recent ANS meeting.[47]

The methods of measuring reactivities described above were mostly developed for thermal reactors; however, several applications to fast reactors were reported in recent years.

FAST REACTOR APPLICATIONS

Bergström[48] describes measurements on Core 1 of the Swedish experimental fast reactor (FR-0), which is an approximate cylinder of 20% enriched uranium metal surrounded by a thick copper reflector (core diameter, 31 cm; height, 30.1 cm). A ^{3}He proportional counter was placed in the center of the core. Subcriticality was measured by both the Garelis and Gozani methods for eight different rod positions. The results agreed quite well with values found by the inverse multiplication method. Further reactivity measurements were made of the worth of a central air gap. The measured values of the prompt decay period were in good agreement with values calculated using Cohn's two-region theory.[49]

Measurements on the Karlsruhe fast subcritical facility (SUAK) were reported.[50] Measurements were made on bare assemblies of 20% enriched uranium, 38 cm high, and about 26 by 26 cm (5 by 5 elements) and 32 by 32 cm (6 by 6 elements) in cross sections. The area methods of Gozani and Garelis–Russell were used to determine the reactivity for the larger assembly. Both methods gave a k_{eff} of 0.88 ± 0.02 in reasonable agreement with a value of 0.86 found by the inverse multiplication method. Calculated values also were in similar agreement. The discrepancy of 2% is supposedly due to parasitic background.

I have measured the reactivity for various control-rod positions and gap widths at Assembly 5 of Argonne's ZPR-VI, a large (2600 liters) ^{235}U carbide core with a depleted uranium reflector.[51] The Simmons and King method (under the assumption of constant lifetime) and the area methods by Gozani and Garelis–Russell were used. Data were taken with fission counters near the core midplane at different radial distances from the center. Results with the three pulsed methods are in satisfactory agreement with nonpulsed reactivity determinations. However, for the area methods the kinetic distortion caused a difference of about 20% in ρ between measurements in the core center and measurements in the blanket.

Spectra Measurements by the Time-of-Flight Method

Over the past few years, the measurement of neutron spectra has been both one of the most promising and one of the most difficult fields in fast reactor physics. A better knowledge of the neutron spectrum is needed for the calculation of many important reactor parameters such as reaction rates and Doppler effects. Further, it provides a very good basis to check the accuracy of calculations, not only with respect to the input cross-section sets but also as a test of the calculational methods themselves.

Quite satisfactory spectra measurements are possible now with various techniques (proton-recoil counters, solid-state devices, and photographic emulsions) for energies from about 1 kev to the high-Mev region; but the low-energy end of the spectrum is largely left to pulsed-source time-of-flight measurements. For assemblies with sufficiently short decay times, the time-of-flight method has also been used at energies up to 15 Mev. In the high-energy ranges, it provides a useful comparison with results gained by other methods, and it is often superior in accuracy and resolution.

Most of the time-of-flight data on the spectra of fast assemblies result from the work of five groups: three center around linear accelerator facilities—at General Atomic,[52–60] Rensselaer Polytechnic Institute,[61–65] and Harwell[66]—and two center around subcritical and critical facilities—at Karlsruhe (SUAK)[67–69] and Aldermaston (VERA).[5–8]

TECHNIQUE

Basically all pulsed-source spectra measurements are similar; ingredients are the pulsed source and assembly, a flight path, and the neutron detector.

Pulsed Source. A pulsed neutron source and the assembly under investigation are set up in such a way that periodic bursts of neutrons can be produced in the interior or at the surface of the assembly. If the assembly is non- (or weakly) multiplying, the pulsed source is usually an electron Linac; only with such a source can the necessary high intensity be achieved. Much cheaper drift-tube accelerators using the $T(d,n)^4He$ reaction have been used successfully with assemblies having high multiplication. When the spectrum is hard (little overlap), the high repetition rates ($\sim 10^5$/sec) possible with the drift-tube accelerators help significantly to overcome intensity problems.

troublesome and cannot be completely avoided. (Any sort of background should be as low as possible.) Time resolution is also very important and must be less than ~30 nsec for experiments at high energy. Finally the spatial location of the detection event must be well defined, particularly when the flight path is short.

Table 3 lists the detectors used most regularly by the different experimental groups. A thorough but older survey of neutron time-of-flight detectors is given in Ref. 20. There are also newer but somewhat briefer accounts oriented directly to the problem of fast spectra measurements.[61,62]

The organic proton-recoil scintillators are particularly suitable for high energies both because of their efficiency characteristic and because of their high time resolution, which is particularly important for short flight times. However, because of their high gamma sensitivity, they must be heavily shielded,

Table 3 DETECTORS USED IN TIME-OF-FLIGHT SPECTRA MEASUREMENTS

	Detector energy range		
Facility	High (3×10^5–1.5×10^7 ev)	Intermediate (10^3–2×10^6 ev)	Low (to 10^4 ev)
RPI Linac[61–65]	Liquid proton-recoil scintillators	$^{10}B_4C + H_2O + NaI(Tl)$	$^{10}B_4C + H_2O + NaI(Tl)$; also, BF_3 counters
GA Linac[52–60]	Liquid proton-recoil scintillators	$^{10}B_4C$ + moderator + organic scintillator	$^{10}B_4C$ + moderator + scintillator; also, BF_3 counters
Harwell Linac[66]	Plastic scintillator	^{10}B + gamma detector	Li glass
SUAK[67–69]		Li glass; also, ^{10}B powder + NaI(Tl)	Li glass; also, ^{10}B powder + NaI(Tl)
VERA[5–8]		Li glass	Li glass

Flight Path. The neutron flight path begins at the inner face of a reentrant hole in the assembly; or, for leakage–spectra measurements, at the surface of the assembly. The detector is located a considerable distance from the assembly (between 10 and several hundred meters). Usually most of the path is taken up by an evacuated tube to reduce air scattering. A system of collimators is placed near the inner end of the flight path to define the area of the assembly which is viewed by the detector. The collimators (e.g., steel or boron combined with lead or with paraffin) also prevent neutrons emerging from the assembly from reaching the wall of the flight tube where they might be scattered into the detector. Concrete cells are often used to shield the assembly and the target of the neutron source; they reduce erroneous counts from neutrons scattered by the collimators and surrounding structures.

Detectors. Demands on the detector are numerous and not easily met. It should cover a large solid angle for there are usually intensity problems. Detector efficiency should be high, well known, and reasonably smooth in the energy range of measurement and low in the thermal region. Sensitivity to gamma rays is

and they generally must be gated off during the gamma burst from the accelerator. Otherwise the electronics would be overloaded and could not recover before the arrival of the neutrons.

Although at low energies such simple devices as BF_3 counters may suffice, more complicated apparatus is necessary in the intermediate-energy range, where the efficiency of these counters would be too low. The linear accelerator groups use slabs containing ^{10}B and usually some moderator in connection with a gamma detector. (When neutrons are captured in the boron, the resulting 480-kev gamma radiation is detected by the gamma detector.) Usually the gamma detector is removed from the flight path of the neutrons and shielded from the assembly. If the neutrons are strongly moderated in the detector, the device has a somewhat poor time resolution. The SUAK and VERA groups have shown the usefulness of lithium-glass scintillators over the whole energy range up to about 2 Mev. They possess good efficiency and time resolution and are relatively easy to calibrate.

Calibration. Reliable calibration of the detector is a very important prerequisite for spectrum measure-

ments by the time-of-flight method. Calibration is easiest for gas-filled counters with known reaction cross sections because direct calculations of efficiency vs. energy are possible. Calculation of the efficiency of the lithium-glass scintillators is more difficult because the energy dependence of the (n,α) cross section is not well known and because the detector material consists of many components. Therefore the SUAK group backed up their calculations by an experimental calibration with monoenergetic neutrons from a Van de Graaff generator, the yield of which in turn had been measured with a long counter. The VERA group calculated the efficiency of their lithium-glass scintillator with a Monte Carlo technique. Extensive work on the determination of cross sections for the calibration of lithium-glass scintillators is described in Ref. 70. The Monte Carlo technique is also used to calibrate detectors consisting of a boron slab and a gamma detector.

Intermediate-energy detectors are often intercalibrated against ^3He and BF_3 chambers of known efficiency. High-energy detectors have been calibrated by the RPI group using the known neutron spectrum from the photodisintegration of deuterium and the (Maxwellian) neutron spectrum from (γ,n) processes in lead. Known spectra from multiplying or nonmultiplying assemblies (usually $1/E$) offer a further method of calibration over almost the whole energy range. Good surveys of these calibration methods may be found in the RPI reports, particularly Refs. 61, 62, and 64.

Time Resolution. A further important factor is the time resolution of the system. In general, it is essentially determined by the decay of the pulse in the assembly. Only for weak and nonmultiplying assemblies, the decay time may be so small that the time uncertainty introduced by the detector becomes comparable. Iteration methods for the unfolding of measured data have been developed by the VERA[5] and SUAK[68] groups. Analytical approaches to the unfolding problem are given in Refs. 71 and 72.

RESULTS

Table 4 shows a survey of time-of-flight spectra measurements performed in recent years. Although the experiments are too numerous to be discussed one by one, there are some common results and significant points. Practically all of the results have been compared to calculations, mostly to transport calculations, because anisotropic effects play a significant role particularly for smaller assemblies.

• The non- or weakly multiplying assemblies had as an important purpose the experimental verification

Table 4 SURVEY OF TIME-OF-FLIGHT MEASUREMENTS USING PULSED NEUTRON FACILITIES

Assembly				
Composition	Size, cm	Source location	Beam extraction	Ref.
GA Linac				
^{238}U block	81 × 76 × 81	Near surface	Variable	53
Lead sphere	15.2 O.D.	Center	Surface	52,54
Lead sphere with graphite reactor	15.2 O.D. 12.7 thick	Center	Surface	52,54
^{235}U sphere (93% enriched)	17.9 O.D.	Center, sphere is target	Surface, variable angles	55,56 58-60
W sphere (heatable)	25, 50 O.D.; 15.2 I.D.	Center	Surface	55
^{238}U block	50.8 O.D.	Center	Variable	57,60
RPI Linac				
Iron block	101.6 × 101.6 × 96.5	30 cm inside block	Variable	63
^{238}U sphere	101.6 × 78.7 × 66	Off center	Variable	64
Harwell Linac				
U_{nat} sphere	32 O.D.	Center	Surface	66
Na cylindrical tank	100 O.D., 100 high	Surface	Center	66
SUAK				
U (20% enriched)	26.9 or 32.3 side, 35.1 high	Center	Center or surface	67-69
U (20% enriched and CH_2)	26.9 or 32.3 side, 33.05 or 35.05 high	Surface	Surface	69
VERA				
5A (U core with H)	32.0 O.D., 28.4 high	Variable	Variable	8
7A (U core with H)	36.3 O.D., 33.5 high	Core edge	Core center	5,6
11A (Pu core, no H)	26.9 O.D., 21.7 high	Core edge	Core center	5
16Z5A (zoned Pu core)		Core edge	Core center	6,7
17Z5J (zoned Pu core with Na)		Core edge	Core center	6,7
19A (PuO_2, UO_2, CH_2)	26.37 long	Core edge	Near core center	8

of techniques used in shielding calculations. A spherical shape was often chosen for the assemblies to facilitate the calculation.

• In the highly multiplying assemblies, the time-of-flight measurements had to close the gap left in the low-energy region by the other methods of spectral measurements. In the comparisons with calculations, the main emphasis has been on the verification of cross sections.

Comparisons of measurements and calculations have shown in almost all cases that the calculated spectra in the very-low-energy region (below 1 kev) are too low. This result agrees with the general experience that measured neutron lifetimes are longer than calculated ones. Incorrect cross sections used in the calculations (particularly inelastic scattering and capture cross sections) are probably the cause of this discrepancy.

Experiments with resistance-heated tungsten spheres deserve mention.[55] Spectra measurements were performed at 800°K (maximum temperature for the spheres) and at room temperature. Reference 55 shows the experimental arrangement and the difference in the measured spectra and gives a qualitative interpretation.

Russian time-of-flight experiments described in Refs. 73 and 74 used the pulsed fast reactor IBR rather than a pulsed source of the types discussed here. Their flight path had the great length of 1 km. Spectra were taken of iron, nickel, and uranium assemblies.

Conclusions

For several fast critical facilities, pulsed neutron experiments are now performed routinely on every assembly built.[75,76] The prompt decay constant [or the prompt-neutron lifetime (extrapolated from $\beta/l_p = \alpha_c$)] is determined and compared to calculations. However, the prompt decay in a reflected system is quite complicated. Often it is analyzed according to a method developed by Cohn who described it in terms of two exponentials resulting from two different lifetimes in core and reflector.[49]

Pulsed neutron studies include general theoretical investigations about the decay of a neutron pulse in nonmoderating assemblies.[77,78] In addition, there are very interesting theoretical and experimental results about the existence of a fundamental decay mode in uranium systems in different hydrogen concentrations.[68,79]

The possibilities of pulsed experiments on fast systems are not yet exhausted. An interesting new proposal would measure (by the time-of-flight method) various reaction rates as functions of energy in the spectrum of an assembly.[59] This method may soon help solve such pressing cross-section problems as the accurate determination of capture-to-fission ratios.

References

1. N. G. Sjöstrand, A Theoretical and Experimental Investigation of the Pulsed Neutron Method as a Means for Neutron Diffusion Studies, collection of papers submitted for Ph.D. degree, Kungliga Tekniska Högskolan, Stockholm, 1959.
2. K. H. Beckurts, Reactor Physics Research with Pulsed Neutron Sources, *Nucl. Instrum. Methods*, 11: 144 (1961). [An alternate source is: G. R. Keepin, Pulsed Neutron Techniques, USAEC Report LAMS-2215, Los Alamos Scientific Laboratory, March 1958.]
3. P. Jessen, Kaman Nuclear Corp., private communication, 1965.
4. W. Eyrich, Two Powerful Neutron Generators for Pulsed and Continuous Operation, *Nukleonik*, 4: 167 (1962).
5. W. J. Paterson et al., Some Measurements of Fast Reactor Spectra by the Time-of-Flight Technique Using a Pulsed Source, in *Pulsed Neutron Research*, Symposium Proceedings, Karlsruhe, 1965, Vol. II, p. 417, International Atomic Energy Agency, Vienna, 1965 (STI/PUB/104).
6. J. W. Weale et al., Neutron Spectrum Measurements in the Zero Power Fast Reactor VERA, in Proceedings of Conference on Radiation Measurements in Nuclear Power, pp. 231-244, Berkeley Nuclear Laboratory, Gloucestershire, England, Sept. 12–16, 1966.
7. J. W. Weale, P. W. Benjamin, and W. J. Paterson, A Comparison of Measured and Calculated Energy Spectra in Two VERA Cores, in Proceedings of the International Conference on Fast Critical Experiments and Their Analysis, USAEC Report ANL-7320, p. 501, Argonne National Laboratory, October 1966.
8. W. J. Paterson et al., Neutron Spectrum Measurements in the Fast Reactor Assembly VERA 19A and Tests of Time-of-Flight Spectrometry Method in VERA 5A and VIPER 1, presented at the International Atomic Energy Agency Symposium on Fast Reactor Physics and Related Safety Problems, Karlsruhe, October 30–November 3, 1967, Paper SM-101/40.
9. W. Eyrich and A. Schmidt, Two Compact, High Intensity Pulsed Neutron Sources, in *Pulsed Neutron Research*, Symposium Proceedings, Karlsruhe, 1965, Vol. II, p. 591, International Atomic Energy Agency, Vienna, 1965 (STI/PUB/104).
10. *Ibid*, p. 598.
11. C. W. Elenga and O. Reifenschweiler, The Generation of Neutron Pulses and Moderated Neutron Fluxes with Sealed-Off Neutron Tubes, in *Pulsed Neutron Research*, Symposium Proceedings, Karlsruhe, 1965, Vol. II, p. 609, International Atomic Energy Agency, Vienna, 1965 (STI/PUB/104).
12. P. D. Lomer et al., High Output Neutron Generating Tubes for Reactivity Measurements, in *Pulsed Neutron Research*, Symposium Proceedings, Karlsruhe, 1965, Vol. II, p. 623, International Atomic Energy Agency, Vienna, 1965 (STI/PUB/104).
13. K. W. Erickson and B. J. Carr, Neutrons on Demand, *Ind. Res.*, 5: 36 (June 1963).
14. J. B. Marion and J. L. Fowler, *Fast Neutron Physics*, pp. 73-176, Interscience Publishers, a division of John Wiley & Sons, Inc., New York, 1960.
15. High Voltage Engineering Company, Two Million Volt Accelerator and Accessories, 1963.
16. L. E. Beghian and M. K. Salomaa, A High Intensity Nanosecond Pulsed Van de Graaff Accelerator, *Nucl. Instrum. Methods*, 17: 181 (1962).
17. A. B. Smith and S. A. Cox, Argonne National Laboratory, personal communication, 1967.
18. W. C. Barber and W. D. George, Neutron Yields from Targets Bombarded with Electrons, *Phys. Rev.*, 116: 1551 (1959).
19. Proceedings of the Symposium on Neutron Physics, Rensselaer Polytechnic Institute, May 1961.

20. Proceedings of the Symposium on Neutron Time-of-Flight Methods, Saclay, France, July 24–27, 1961.
21. J. R. Beyster and J. L. Russell, Jr., Repetitively Pulsed Accelerator Boosters, in Proceedings of Symposium on Pulsed High Intensity Fission Neutron Sources, Washington, D. C., February 1965, USAEC Report CONF-650217.
22. E. R. Gaerttner et al., Operating Experience with the RPI Linac, *IEEE (Inst. Elec. Electron. Eng.), Trans. Nucl. Sci.*, 9(5): 23 (1962).
23. Gulf General Atomic Inc., unpublished.
24. L. E. Beghian et al., The Investigation of Neutron Kinetics and Cross Sections in Fast Nonmoderating Assemblies by the Nanosecond Pulsed Neutron Source Technique, *Nucl. Sci. Eng.*, 15: 375 (1963).
25. L. E. Beghian et al., The Investigation of Nonelastic Cross Sections for Iron by the Nanosecond Pulsed Source Technique, *Nucl. Sci. Eng.*, 17: 82 (1963).
26. L. E. Beghian and S. Wilensky, The Pulsed Neutron Technique Applied to Fast Nonmultiplying Assemblies, in *Pulsed Neutron Research*, Symposium Proceedings, Karlsruhe, 1965, Vol. II, p. 511, International Atomic Energy Agency, Vienna, 1965 (STI/PUB/104).
27. L. E. Beghian, F. Hofmann, and S. Wilensky, Experimental Investigation of Fast Neutron Decays in Lead Assemblies, *Nucl. Sci. Eng.*, 27: 80 (1967).
28. G. Deconninck, P. d'Oultremont, and M. Stievenart, Contribution to the Study of Fast Neutron Nonmultiplying Assemblies by the Pulsed Neutron Technique, in *Pulsed Neutron Research*, Symposium Proceedings, Karlsruhe, 1965, Vol. II, p. 493, International Atomic Energy Agency, Vienna, 1965 (STI/PUB/104).
29. E. Arai, H. Miessner, and K. H. Beckurts, Measurements of Effective (Self-Shielded) Neutron Cross Sections by a Fast Pulsed Method, *Nucl. Sci. Eng.*, 26: 573 (1966).
30. R. G. Cockrell, R. B. Perez, and G. R. Dalton, One Speed Transport Study of Fast Neutron Pulses in Nonmoderating Media, *Nucl. Sci. Eng.*, 19: 423 (1964).
31. N. C. Paik, Application of the Spatial Expansion Method to the Solution of the Boltzmann Equation in Three Dimensions, Ph.D. Thesis, Massachusetts Institute of Technology, September 1965.
32. N. C. Paik, A. Travelli, and I. Kaplan, Asymptotic Decay Constants in Small Slabs and Cubes by Spatial Expansion Method, *Trans. Amer. Nucl. Soc.*, 8: 292 (1965).
33. B. E. Simmons and J. S. King, A Pulsed Neutron Technique for Reactivity Determination, *Nucl. Sci. Eng.*, 3: 595 (1958).
34. T. Gozani, The Concept of Reactivity and Its Application to Kinetic Measurements, *Nukleonik*, 5: 55 (1963).
35. C. F. Masters and K. B. Cady, A Procedure for Evaluating Modified Pulsed Neutron Source Experiments in Subcritical Nuclear Reactors, *Nucl. Sci. Eng.*, 29: 272–282 (1967).
36. C. H. Preskitt et al., Interpretation of Pulsed Source Experiments in the Peach Bottom HTGR, *Nucl. Sci. Eng.*, 29: 283 (1967).
37. A. F. Henry, Definition and General Considerations Concerning Large Changes in Reactivity, *Trans. Amer. Nucl. Soc.*, 9(1): 235 (1966).
38. A. E. Waltar and L. Ruby, Interpretation of Pulsed Source Experiments in Reflected Reactor, *Nukleonik*, 8: 287 (1966).
39. A. E. Waltar and L. Ruby, Initial Tests of a Two-Region Theory for Pulsed Neutron Reactivity Measurements, *Trans. Amer. Nucl. Soc.*, 9(1): 169 (1966).
40. M. Becker and K. S. Quisenberry, The Spatial Dependence of Pulsed Neutron Reactivity Measurements, in *Neutron Dynamics and Control*, Tucson, Ariz., April 5–7, 1965, David L. Hetrick and Lynn E. Weaver (Coordinators), AEC Symposium Series, No. 7 (CONF-650413), 1966.
41. S. K. Wallace, A Note on the Analysis of Pulsed Neutron Shutdown Measurements, *Nucl. Sci. Eng.*, 21(1): 116 (1965).
42. N. G. Sjöstrand, Measurements on a Subcritical Reactor Using a Pulsed Neutron Source, *Ark. Fys.*, 11: 223 (1956).
43. T. Gozani, A Modified Procedure for Evaluation of Pulsed Source Experiments in Subcritical Reactors, *Nukleonik*, 4: 348 (1962).
44. E. Garelis and J. L. Russell, Jr., Theory of Pulsed Neutron Source Measurements, *Nucl. Sci. Eng.*, 16: 263 (1963).
45. E. Garelis, Theory of Pulsing Techniques, *Nucl. Sci. Eng.*, 18: 242 (1964).
46. L. Ruby, Modification to Prescription for β/l Pulsing, *Nucl. Sci. Eng.*, 21: 115 (1965).
47. Session About Determination of Large Negative Reactivity Changes, *Trans. Amer. Nucl. Soc.*, 9(1): 235–238 (1966).
    a. A. F. Henry, Definition and General Considerations Concerning Large Changes in Reactivity.
    b. Tsahi Gozani, Subcritical Reactivity Determinations: Comparison of Experimental Methods.
    c. Martin Becker, Principles of, and Problems with, Pulsed-Neutron Reactivity Measurements.
    d. Gordon E. Hansen, Special Problems Associated with the Determination of Large Negative Reactivity Changes in Fast Systems.
    e. Robert W. Albrecht, Application of Correlation Techniques To Determination of Subcritical Reactivity.
48. A. Bergström et al., Determination of Neutron Lifetimes and Reactivities in the Fast Critical FR-0 Assembly, in *Pulsed Neutron Research*, Symposium Proceedings, Karlsruhe, 1965, Vol. II, p. 357, International Atomic Energy Agency, Vienna, 1965 (STI/PUB/104).
49. C. E. Cohn, Reflected Reactor Kinetics, *Nucl. Sci. Eng.*, 13: 12 (1962).
50. H. Borgwaldt et al., SUAK, A Fast Subcritical Facility for Pulsed Neutron Measurements, in *Pulsed Neutron Research*, Symposium Proceedings, Karlsruhe, 1965, Vol. II, p. 399, International Atomic Energy Agency, Vienna, 1965 (STI/PUB/104).
51. F. Helm, Argonne National Laboratory, unpublished report, 1967.
52. J. L. Russell, Jr., Neutron Spectra in Shields by Time-of-Flight, in Proceedings of Special Session on Fast Neutron Spectrometry, 1964 Winter Meeting of ANS, San Francisco, Calif., Shielding Division Report ANS-SD2.
53. W. Y. Kato et al., Fast Reactor Physics Parameters from a Pulsed Source, in *Pulsed Neutron Research*, Symposium Proceedings, Karlsruhe, 1965, Vol. II, p. 373, International Atomic Energy Agency, Vienna, 1965 (STI/PUB/104).
54. J. L. Russell, Jr., et al., Determination of Neutron Spectra in Bulk Media by Time-of-Flight, in *Pulsed Neutron Research*, Symposium Proceedings, Karlsruhe, 1965, Vol. II, p. 445, International Atomic Energy Agency, 1965 (STI/PUB/104).
55. A. E. Profio et al., Time-of-Flight Measurements of Neutron Spectra in ^{235}U and Tungsten, in Proceedings of the International Conference on Fast Critical Experiments and Their Analysis, USAEC Report ANL-7320, p. 524, Argonne National Laboratory, October 1966.
56. J. L. Russell, Jr., et al., Accelerator Pulsed Fast Assembly, Operational Experience, *Trans. Amer. Nucl. Soc.*, 8(2): 437 (1965).
57. R. A. Moore et al., Fast Neutron Spectra in a Depleted Uranium Sphere, *Trans. Amer. Nucl. Soc.*, 10(1): 267 (1967).
58. J. R. Beyster et al., Integral Neutron Thermalization, Annual Summary Report, Oct. 1, 1964–Sept. 30, 1965, USAEC Report GA-6824, Gulf General Atomic Inc.
59. J. L. Russell, Jr., and A. E. Profio, Adequacy of Fast and Intermediate Cross Section Data from Measure-

ment of the Neutron Spectra in Bulk Media, USAEC Report GA-7059, Gulf General Atomic Inc., Apr. 27, 1966.

60. H. Antunez et al., Integral Neutron Thermalization, Quarterly Progress Report for the Period Ending March 31, 1966, USAEC Report GA-7091, Gulf General Atomic Inc.
61. Linear Accelerator Project, Progress Report, January–March 1966, USAEC Report RPI-328-56, Rensselaer Polytechnic Institute.
62. Linear Accelerator Project, Annual Technical Report During FY 1966, USAEC Report RPI-328-68, Rensselaer Polytechnic Institute.
63. Linear Accelerator Project, Progress Report, January–March 1967, USAEC Report RPI-328-87, Rensselaer Polytechnic Institute.
64. Linear Accelerator Project, Progress Report, April–June 1967, USAEC Report RPI-328-97, Rensselaer Polytechnic Institute. [An alternate source of information about recent work at the RPI Linac, including that described in Refs. 63 and 64, is: Linear Accelerator Project, Annual Technical Report, July 1, 1966–September 30, 1967, USAEC Report RPI-328-100, Rensselaer Polytechnic Institute.]
65. B. K. Malavija et al., Fast Neutron Spectrum Program from Reports to the AEC Nuclear Cross Sections Advisory Group, USAEC Report WASH-1074, p. 111, April 1967.
66. D. B. Gayther and P. D. Goode, Measurements of Fast Neutron Spectra in Reactor Materials, in *Pulsed Neutron Research*, Symposium Proceedings, Karlsruhe, 1965, Vol. II, p. 435, International Atomic Energy Agency, Vienna, 1965 (STI/PUB/104).
67. H. Borgwaldt et al., SUAK, A Fast Subcritical Facility for Pulsed Neutron Measurements, in *Pulsed Neutron Research*, Symposium Proceedings, Karlsruhe, 1965, Vol. II, p. 399, International Atomic Energy Agency, Vienna, 1965 (STI/PUB/104).
68. M. Küchle et al., Measurements of Neutron Spectra and Decay Constants with the Fast Subcritical Facility SUAK, in Proceedings of the International Conference on Fast Critical Experiments and Their Analysis, USAEC Report ANL-7320, p. 506, Argonne National Laboratory, October 1966.
69. E. D. A. Wattecamps, On Neutron Spectra Measurements by the Time-of-Flight Method and Neutron Spectra Calculations of the Fast Subcritical Assembly SUAK, Ph. D. Thesis, University of Ghent, Belgium, 1968, to be published.
70. S. Schwarz, L. G. Strömberg, and A. Bergström, A Relative Measurement of the $^{6}Li(n,\alpha)^{3}H$ Reaction Cross Section in the Range $1 < E_n < 600$ Kev, *Nucl. Phys.*, 63: 593 (1965).
71. E. Garelis and W. J. Ozeroff, Resolution of Time-of-Flight Measurements, *Nukleonik*, 9: 142 (1967).
72. E. A. Kramer-Ageev et al., Treatment of Intermediate Spectra with Time-of-Flight, from Dosimetry and Radiation Protection Collection No. 4, USAEC Report AEC-tr-6719, translated from *Vop. Dozim. Zashch. Izluch., Mosk. Inzh. Fiz. Inst., Sb. Statei*, No. 4 (1965).
73. A. I. Leipunsky et al., Experimental Studies on Fast Neutron Reactor Physics, in *Proceedings of the Third International Conference on the Peaceful Uses of Atomic Energy, Geneva, 1964*, Vol. 6, p. 167, United Nations, New York, 1965.
74. A. V. Zvonarev et al., Research in Reactor Physics by Time-of-Flight with Reactor IBR (in Russian), *Kernenergie*, 10: 101 (1967).
75. G. S. Brunson and R. J. Huber, Pulsed Neutron Die Away Measurements in Three Fast Critical Assemblies, *Trans. Amer. Nucl. Soc.*, 9(1): 168 (1966).
76. L. Barleon et al., Physics Investigations of a 670 l Steam Cooled Fast Reactor System in SNEAK, Assembly 3A-1, USAEC–Euratom Report EURFNR-396, Kernforschungszentrum, Karlsruhe, October 1967.
77. F. Storrer, Pulsed Neutron Experiments on Fast and Intermediate Systems, in *Pulsed Neutron Research*, Symposium Proceedings, Karlsruhe, 1965, Vol. II, p. 317, International Atomic Energy Agency, Vienna, 1965 (STI/PUB/104).
78. M. Stievenart, Theoretical Consideration Concerning the Pulsation of Fast Subcritical Assemblies, in *Pulsed Neutron Research*, Symposium Proceedings, Karlsruhe, 1965, Vol. II, p. 461, International Atomic Energy Agency, Vienna, 1965 (STI/PUB/104).
79. F. Mitzel, Untersuchungen über Instationare Neutronenfelder in Schnellen Multiplizierenden Systemen, Ph. D. Thesis, Karlsruhe, Germany, 1967.

Superheating of Liquid Metals in Relation to Fast Reactor Safety

By Hans K. Fauske

As the coolant in a liquid-metal-cooled fast breeder reactor (LMFBR), sodium offers highly desirable properties—high thermal conductivity and specific heat, high boiling point, low neutron absorption, and good electrical conductivity. However, sodium also has some undesirable characteristics, one of which is the superheat problem—the possible large overheating of the coolant before boiling occurs. During steady-state operation the coolant in an LMFBR is considerably below its boiling temperature throughout the core. But abnormal conditions may greatly increase coolant temperature due to rapid heat insertion, a decrease in flow, or both, and may initiate boiling. In fast reactors with positive void coefficient, accidents that initiate boiling may lead to undesirable reactivity insertions and possible core damage.

When boiling occurs, reactivity may increase, but the rate of increase depends primarily on how rapidly sodium is ejected from fuel-coolant channels. The amount of superheat present when boiling occurs, together with the rate of superheat release, governs the driving pressure for liquid-sodium ejection.[1,2] These factors also determine whether the reactor heat flux is an important parameter in subsequent vapor production that may force all the sodium out of the coolant channels.

A considerable amount of basic liquid-metal superheat data has become available (mostly for sodium), but the data show large variation. As a result, these data are currently of limited value in determining design safety criteria for fast reactors. This article reviews the data and their applicability to reactor design.

Superheat

The boiling process of liquid metals differs from that of nonmetallic fluids primarily because of the larger superheats required to initiate nucleation. This is illustrated in the following expression for superheat, $T - T_s$:

$$T - T_s \approx \frac{T_s}{\rho_v h_{fg}} \frac{2\sigma \cos \theta}{R_c} \qquad (1)$$

where T_s = saturation temperature
ρ_v = vapor density
h_{fg} = latent heat of vaporization
σ = liquid surface tension
R_c = cavity radius
θ = dynamic contact angle (see Ref. 3 for details)

Figure 1 shows superheat values for sodium and for water as calculated from Eq. 1 for a single set of assumptions. These superheat values are roughly 10 times larger for sodium than for water, primarily due to the higher boiling point and surface tension, and the lower vapor density, of sodium.

The large superheat required to initiate boiling in liquid metals has caused considerable concern in fast reactor safety analysis as evidenced by the new data and great interest expressed at the recent Aix conference on fast reactor safety.[4]

SUPERHEAT DATA

Four papers dealt directly with new experimental data on superheat of potassium and sodium.[5,8] These data (Fig. 2) were particularly noteworthy by their large variation, 9 to 1480° F, as compared to the variation in previously published data, 0 to 500° F (Fig. 3). Surprisingly, there was little (in some cases[5,6] zero) discussion of the older data.

Influential Variables

Extrinsic variables that can affect superheat behavior include the heat flux, heating surface, fluid velocity, pressure, and pressure–temperature history, aging, purity, radiation, heating method . . . and perhaps many more.

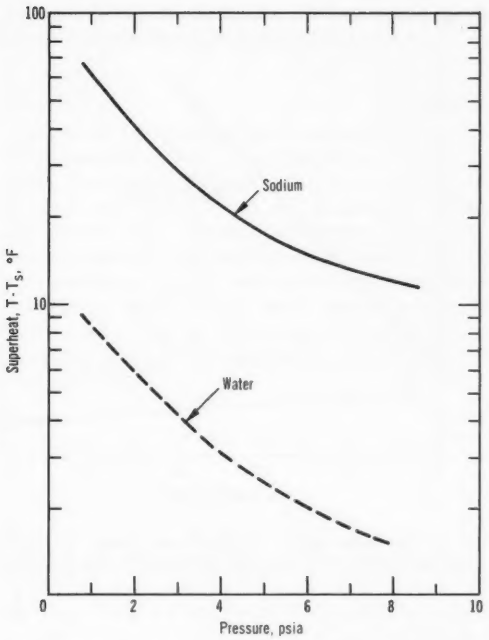

Fig. 1 Superheat values for sodium and water calculated from Eq. 1 for a given cavity size (R_c = 0.003 in.) and cos θ = 1.

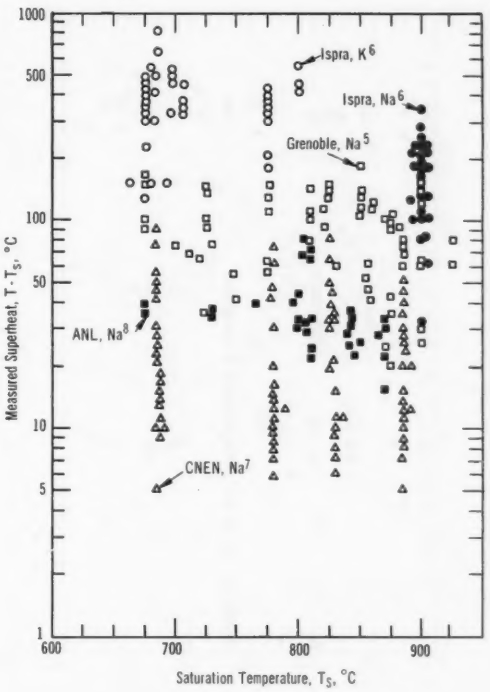

Fig. 2 Recent superheat data, presented at the Aix conference, scatter from 5 to ~800°C.

HEATING METHOD

Investigators who have used direct heating[5,6] (joule heating in the liquid metal itself) report superheats considerably higher than do those who have used indirect heating methods[7,8] (conduction heating through the coolant-channel wall). The latter are more representative of the type of heating that takes place in an actual reactor coolant channel. Considering the direct-heating studies of Ref. 5 and taking into account the resistivities and thermal capacities of steel and sodium, it appears that approximately two-thirds of the thermal energy supplied was dissipated in the sodium and that one-third was stored in the wall. Perhaps direct heating causes homogeneous nucleation (and therefore higher superheats) rather than the wall nucleation that occurs with indirect heating. [And perhaps not; Fig. 3 shows earlier Argonne National Laboratory (ANL) data[9] obtained via direct heating where observed superheat values are relatively small.] It should also be noted that, quite possibly, variables other than the heating method may have caused the differing results, as will be seen later.

The importance of indirect heating is emphasized by the results of experiments in which subcooled nucleate boiling occurred.[10] (Negative bulk superheat could be an important consideration in the analysis of transient expulsion.) Measurements of the actual wall superheat present during these experiments would be most welcome and are being obtained in experiments now in progress.[10]

SURFACE CONDITION

French superheat data[5] spread from about 20 to 200°C, values that they consider compatible with the condition of the surface of the experimental tube used. The importance of surface roughness is indicated in Eq. 1 by the variable R_c, the cavity radius.

Thorough studies of the relation between surfaces and incipient boiling have been published,[11-13] and they clearly show the effect of roughness. With as-received surfaces (commercially smooth), measured potassium superheats have ranged from 500°F at 1500°F (saturation temperature) down to 230°F at 1770°F, but, when eight 0.006-in.-diameter holes were drilled 0.040 in. deep in the same surface, the superheat was reduced[12] about 40-fold. These data agree reasonably well with predictions from an expression similar to Eq. 1 when cos θ is equal to 1. However, it is important to note that Ref. 12 indicates some doubt as to whether the data illustrated in Fig. 3 represent incipient superheat measurements or stable nucleate-boiling superheats. In a more recent paper,[13] it appears that these data represent the behavior of the

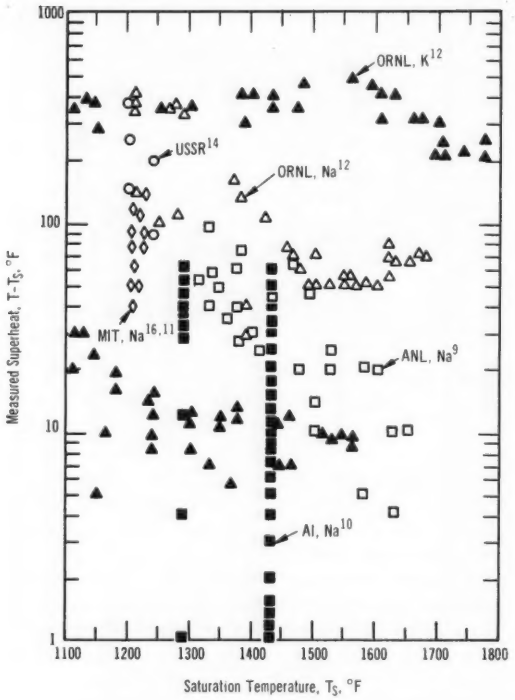

Fig. 3 Variation is characteristic of superheat data; these measurements, older than those of Fig. 2, spread from 1 to 500°F.

superheat existing in the stable boiling mode and that the incipient superheat is more closely related to the saturation temperature than to the cavity size or surface condition.

AGING

In the recent French experiments,[5] the mean value of the superheats reached for a given pressure appears to increase slowly with time. This observation is in agreement with the Ispra data[6] and indicates that the larger nucleation sites are eliminated as boiling goes on, i.e., the larger nucleation sites get washed out and completely wetted with sodium; thus smaller cavities are activated, and—according to Eq. 1—superheat increases. However, earlier experimental data[9] show the opposite trend, as noted in Fig. 4. Aging effects were not reported by the experimenters who used conduction heating techniques.[7,8]

The possible increase in superheat with time appears to be an important consideration in further studies on superheat. During the life of a fast reactor, the coolant could conceivably clean the heating surface to a large degree, leaving smaller and smaller cavities available for nucleation.

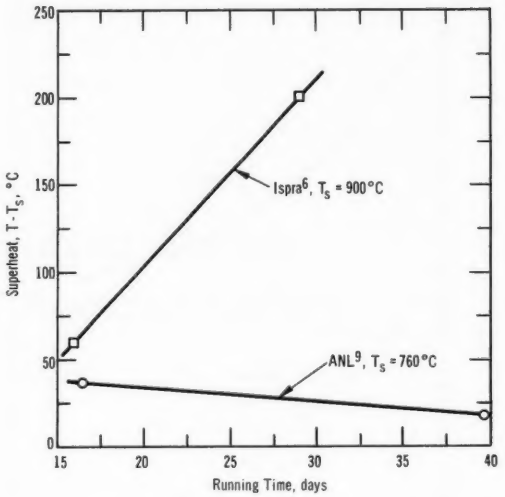

Fig. 4 Superheat values evidently can change as experiments age. In fast reactors the aging effect may be important.

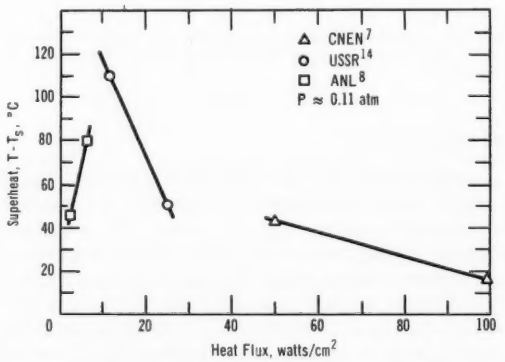

Fig. 5 Heat flux may influence superheat, as indicated by these values for sodium.

HEAT FLUX

Differing results were reported at the Aix conference concerning heat flux. Heating power sometimes appears to be an unimportant parameter,[5,6] but Refs. 7 and 8 indicated a definite heat-flux dependency. Reference 7 reports a decrease in superheat with increasing heat flux—Ref. 8 an increase—as shown in Fig. 5. Also indicated in Fig. 5 are data from a Russian paper[14] published in 1966. Quoting this paper: "The tendency of the nucleate boiling to change to natural convection can be noticed at low heat fluxes. In this case, the value of the liquid superheat sharply increases." In a more recent study,[13] there was no sizable effect of heat

flux upon incipient superheat. Obviously, the possible heat-flux dependency deserves further study.

VELOCITY

In recent Ispra experiments, measured superheats were generally lower under forced or natural circulation than under stagnant conditions, for the same mockup and filling,[6] but no quantitative velocity dependency was reported. However, this velocity relation agrees with earlier data[9] where relatively low superheat values were observed during forced circulation. More recent data[10] show a definite velocity effect (Fig. 6). These data are for bulk superheats and could differ significantly from results with wall superheat.

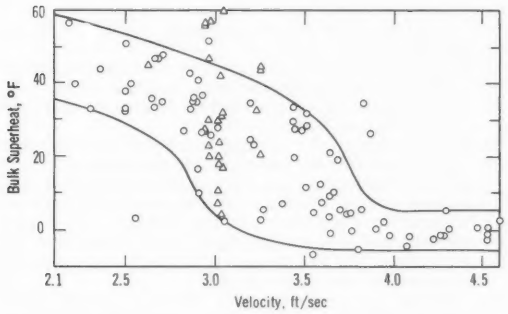

Fig. 6 A velocity effect is apparent in these data[10] for bulk superheat in sodium at 5 psia.

PRESSURE AND PRESSURE–TEMPERATURE HISTORY

Both pressure and pressure–temperature history were shown by ANL to be important variables.[8] The pressure effect—increasing superheat with decreasing pressure according to Eq. 1 and Fig. 1—is also apparent (but to a lesser degree) in the French data.[5] Earlier published data[9,12] also clearly show the expected pressure effect on the incipient superheats (Fig. 7). A simplified analysis[15] appeared to predict the effects of pressure–temperature history reasonably well,[8] and may explain part of the variation found in published data where this variable is not accounted for.

INSTABILITY

The characteristic instability of boiling sodium—intermittent bubbling—was noted only at low heat fluxes and pressures.[7,8] Recent observations are in agreement with previous work,[3,14,16] where analyses have shown that stability increases with increasing heat flux and pressure. Two new papers[13,17] also discuss the instability of alkali-metal boiling. An instability map that indicates pressure levels and heat

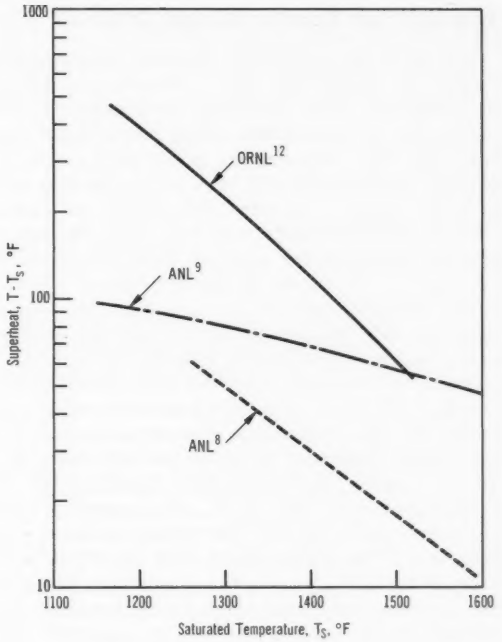

Fig. 7 Incipient-boiling superheats in sodium show a definite pressure (or temperature) effect.

fluxes nucessary to maintain stable boiling for a particular surface is given in Ref. 8.

PURITY AND GAS CONTENT

The extremely high values of superheat reported in the Ispra paper[6] were attributed primarily to a more efficient purification of the liquid metals before testing. System cleanliness undoubtedly is very important. However, in most experiments reported, neither the actual purity of the liquid metal nor the dissolved gas content has been very well known. Better agreement among various laboratories will be achieved when the systems and the fluids in them are better defined.

RADIATION

The effects of nuclear radiation on incipient boiling were discussed in a British paper at the Aix conference.[18] Several different types of radiation were considered: electrons, protons, alpha particles, photons, neutrons, fission fragments, and alpha recoils. It was concluded to be highly unlikely that, at saturation pressures near 1 atm, any nuclear radiation encountered would induce nucleation of vapor bubbles in bulk sodium before boiling would occur at surface cavities. However, a number of assumptions were made in these theoretical calculations; experimental verification seems in order.

Toward Fast Reactor Design Criteria

It is quite obvious that the superheat phenomenon is extremely complex and that it depends on a number of variables. These variables have generally been recognized in nonmetallic boiling research for some time, but their understanding is still quite empirical. Effects often conflict and, as a result, the data show a large range of scatter, with values as high as ~800°C. Because these data have been obtained in systems generally far removed from actual reactor conditions, and because no major progress toward a basic understanding of the superheat problem is apparent, the data are of limited use for reactor-safety design criteria at the present time.

There are reasons to believe that, under realistic reactor conditions, very little superheat will be sustained. At least this appeared to be the consensus of the reactor designers attending the Aix conference. These opinions were generally expressed by the U. K., German, French, U. S., and, especially, USSR designers. Actually, the USSR group appeared very surprised at the great concern about superheat. However, in the USSR fast reactor development program, the presence of large numbers of entrained gas bubbles eliminates the problem of superheat. (But the entrained gas bubbles themselves can pose a severe safety problem.)

THE NEXT STEP—A CAREFUL MOCKUP

Experiments should be designed, built, and tested *now* which closely simulate reactor conditions. Particular emphasis should be on the following:

1. Heating surfaces that simulate coolant channels after long periods of reactor operation.
2. Heat fluxes of $1-2 \times 10^6$ Btu/(hr)(sq ft) from indirect heating techniques (which require extensive development).
3. Coolant of defined (and monitored) composition, i.e., oxide and gas content, entrained bubbles, etc.
4. Geometry and velocity that closely resemble reactor conditions.

Preventing High Superheats. If large superheats exist under typical reactor conditions, methods that can be incorporated in the core to prevent superheating must receive special attention. From Eq. 1, detailed studies of the variables R_c and θ (roughness and wettability) seem appropriate. Ultrasonic energy excitation, vapor traps in the form of metal sleeves mechanically attached to heat-transmitting surfaces, and vapor discharges into the boiler pool have already shown good results.[19,20] However, application of these techniques to prevent overheating may introduce additional safety problems.

Prognosis. Experiments at typical reactor conditions should greatly aid the design of commercial fast breeder reactors. If past performance is any guide, complete understanding of the superheat phenomena will require many years of research—probably too long for establishing safety criteria.

References

All references except 1, 3, 4, and 9 to 17 are papers presented at the International Conference on the Safety of Fast Reactors, Aix-en-Provence, France, September 19–22, 1967, and the proceedings are in preparation.

1. W. G. Meinhardt, Calculating Vapor Growth in a Superheated Liquid Metal Within a Heated Channel, *Trans. Amer. Nucl. Soc.*, 9(2): 566-568 (1966).
2. W. Peppler et al., Sodium Boiling and Fast Reactor Safety.
3. P. J. Marto and W. M. Rohsenow, Nucleate Boiling Instability of Alkali Metals, *J. Heat Transfer*, 88(2): 183 (1966).
4. C. E. Dickerman, Highlights of the Aix Conference on Fast Reactor Safety, *Reactor Fuel-Process Technol.*, 11(1): 1-4 (Winter 1967–1968).
5. B. Le Gonidec et al., Experimental Studies on Sodium Boiling.
6. G. Grass et al., Measurements of the Superheating and Studies About Boiling Phenomena in Liquid Metals.
7. G. C. Pinchera et al., Experimental Boiling Studies Related to Fast Reactor Safety.
8. R. E. Holtz and R. M. Singer, On the Superheating of Sodium and the Generation of Pressure Pulses.
9. J. B. Heineman, Forced-Convection Boiling Sodium Studies at Low Pressure, in Proceedings of the Conference on Application of High-Temperature Instrumentation of Liquid Metal Experiments, September 28–29, 1965, USAEC Report ANL-7100, pp. 189-194, Argonne National Laboratory.
10. Atomics International, AEC Unclassified Programs Quarterly Technical Progress Report, January–March 1967, USAEC Report NAA-SR-12395, May 31, 1967.
11. P. J. Marto and W. M. Rohsenow, Effects of Surface Conditions on Nucleate Pool Boiling of Sodium, *J. Heat Transfer*, 88(2): 196 (1966).
12. J. A. Edwards and H. W. Hoffman, Superheat with Boiling Alkali Metals, in Proceedings of the Conference on Application of High-Temperature Instrumentation to Liquid-Metal Experiments, September 28–29, 1965, USAEC Report ANL-7100, pp. 515-534, Argonne National Laboratory.
13. J. A. Edwards and H. W. Hoffman, Incipient and Stable Boiling Superheat for Potassium Boiling on a Surface Containing Reentrant Cavities, JSME Semi-International Symposium, Tokyo, Japan, September 4–8, 1967, in preparation.
14. B. S. Petukhov, S. A. Kovaler, and V. M. Zhukov, Study of Sodium Boiling Heat Transfer, in *Proceedings of the Third International Heat Transfer Conference, Chicago, Illinois*, Vol. V, p. 80, August 1966.
15. R. E. Holtz, The Effect of the Pressure–Temperature History upon Incipient-Boiling Superheats, USAEC Report ANL-7184, Argonne National Laboratory, June 1966.
16. I. Shai, The Mechanism of Nucleate Pool Boiling Heat Transfer to Sodium and the Criterion for Stable Boiling, USAEC Report TID-23790 (DSR-76303-45), Massachusetts Institute of Technology, January 1967.
17. G. I. Bobrovich, B. P. Auksentyuk, and N. N. Mamontova, On the Mechanism of Boiling of Liquid Metals, JSME Semi-International Symposium, Tokyo, Japan, September 4–8, 1967, in preparation.
18. K. T. Claxton, The Influence of Radiation on the Inception of Boiling in Liquid Sodium.
19. M. M. Yarosh, Experiment Employing Ultrasonic Energy To Promote Boiling in Liquid Metals.
20. R. E. MacPherson, Techniques for Stabilizing Liquid Metal Pool Boiling.

Letters to the Editor

Realistic Analysis of Fuel Elements

In the article entitled, "Realistic Data Are Needed for Mechanical Analysis of Reactor Fuel Elements," *Reactor and Fuel-Processing Technology*, 11(1): 13-16 (Winter 1967–1968), by Richard A. Valentin, the assumption of incompressibility of the fuel is a severe limitation: it may be applicable to fuels of a density approximating the true theoretical density of the substance. Low-density fuels (e.g., approximately 80% TD oxides) may behave quite compressibly. Furthermore, the assumption of full radial symmetry of heat flow and of stress ignores the cracking of ceramic fuels. Such cracks not only disturb the radial temperature and stress profiles, but also generate local (microscopic and macroscopic) hot spots within the fuel matrix which cause local plasticity effects permitting fuel dilation (into voids) both by flow and by sublimation (in the case of oxides).

A further limitation on the applicability of the method arises from the assumption of constant thermal conductivity of fuel material and from neglect of cladding fuel gap effects which may govern the mechanical interaction between fuel and clad over a major fraction of the burnup cycle.

In summary, it may be argued that the methods proposed are applicable to metallic fuels; however, their applicability to oxide or ceramic fuels may be limited.

Louis Bernath
Atomics International

Author's Reply

I agree with Dr. Bernath's observation that the methods discussed may have limited applicability for oxide and ceramic fuels. An assumption pervading the entire article, which was unfortunately never stated explicitly, required that a strictly continuum approach to modeling the mechanical behavior of the fuel be valid for the entire fuel-element lifetime. While this is perhaps reasonable for metallic fuels, it does not follow that concepts such as stress, strain rate, etc., have any meaning in explaining the behavior of a material known to crack or sublime during normal operation. Requiring radial symmetry, constant thermal conductivity, incompressibility, etc., seriously limits the applicability of a fuel-element model; however, if added complexity can be tolerated, there is no *essential* restriction inherent in these assumptions and one or all may be relaxed as necessary. Questions relating to the plausibility of a continuum model are of much more basic nature and whether ceramic and oxide fuels may be treated as such methods should perhaps be viewed as an open question.

Richard A. Valentin
Argonne National Laboratory

Letter to the Editor

Shippingport Hot-Channel Factors

On reading my article, "The Evolution of Hot-Channel Factors for Shippingport Reactor Cores" [Vol. 10, No. 4], I find that I am embarrassed to report two errors, as follows:

1. In Fig. 2, p. 262, the plates contain highly enriched uranium–zirconium alloy—not uranium dioxide.
2. In Fig. 5, p. 264, the seed wafer dimensions are 1.5 × 0.25 × 0.036 in., not 0.1 in.

Richard Atherton
Westinghouse Electric Corporation

GLOSSARY OF NUCLEAR TERMS*

The United States of America Standards Institute has published *USA Standard Glossary of Terms in Nuclear Science and Technology*, a revision of an early glossary published in 1957 by the National Research Council and the American Society of Mechanical Engineers.

The revision, which was sponsored by the Atomic Industrial Forum, Inc., includes terms distinctive to the nuclear field, terms used in the nuclear field with meanings different from their common usage or from their meanings in other fields, and terms used in the same way in related fields but which are important enough to warrant inclusion also in the nuclear glossary. Terms in the glossary whose definitions are substantially the same as those accepted or being considered by the International Organization for Standardization are so indicated.

The terminology committee that revised the glossary included representatives from the American Chemical Society, the American Institute of Chemical Engineers, the American Institute of Mining, Metallurgical, and Petroleum Engineers, the American Nuclear Society, the American Society of Mechanical Engineers, the American Society for Testing and Materials, the Health Physics Society, the Institute of Electrical and Electronics Engineers, and the Institute of Nuclear Materials Management.

**USA Standard Glossary of Terms in Nuclear Science and Technology*, USAS N1.1-1967 (Revision of N1.1-1957), 111 pp., published by United States of America Standards Institute, 10 East 40th Street, New York, N. Y. 10016, $7.95.

Research and Development on Aqueous Processing

By C. E. Stevenson and D. M. Paige

Factors affecting the acid dissolution of PuO_2, ThO_2, and of UO_2–Mo are discussed, along with the preparation of graphite-matrix fuels by grinding and leaching. A ZrO_2–UO_2 compact is dissolved in fused ammonium bifluoride in preparation for aqueous dissolution, and a process for decladding Zircaloy-jacketed UO_2-blanket material from the Shippingport Pressurized Water Reactor (PWR) with NH_4F–NH_4NO_3 solution is described.

A flow sheet using high concentrations of acid is proposed for extraction of solutions prepared from graphite fuels to overcome emulsion formation.

Dissolution of Plutonium Oxide

The conversion of plutonium metal to oxide may be effected most simply by burning in air. This method is often used as a step in a recovery operation for metallic scrap, but such oxide may also be used in the preparation of nuclear fuels. Some time ago, a report[1] on work at the Rocky Flats plant of Dow Chemical Co. indicated that HBr dissolved such PuO_2 more rapidly than did HNO_3 or HCl. Recently, Molen, from the same facility, reported the results of work on the factors controlling dissolution of such PuO_2 in $12M$ HNO_3–$0.1M$ CaF_2 and in $12M$ HCl–$0.5M$ $SnCl_2$ at refluxing temperatures.[2]

The oxide resulting from burning the metal without temperature control contains 82 to 90% plutonium and has a specific surface area of 0.4 to 6.7 m^2/g and mean crystallite sizes of 210 to 450 A. In both acid systems, HCl and HNO_3, a small increase in the mean crystallite sizes (<100 A), or a small decrease (<0.8 m^2/g) in the specific surface area, did not significantly change the rate at which the PuO_2 dissolved; however, larger changes in either the crystallite sizes or the specific surface area did affect the rates of dissolution. Such effects were minimal above a specific surface area of 4.0 m^2/g or a mean crystallite size of 480 A. Rates of dissolution were also increased by increasing the solid-to-liquid ratio, i.e., from 150 to 250 g of PuO_2 per liter of acid, although in the HCl system, for material of a given specific surface area or crystallite size, the percentage of the PuO_2 present which was dissolved was not increased by increasing the solid-to-liquid ratio.

The use of the HCl solvent and burning to produce PuO_2 particles with surface area of >3.5 m^2/g and mean crystallite size of <250 A is recommended to achieve a maximum dissolution rate.

Dissolution of Thorium Oxide

The dissolution of sol-gel ThO_2 in strong HNO_3 and the use of $0.025M$ F^- and $0.1M$ $Al(NO_3)_3$ were discussed recently in reporting work of the Savannah River Laboratory.[3] Phillips and Huber of the Pacific Northwest Laboratory have since presented the results of a factorial experiment aimed at describing the effects of concentrations of HNO_3, $Th(NO_3)_4$, $Al(NO_3)_3$, and HF, and their interactions, on the rate of dissolution of ThO_2 under boiling conditions.[4] Material from a single lot of Mallinckrodt sol-gel ThO_2 (8 to 10 mesh) was reacted for 2 to 10 min with 25 ml of the boiling dissolution reagent, and unreacted ThO_2 was removed, washed, and weighed after drying. From the results of duplicate dissolution-rate measurements for 25 sets of concentrations, in which the ranges of variables were HNO_3 8 to $12M$, $Th(NO_3)_4$ 0.0 to $1.0M$, $Al(NO_3)_3$ 0.0 to $0.7M$, and HF 0.01 to $0.07M$, least-squares estimates of the coefficients were developed for the following polynomial expression:

$$\log R = \beta_0 + \sum_{i=1}^{4} \beta_i X_i + \sum_{i=1}^{4} \sum_{j=1}^{4} \beta_{ij} X_i X_j$$

where R is the dissolution rate [mg/(cm^2)(min)], and X_1, X_2, X_3, and X_4 are the HNO_3, $Th(NO_3)_4$, $Al(NO_3)_3$,

and HF concentrations (M), respectively. The coefficients are as follows:

$\beta_0 = -1.68235$	$\beta_{11} = -0.00569767$	$\beta_{13} = -0.116316$
$\beta_1 = 0.226343$	$\beta_{22} = 0.150163$	$\beta_{14} = -0.945428$
$\beta_2 = -1.12611$	$\beta_{33} = -0.0587321$	$\beta_{23} = -0.171565$
$\beta_3 = -0.241396$	$\beta_{44} = -323.915$	$\beta_{24} = 1.99954$
$\beta_4 = 44.2611$	$\beta_{12} = 0.0751640$	$\beta_{34} = 17.3178$

These data were used to develop average effect curves for each of the variables. These curves indicate a twofold linear increase in dissolution rate with increase in HNO_3 concentration over the range studied, an almost linear 25% decrease in dissolution rate with increase in $Th(NO_3)_4$ concentration, an almost linear twofold decrease in dissolution rate with increase in $Al(NO_3)_3$ concentration, and a fivefold and leveled-off increase in dissolution rate with increase in HF concentration.

Because significant interactions were found between HF and $Al(NO_3)_3$, HNO_3 and $Al(NO_3)_3$, and HNO_3 and $Th(NO_3)_4$ concentrations, the average individual effects do not adequately summarize the reagent composition effects, and contour curves for constant dissolution rate were developed for two-variable plots. Such a curve is shown for the effects of $Th(NO_3)_4$ and HF concentrations in $13M$ HNO_3 in Fig. 1;

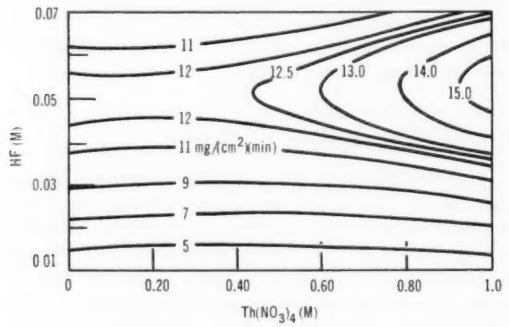

Fig. 1 ThO_2 dissolution rate in $13M$ HNO_3–$0M$ $Al(NO_3)_3$ containing varying concentrations of $Th(NO_3)_4$ and HF.

contour curves for combinations of varying concentrations of $Al(NO_3)_3$ and HF with $13M$ HNO_3–$0M$ $Th(NO_3)_4$, $11M$ HNO_3–$0.5M$ $Th(NO_3)_4$, and $9M$ HNO_3–$1.0M$ $Th(NO_3)_4$ are also given in the article.

The contour plots indicate that, in $13M$ HNO_3 in the absence of $Al(NO_3)_3$, the maximum dissolution rate occurs in $0.052M$ HF, and that, in 11 and $9M$ HNO_3, the pattern remains the same. The presence of $Al(NO_3)_3$ markedly reduces the dissolution rate and tends to increase the optimum HF concentration, in line with its known tendency to complex fluoride.

In the presence of $Th(NO_3)_4$, there is a similar optimum HF concentration. However, the effects of varying $Th(NO_3)_4$ concentration are more complex. In $13M$ and $11M$ HNO_3 with less than $0.02M$ HF, the dissolution rate is almost independent of the $Th(NO_3)_4$ concentration, and above $0.02M$ HF the rate increases with increasing $Th(NO_3)_4$ concentration. In $9M$ HNO_3, on the contrary, the rate decreases with increasing $Th(NO_3)_4$ concentration.

To maximize dissolution rate, the HNO_3 concentration should be as high as possible, both because of the direct effect of HNO_3 concentration on dissolution rate, and because in $11M$ and higher HNO_3 concentrations, increasing $Th(NO_3)_4$ concentration has little adverse effect on dissolution rate.

Dissolution of UO_2 Pellets Containing Molybdenum

The use of 10 to 20% molybdenum as a structural and heat-transfer medium in the preparation of UO_2-pellet fuels has been proposed. Bähr, in a recent report from Karlsruhe, has described studies of the dissolution of such fuel compositions in 3 to $14M$ HNO_3, and in HNO_3 containing $Fe(NO_3)_3$ as a complex former for molybdenum.[5] The use of ferric iron for this purpose has been previously discussed in connection with the dissolution of U–3% Mo alloy fuels.[6] In HNO_3 at 100°C, UO_2 compositions containing 10, 15, or 20% molybdenum dissolved about 10 times as fast as pellets containing UO_2 alone, and in all cases dissolution was speeded by increased acidity. For example, the rate of attack on UO_2 increased from about 0.2 mg/(cm^2)(min) in $3M$ HNO_3 to 10 mg/(cm^2)(min) in $14M$ acid; the corresponding rate increase for the 10 to 20% molybdenum compositions was from 1.1 to 1.4 mg/(cm^2)(min) in $3M$ acid to 100 to 200 mg/(cm^2)(min) in $14M$ acid. The molybdenum was only partially dissolved (10 to 30% in $3M$ HNO_3 to 2 to 5% in $10M$ HNO_3); the bulk of the molybdenum was precipitated as molybdic acid, which required washing to obtain complete dissolution of the uranium. The concentrations of molybdenum in solution were 0.01 to $0.04M$. Rates of dissolution of UO_2 were increased twofold to threefold by the application of ultrasonic energy with a frequency of 20 kc and an intensity of 55 to 60 watts/cm^2. The presence of $1M$ $Fe(NO_3)_3$ also markedly increased the rates of dissolution of UO_2. Fission products (Cs, Ru, Ce, and Zr) were significantly sorbed by the precipitated MoO_3.

Treatment of Coated-Particle Fuels

It has been proposed to prepare graphite-matrix fuels, such as High Temperature Gas-Cooled Reactor (HTGR) fuel elements composed of pyrolytic carbon-coated $(Th,U)C_2$ or $(Th,U)O_2$ particles dispersed in a graphite compact, for processing by mechanical or chemical disintegration of the coating and matrix followed by dissolution of the particles in HNO_3. In

studies of such carbide fuels at Oak Ridge National Laboratory (ORNL), it was recently reported[7] that it was difficult to achieve adequate uranium recovery. Goode and Flanary[8] now report that greater success is achieved with irradiated coated oxide (and carbide) particles that are not dispersed in graphite. The material treated consisted of sol-gel ThO_2, $(Th,U)O_2$, and $(Th,U)C_2$ particles, with duplex coatings of pyrolytic carbon, which had been irradiated as loose particles (i.e., not in a graphite matrix) to levels of 15,000 to 17,500 Mwd/metric ton, and allowed to cool 10 to 19 months.

For recovery of the nuclear materials, the particles were ground to −100 mesh and leached three times with boiling $13M$ $HNO_3-0.05M$ $HF-0.1M$ $Al(NO_3)_3$, followed by washing residue with water. In four tests, recovery of uranium was 99.6 to 99.9% and that of thorium was >99.9%. The residue from the oxide fuels contained 2 to 14% of the gamma activity, whereas that from a single test of carbide fuel contained ~60% of the gamma activity. Although the high Th−U recovery was encouraging, the authors questioned the feasibility of treating carbide fuels in this manner because of the quantity of fission products retained in the leached carbon residue.

Dissolution of Zircaloy-Clad ZrO_2–UO_2 Fuel

A three-step process for the dissolution of a Shippingport PWR Core-2 Seed-1, composed of pyrolytic carbon-coated ZrO_2-UO_2 wafers clad in Zircaloy-4, was recently described.[9] This process was developed at the Idaho Chemical Processing Plant (ICPP) and consists in removal of cladding with $5M$ HF, disintegration of pyrolytic carbon and dissolution of ZrO_2 in $20M$ HF, and dissolution of UO_2 in $0.1M$ chromic acid. An alternative procedure[10] has been developed by ICPP workers in which decladding is conducted in $10M$ rather than $5M$ HF, and the ZrO_2-UO_2 wafer is totally dissolved in fused NH_4HF_2. The fusion product is dissolved in a dilute $Al(NO_3)_3-CrO_3$ solution to prepare a feed for solvent extraction, to which the decladding solution may also be added, if it contains sufficient uranium to warrant recovery. The flow sheet for this process is shown in Fig. 2.

The feasibility of the process is based on the high concentration of fluoride ($42M$) available in fused NH_4HF_2 and on the elevated temperature (>190°C) that may be used with this dissolution medium. The cladding could also be attacked by this medium, but the zirconium solubility is quite limited, and a thick slurry would be formed; furthermore, the resulting fluoride concentration, after conversion to an aqueous medium, would not permit uranium recovery by solvent extraction in stainless-steel equipment. At present, the authors conclude that the two-step aqueous–fused-salt process does not offer significant advantages over the three-step aqueous process.

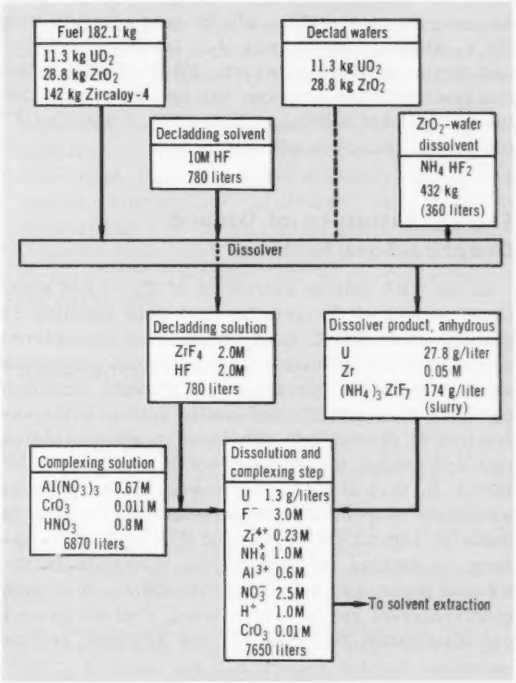

Fig. 2 Two-step aqueous–fused-salt dissolution of advanced PWR fuel.

Decladding and Dissolution of Shippingport Blanket Elements

The initial blanket assemblies used in the Shippingport PWR consisted of UO_2 pellets contained in 0.411-in.-diameter by 10.2-in.-long Zircaloy tubes, 120 of which are assembled between 5.2-in.-square tube sheets. A dissolution flow sheet has been developed for use in processing 13 tons of this material in the Hanford Redox plant.[11] The flow sheet is based on the dissolution of cladding in $5.5M$ $NH_4F-0.5M$ NH_4NO_3 and the dissolution of UO_2 in HNO_3. Because of equipment limitations, and to secure its most effective use, a seven-stage process is planned. Since laboratory studies have shown that multiple exposures to NH_4F are necessary to penetrate the heavily oxidized Zircaloy cladding, the annular dissolver will be loaded with about 4 tons of blanket assemblies, and treated twice with 1100 gal of the Zircaloy-dissolving reagent. It is anticipated that the cladding will be penetrated sufficiently by the two attacks to permit HNO_3 dissolution of the UO_2. Consequently the dissolver will next be flushed with 1100 gal of water, and then $Al(NO_3)_3$ (to complex residual fluoride), H_2O, and $12.2M$ HNO_3 will be added in increments in sufficient volume to dissolve the UO_2. So that complete dissolution of all solid material in the dissolver can

be assured, the residue will be treated again with $NH_4F-NH_4NO_3$, flushed with H_2O, treated with HNO_3, and again treated twice with $NH_4F-NH_4NO_3$. The combined uranium solutions will be adjusted to 1.5*M* $UO_2(NO_3)_2$, 0.4*M* $Al(NO_3)_3$, 0.25*M* HNO_3, 0.08*M* $Cr_2O_7^{2-}$ for solvent extraction with hexone.

Solvent Extraction of Ground Graphite-Base Fuels

In the TBP solvent extraction of Th–U fuel solutions, prepared by grinding and acid leaching of graphite-base HTGR fuels, difficulties encountered are due to the formation of troublesome emulsions arising from the presence of graphite oxidation products (i.e., mellitic and oxalic acids), if the extraction is carried out with aqueous-phase acidities that are normal for Purex-process conditions (~ 3*N* HNO_3). In work at ORNL,[12] however, the formation of emulsions is avoided if the aqueous-phase acidity is made as high as 4.6*N* HNO_3, and it is then not necessary to destroy the emulsifying materials in the aqueous phase, i.e., by boiling with $KMnO_4$. In a batch countercurrent run at tracer level, a gross gamma decontamination factor of 400 was achieved, and the uranium loss was <0.01%. Although the thorium loss was ~ 5%, the author indicated that this could readily be reduced with additional extraction stages. Hot-cell tests of the high-acid process, with feeds prepared from both burn–leach and grind–leach products of irradiated HTGR fuels, were also successful in demonstrating adequate uranium and thorium recovery and acceptable one-cycle decontamination.

At ORNL, preliminary work has also been done on the direct leaching of uranium and thorium by 30% TBP in dodecane from crushed graphite fuel that had been wetted with 13*M* HNO_3. The majority of the thorium and uranium present in the fuel was transferred to the solvent phase, but recovery yields, and the fate of the fission products, were not established.

Plant and Equipment Design and Operation

THE GERMAN REPROCESSING PLANT WAK

A new fuel-reprocessing plant (WAK) is being constructed at the Karlsruhe Nuclear Research Center by several German contractors. A recent report[13] (in German) gives a detailed description of this facility.

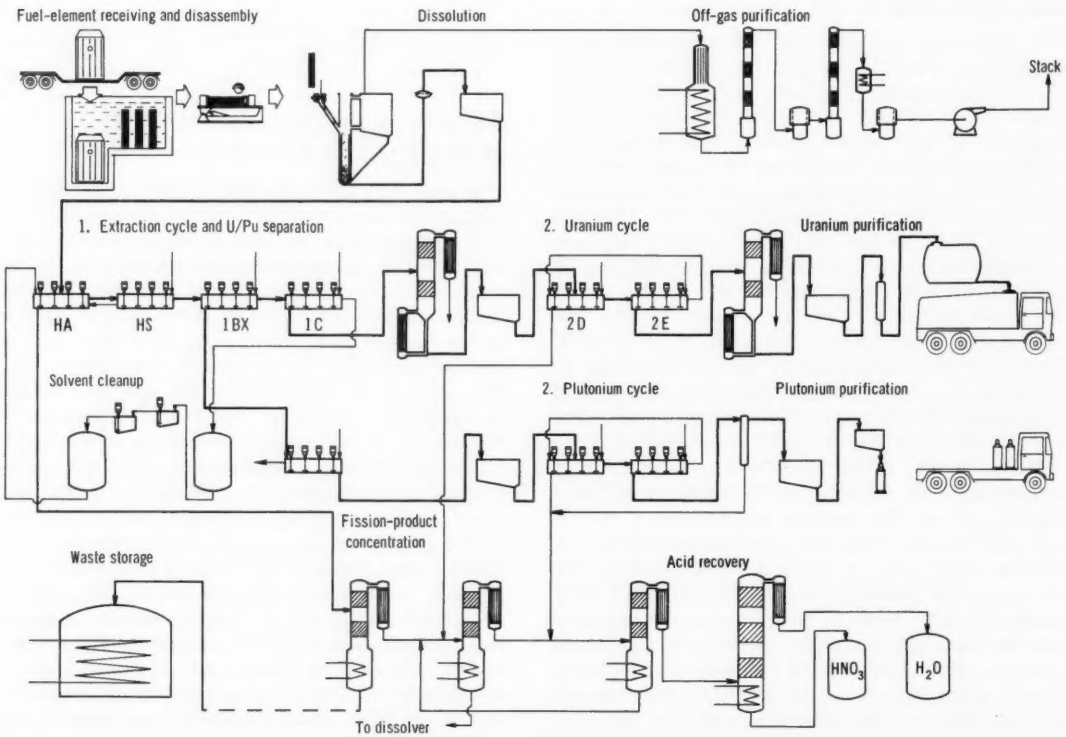

Fig. 3 Process flow sheet for WAK.

The facility will process 40 metric tons of slightly enriched UO_2 per year (200 operating days). It will also provide German industry with experience in planning, construction, and operation of a reprocessing plant. The well-proved solvent extraction process was chosen for the fuel reprocessing. The WAK plant will be used to further develop aqueous processing and will be adaptable to new fuel compositions. Economics and capacity were given only minor consideration.

The process-equipment flow sheet is shown in Fig. 3. Spent fuel elements are accepted at the entrance area, cleaned and, after having been checked for leaking fuel elements, transferred to a storage pond.

A chop–leach[14] head-end process is provided. The fuel assemblies are first dismantled into their individual rods and then cut into 5-cm sections. The shear is directly coupled to the dissolver. Nitric acid (7.5M) is used to dissolve the UO_2 out of the stainless-steel or Zircaloy cans.

Mixer–settlers are used in the first-cycle fissile-material extraction with 30% TBP in n-dodecane. The aqueous waste containing 99.9% of the fission products is concentrated and sent to waste storage. After two washes the separation of uranium from plutonium is effected by reduction with U(IV) nitrate.

Uranium, as well as plutonium, is then stripped of residual fission products in a second extraction cycle. For final purification a silica-gel column is used for uranium and an anion-exchange column for plutonium. Except for these two purification columns, the extractions and reextractions are carried out in mixer–settlers.

The authors state that this plant should produce uranyl nitrate with a concentration of 450 g/liter and a specific activity of 0.6 μc per gram of uranium. The concentration of plutonium nitrate will be 50 g/liter with a specific activity of 25 μc per gram of plutonium.

The process is performed in 10 single thick-walled concrete cells. Only the cell for the mechanical head-end step is equipped with lead-glass windows and facilities for remote handling. In the other cells the process is operated by remote control from a central control room. Operation of the flow sheet is controlled, on the one hand, by remotely actuated sampling of liquids and their analysis and, on the other hand, through process variables such as level, density, temperature, pressured, etc., which are measured by well-known control instrumentation.

Construction work on the facility was started in January 1967. Test runs will be started probably by the end of 1969.

References

1. *Reactor Fuel Process.*, 8(1): 11 (Winter 1964–1965).
2. G. F. Molen, Dissolution of Plutonium Oxide, USAEC Report RFP-922, Dow Chemical Co., Aug. 29, 1967.
3. *Power Reactor Technol. Reactor Fuel Process.*, 10(2): 154 (Spring 1967).
4. J. F. Phillips, Jr., and H. D. Huber, Dissolution of Thorium Oxide, USAEC Report BNWL-SA-1154, Pacific Northwest Laboratory, Apr. 1, 1967.
5. W. Bähr, Investigation on Dissolution of UO_2–Mo Fuel Cores in Nitric Acid, German Report KFK-573, February 1967.
6. *Reactor Fuel Process.*, 5(1): 9 (Winter 1961–1962).
7. *Reactor Fuel-Process. Technol.*, 10(4): 305 (Fall 1967).
8. J. H. Goode and J. R. Flanary, Hot-Cell Evaluation of the Grind–Leach Process with Irradiated Pyrolytic Carbon-Coated Sol-Gel Thoria–Urania Particles, USAEC Report ORNL-TM-1880, Oak Ridge National Laboratory, May 26, 1967.
9. *Reactor Fuel-Process. Technol.*, 10(3): 243 (Summer 1967).
10. J. R. Bower (Ed.), Chemical Technology Branch Annual Report, Fiscal Year 1967, USAEC Report IN-1087, Idaho Nuclear Corporation, October 1967.
11. D. F. Davis, Proposed Redox Dissolution and Head-End Flow Sheets for PWR-1 (Shippingport) Blanket Fuel Elements, USAEC Report ISO-595, Isochem Inc., November 1966.
12. Oak Ridge National Laboratory, Chemical Technology Division Annual Progress Report for Period Ending May 31, 1967, USAEC Report ORNL-4145, October 1967.
13. Von H. Tebbert, W. Schüller, and P. Zühlke, The German Reprocessing Plant WAK, (in German) *Atomwirtschaft*, 12: 194-200 (April 1967).
14. *Reactor Fuel Process.*, 9(2): 78 (Spring 1966).

Compact Pyrochemical Processes

By W. E. Miller and R. K. Steunenberg

Pyrochemical processes may be used to process reactor fuels or to purify or produce materials of interest to the nuclear industry. The processing of irradiated reactor fuels separates fissile, fertile, and fission-product elements from each other. In most cases liquid metals and/or salts are used as process solvents. Separations are effected at high temperatures by volatilization, precipitation, liquid metal–salt extraction, and electrolysis. Much of the development work is directed toward reprocessing fuels from reactors whose operating economy would benefit from on-site plants that would process the fuel with little or no cooling time. Homogeneous molten-salt reactors and fast reactors are examples of these reactor types.

Salt-Transport Process for Fast Breeder Reactor Fuels

Present work at Argonne National Laboratory (ANL) is concerned with the investigation of a number of pyrochemical processing steps, some of which have been combined into a conceptual process for treating oxide fuel from a fast breeder reactor. The flow sheet for this process was presented in an earlier issue of *Power Reactor Technology and Reactor Fuel Processing*.[1] In the conceptual process, PuO_2–UO_2 irradiated fuel elements are first declad with liquid zinc at 750 to 800°C. The declad oxide is then reduced by a liquid Cu–Mg alloy in the presence of a molten-salt flux. The salt waste from the reduction contains the oxygen as MgO and the rare-earth and alkaline-earth fission products. The Cu–Mg metal phase from the reduction contains plutonium, uranium, and noble-metal fission products. A salt-transport separation removes the plutonium from the Cu–Mg phase and deposits it into a Zn–Mg phase. The details of salt-transport separations processes were discussed in an earlier issue of *Reactor and Fuel-Processing Technology*.[2] The Zn–Mg phase is retorted to recover the plutonium. To recover the uranium, which is present as a precipitate in the Cu–Mg alloy, workers decant the supernatant liquid and wash the precipitate with magnesium, a procedure that removes noble-element fission products and copper from the uranium. Residual magnesium is removed from the uranium by retorting.

The work at ANL is divided into a number of interrelated studies. In addition to process demonstrations, investigations are conducted on process development, process chemistry, corrosion, process kinetics, and equipment design.

DEMONSTRATION OF PROCESSING STEPS

A recent flow-sheet demonstration experiment has been reported[3] in which an oxide fuel was simulated by a charge consisting of 199 g of plutonium as PuO_2, 458 g of UO_2, and 24 inactive fission-product elements having a total weight of 52.4 g. The equipment used in this demonstration run was described previously.[4]

A reduction step was performed in which 99% of the uranium and 99.9% of the plutonium in the oxide charge were reduced in 4 hr at 800°C. The salt was 47.5 mole % $MgCl_2$–47.5 mole % $CaCl_2$–5 mole % CaF_2, and the metal phase was Cu–33 wt.% Mg. The metal alloy from the reduction step was then contacted with fresh reduction salt in two scrub steps to provide further rare-earth removal from the plutonium. Each scrub step was conducted at 800°C for 2.5 hr. The composition of the waste-reduction salt was altered by the addition of lithium and calcium metals to lower the plutonium distribution coefficient (wt.% Pu in salt/wt.% Pu in metal) in subsequent plutonium strip steps. In these strip steps, the waste-reduction salt was contacted with a Cu–36 wt.% Mg alloy for 5 hr at 700°C to remove residual plutonium from the salt.

Two plutonium salt-transport steps were carried out in the experiment. In the first, 99.3% of the plutonium charged was transported from the Cu–33 wt.% Mg reduction alloy to a Zn–2 wt.% Mg acceptor alloy using a 50 mole % $MgCl_2$–30 mole % NaCl–20 mole % KCl transport salt at 600°C. Fourteen cycles

were conducted. However, more than 90 at.% of the plutonium was transported in the first five cycles, and this fact indicates that the technique is quite effective.

The second salt-transport step was conducted to separate the plutonium in the Zn–2 wt.% Mg acceptor alloy of the first salt-transport step from about 1 g of copper that was carried over into the alloy. Before this acceptor alloy can serve as a donor alloy, it is necessary to reduce the concentration of magnesium in the alloy. This was done by treating the alloy with $ZnCl_2$ at 600°C, whereby the magnesium and plutonium were oxidized to $MgCl_2$ and $PuCl_3$. The plutonium was subsequently salt transported to a Zn–4 wt.% Mg acceptor alloy in six cycles at 600°C using the transport salt from the first salt-transport step. The resulting Zn–Mg–Pu acceptor alloy contained only the amount of copper that was contributed by the reagents used to make up the alloy prior to the salt transport of the plutonium.

The Cu–Mg alloy from the donor vessel of the first salt-transport step was poured away from the precipitated uranium. The precipitate was then washed three times at 700 to 750°C with 1.0, 1.5, and 1.0 kg of magnesium to remove residual copper and fission products.

In the run described above, fission-product removals exceeded 99% for Ba, Cs, Mo, Pd, Rb, Rh, Ru, and Sm. Removals of several other fission-product elements (Ag, Ce, Eu, La, Nd, Pr, and Zr) ranged from 96 to 98.5%. The amounts of the remaining fission-product elements in the product (Cd, Gd, In, Nb, Sb, Se, Sn, Sr, and Y) were below the analytical detection limits. It is believed that the removals of the major rare-earth elements can be improved to ~99.9% through modification of operating procedures.

PROCESS DEVELOPMENT

The first step in the pyrochemical flow sheet is the decladding of stainless-steel-clad ceramic reactor fuel. The dissolution of the cladding (and possibly of some of the stainless-steel structural material of the fuel subassembly) in molten zinc appears to be a promising decladding method. Because it might be desirable to reclaim the solvent zinc for reuse, simple methods of separating iron, chromium, and nickel from zinc are being investigated.

A previous experiment had shown that the levels of iron, chromium, and nickel in the solvent zinc could be reduced significantly by adding aluminum to form insoluble intermetallic compounds with the impurities.[2] However, the residual aluminum concentration in the zinc was somewhat high (0.9 wt.%) and could cause reduction of PuO_2 in a subsequent decladding step with a consequent loss of plutonium to the zinc solution. Therefore an experiment[5] was performed in which 44 g of aluminum, the stoichiometric amount, was added to a zinc solution containing 37 g of iron (6.4 wt.% iron) to form Fe_2Al_5. (Chromium and nickel were omitted in this experiment because they are present in relatively small quantities in stainless steel and also because the previous experiment had shown that these elements are readily removed by aluminum addition.) After all the aluminum had been added to the Zn–Fe solution at 800°C, the temperature was lowered to 500°C and a filtered sample of the zinc phase was taken. Analysis of this sample showed that only 0.048 wt.% iron and 0.18 wt.% aluminum were present. These results indicate that, by adding the proper amount of aluminum, iron can be removed effectively from zinc through the formation of an aluminum intermetallic compound, without leaving an undesirably large amount of aluminum in the zinc.

PROCESS CHEMISTRY

A system consisting of a molten $CaCl_2$–20 mole % CaF_2 salt mixture and a liquid Cu–33 wt.% Mg alloy containing calcium as the reductant is being considered as an alternative system for use in the oxide-reduction step of the process. Because the salt in this system becomes a waste stream, it is desirable to decrease its plutonium content to the lowest possible level. Therefore measurements are being made of the distribution coefficients (wt.% in salt/wt.% in metal) of plutonium and selected fission-product elements between the salt mixture and the metal alloy. Measurements of the plutonium distribution coefficient were made at 700 and 800°C with calcium concentrations in the alloy ranging from 0.1 to 6 wt.%. The results are presented along with previous data on the distribution of cerium in the same system.[6] The distribution coefficient of plutonium at 700°C ranged from 2.4×10^{-4} to 2.6×10^{-5} for nominal calcium concentrations in the alloy of from 0.1 to 6 wt.%. At 800°C the distribution coefficient ranged from 7.6×10^{-5} to 2.9×10^{-5} for the same respective calcium concentrations. (Subsequent analytical data show that the actual range of calcium concentrations in these experiments[15] was from 0.13 to 3.5 wt.%.) These values indicate that the loss of plutonium by distribution to the reduction salt under the above conditions would be less than 0.01%. This salt–alloy system appears to be very promising for the reduction step of the process.

The distribution behavior of barium in the $CaCl_2$–CaF_2/Cu–Mg–Ca reduction system was determined at temperatures between 775 and 850°C. The distribution coefficient of barium in this system is approximately 700, with no apparent variation over the temperature range. As with rubidium, essentially all the barium appears in the salt phase of the system and would be removed with the waste salt.

The solubility of neptunium in liquid cadmium is being measured to determine possible methods for

the recovery of neptunium from fast breeder reactor fuels by pyrochemical processes.[6,7] The solubility of neptunium in liquid cadmium, over the temperature range 330 to 450°C, may be represented by the equation: log (at.% Np) = $6.054 - 4384/T(°K)$. The heat of solution, –20.1 kcal/mole, is intermediate between the heats of solution of uranium and plutonium, which are –20.8 and –19.6 kcal/mole, respectively. The solubility values for neptunium in cadmium and the heat of solution suggest that the solid phase in equilibrium with this solution is $NpCd_{11}$. The nature of the solid phase is being investigated further by X-ray diffraction measurements.

CORROSION OF MATERIALS

In many of the steps of the salt-transport process, zinc-rich alloys in combination with salts are employed as solvents. Container materials such as tungsten, tungsten alloys, and certain ceramics such as alumina are not corroded by these solvents. These materials, however, are difficult to fabricate; therefore more easily fabricated materials are being sought.

Two ductile rhenium alloys, W–25 wt.% Re and Mo–50 wt. % Re, were tested as agitator blades in a system consisting of pure zinc and a $MgCl_2$–30 mole % NaCl–20 mole % KCl salt mixture at 800°C.[5] In this method of testing, four samples of the material to be exposed are placed on an agitator shaft so that one blade is exposed to the metal phase, one to the metal–salt interface, one to the salt phase, and one to the vapor phase of the metal–salt system in which the material is being tested. The W–Re alloy was tested for 192 hr, and the Mo–Re alloy was tested for 50 hr. Metallographic examination after exposure of the alloys showed no detectable corrosion (limit of detection = 0.01 mm) of the W–Re alloy and only 0.02-mm corrosion of the Mo–Re alloy, primarily by surface dissolution. These results indicate that rhenium alloys could be useful for containing systems with high concentrations of zinc; the alloys would probably be used only as thin vessel liners or for special applications, such as valves, because of the high cost of rhenium.

Another potential container material, vitreous carbon, was tested for corrosion resistance to systems containing halide salts and Zn–Mg–U or Cu–Mg–U alloys. Small crucibles (1.6 in. in outside diameter by 1.6 in. high by 0.10 in. in wall thickness) were not wetted by the metal phases of the systems tested, and these crucibles displayed only limited wetting by the salt phases. Larger crucibles (3.9 in. in outside diameter by 7.1 in. high by 0.10 in. in wall thickness) were chosen for more extensive tests of this material. Analyses of failures experienced with the large crucibles in these experiments indicate that thermal shock was the major factor. An attempt was made to reduce the thermal shock by placing a crucible within a tight-fitting graphite secondary container. This procedure did not prevent the crucible from failing during the course of an experiment. It is concluded that, although vitreous carbon has desirable chemical properties for a container material, it is not suitable for use in these systems because of its low resistance to physical and thermal shock.

PROCESS KINETICS AND EQUIPMENT DESIGN

A high-temperature extraction facility has been designed and constructed to study mass-transfer rates between liquid-metal and molten-salt solvents in packed, countercurrent extraction columns.[3] In addition, information on the design and operation of such equipment is being obtained, limiting flow rates for columns of this type are being determined, and the entrainment of metal in the effluent salt stream is being investigated.

The equipment consists of the column, a jackleg to control the position of the metal–salt interface in the column, supply and receiver tanks for the metal and salt solvents, a column drain tank, and bellows-sealed valves to control the flow of the fluids (see Fig. 1).

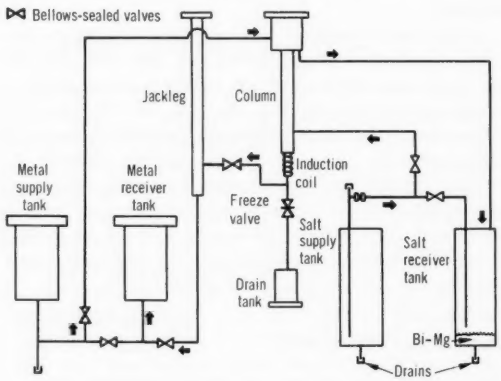

Fig. 1 Schematic diagram of facility for high-temperature extraction.

The entire facility is constructed of 304 stainless steel. The column consists of a 1-in. pipe, 3 ft long, packed with 1/4-in. Raschig rings. Liquid metal (the discontinuous phase) is sprayed into the top of the column through small holes in a horizontal tube in the top disengaging section. Liquid salt (the continuous phase) enters the bottom of the column beneath the packed section. The position of the metal–salt interface below the packed section is determined by a mutual-inductance probe that surrounds the ½-in. tube where the interface is maintained. The salt and metal supply and receiver tanks are equipped with agitators, thermocouple wells, sample ports, and movable resistance level probes for liquid-level

detection. In addition, the metal tanks have mutual-induction probes, and the salt tanks have time-delay reflectometry probes for liquid-level determination. Each tank has connections to the pressure-vacuum manifold to provide for movement of the solvents by pressure siphoning from tank to tank and to and from the column.

A single extraction experiment lasts from 20 to 120 min, depending on the flow rates, and is terminated when the supply of metal or salt is exhausted. Prior to a subsequent experiment, the solute that was extracted from the metal into the salt is removed from the salt by contacting it with a Bi–6 wt.% Mg alloy in the salt-receiver tank. Additional solute is then dissolved in the alloy in the metal-receiver tank for the next run. The entire apparatus is kept at operating temperature between experiments and is shut down completely only at the end of a series of experiments.

An experiment was performed in the facility to study the extraction of cerium from a Cd–6.9 wt.% Mg–2.2 wt.% Zn–9.65 wt.% Ce alloy into a 52.4 mole % $MgCl_2$–28.6 mole % NaCl–19 mole % KCl salt mixture at 600°C. In this experiment, 40 kg of metal was contacted with about 7 kg of salt over a 32-min period. The 33 in. of packed column length provided about 2.4 theoretical extraction stages. An extraction rate of 1.2 g of cerium per minute was realized with a metal flow rate of 1080 g/min and a salt flow rate of 181 to 276 g/min. During this run, only 0.1 g of cadmium from the alloy was carried into the effluent salt.

Processes for Molten Salt Breeder Reactor (MSBR) Fuel

A thermal breeder reactor that operates on a Th–U fuel cycle is being developed by Oak Ridge National Laboratory (ORNL). The reactor concept is a two-region breeder in which the core fuel is a molten fluoride salt (66 mole % LiF–34 mole % BeF_2) containing uranium (235 or 233) fluoride as the fissile material and ZrF_4 as a stabilizing agent to prevent uranium oxide precipitation. The reactor breeder blanket is a molten fluoride salt of the nominal composition 71 mole % LiF–2 mole % BeF_2–27 mole % ThF_4. In a thermal breeder it is necessary to maintain the fission-product neutron poisons at a low concentration by processing the core. It is also desirable to remove ^{233}Pa as it is bred in the blanket by thermal-neutron capture in ^{232}Th. Both of these requirements make it advantageous to process the fuel and blanket at the reactor site. Processing methods were discussed in the preceding issue of *Reactor and Fuel-Processing Technology*.[4] In a recent ORNL report, the status of processing work is reviewed and a program of needed development work is presented.[8]

Spectra of U(IV) and U(III) in molten salts were obtained to gain a better understanding of the chemistry of the molten-salt reactor system. Spectra in molten LiF–BeF_2, LiF–BeF_2–ZrF_4, and LiF–NaF–ZrF_4, and LiF–NaF–KF were obtained at temperatures up to 540°C over the wavelength range[9] of 200 to 2400 nm. On the basis of comparison of these spectra with those obtained in other molten-salt systems and aqueous systems, it is suggested that the coordination number of the uranium species in the molten-fluoride media studied is possibly 8 or 9. By chemical means, it was not possible to obtain a solution of U(III) free of U(IV). The reaction of U(III) with alkali fluorides is discussed.

Electrolytic Processes

A French report[10] describes an electrolytic cell that produces plutonium metal from PuO_2. The anode of the cell is a graphite toroid with a groove cut in the top to form a container for the PuO_2 solid. A graphite rod inside a ceramic insulating tube is attached to the anode and forms the anode current lead. The cathode lead is a tungsten rod with the lower end set in an alumina crucible. The alumina crucible is located in the center space of the anode toroid. The anode–cathode assembly is submerged in the molten electrolyte that is contained in another alumina crucible. The electrolyte is the NaCl–KCl eutectic containing 15 to 25 wt. % plutonium trichloride. The cell is operated at 750°C.

In the cell, chlorine in the electrolyte reacts with carbon and PuO_2 at the anode to form $PuCl_3$ and CO and CO_2 gases that are expelled. The $PuCl_3$ is reduced at the cathode to form plutonium liquid metal, which collects in the alumina crucible, and chlorine, which dissolves in the electrolyte. Parameters that affect the performance of the cell are discussed.

Studies were made to determine the feasibility of producing yttrium by fused-salt electrorefining in a controlled atmosphere.[11] Tests were conducted in a LiCl–YCl_3 electrolyte system at 710°C. The major variables studied were the YCl_3 content of the electrolyte, from 1.7 to 13.4 mole %, and the initial cathode current density, from 410 to 1630 A/sq ft. Vacuum distillation was employed to remove salt from the deposited metal. Metallic impurities, except for lithium, could be reduced to near or below their lower analytical limits, ranging from 10 ppm for copper to 300 ppm for tantalum; reduction of oxygen content, however, was accomplished only in metal produced from electrolytes with 5.4 mole % YCl_3 or less. Initial cathode current density had little effect on the purity of the product.

A recent U. S. patent describes the electrolytic separation of pure actinide oxides by cathodic deposition from a molten alkali-metal chloride.[12] (This

separation is one step in the salt-cycle process described in a previous report.[7]) A chlorinating gas is passed through the melt, and graphite electrodes are used. The cathode is coated with pyrolytic carbon to ease removal of the actinide oxides.

Miscellaneous Developments

A report from Ames Laboratory describes the preparation of thorium chloride.[13] In exploratory investigations, various thorium source materials and chlorinating agents were studied. On the basis of the results of preliminary investigations, the chlorination of thorium oxalate with mixtures of CO_2 and CCl_4 was selected for a more detailed study. In the present state of development, a charge of thorium oxalate is chlorinated in a fixed-bed reactor with approximately 1:1 mole mixtures of CO_2 and CCl_4. The reaction temperature is raised from 300 to 610°C in the course of the reaction, which takes from 5 to 6 hr. Analytical data indicate that the product is approximately 99.4% thorium tetrachloride (less than 0.08% oxygen). Batches as large as ¾ lb have been prepared by this technique. Magnesium reductions were made to further evaluate the quality of the tetrachloride and to demonstrate that it is of acceptable quality for metal preparation. The thorium obtained from these reductions was arc melted to yield good-quality metal.

A Japanese report describes the reduction of thoria by calcium.[14] Calcium chloride flux was used as carrier for the oxide. Equipment, quantities of flux relative to the oxide, operating conditions, and yields are discussed.

A French report discusses the fusion decladding of certain types of fuel elements that are clad with magnesium-rich Mg–Zr alloy.[10] It was found that the cladding could be removed by melting at 740°C, but the loss of uranium and plutonium to the liquified cladding needed to be determined. The rates of loss of uranium and plutonium to magnesium were measured in tests with simulated fuel elements. The rate of plutonium loss was lower than predicted rates based upon the diffusion rate of plutonium in the U–1 to 2 wt.% Pu alloy. It was assumed that the low rates resulted from the presence of a film barrier of oxide or carbide on the surface of the element. The observed losses were acceptable for a decladding operation.

References

1. *Power Reactor Technol. Reactor Fuel Process.*, 10(1): 80 (Winter 1966–1967).
2. *Reactor Fuel-Process. Technol.*, 10(4): 314-317 (Fall 1967).
3. R. M. Adams and A. Glassner (Comps.), Reactor Development Program Progress Report, September 1967, USAEC Report ANL-7382, pp. 119-122, Argonne National Laboratory, Oct. 31, 1967.
4. *Reactor Fuel-Process Technol.*, 11(1): 60 (Winter 1967–1968).
5. R. M. Adams and A. Glassner (Comps.), Reactor Development Program Progress Report, October 1967, USAEC Report ANL-7391, pp. 152-153, Argonne National Laboratory, Nov. 30, 1967.
6. R. M. Adams and A. Glassner (Comps.), Reactor Development Program Progress Report, August 1967, USAEC Report ANL-7371, pp. 96-97, Argonne National Laboratory, Sept. 28, 1967.
7. *Reactor Fuel-Process. Technol.*, 10(3): 237-238 (Summer 1967).
8. W. L. Carter and M. E. Whatley, Fuel and Blanket Processing Development for Molten Salt Breeder Reactors, USAEC Report ORNL-TM-1852, Oak Ridge National Laboratory, June 1967.
9. J. P. Young, Spectra of Uranium IV and Uranium III in Molten Fluoride Solvents, *Inorg. Chem.*, 6(8): 1486-1488 (August 1967).
10. Semiannual Report of the Chemistry Department [CEN, Fontenay-aux-Roses], June 1966–November 1966, Research on Dry Treatment Process, USAEC Report ANL-Trans-544, September 1967 (translated from French Report CEA-N-816).
11. C. C. Merrill and M. M. Wong, Electrorefining Yttrium, Report BM-RI-7018, U. S. Bureau of Mines, Washington, September 1967.
12. J. H. Kleinpeter and G. Jansen, Electrolytic Deposition of Actinide Oxides, U. S. Patent No. 3,314,865 to USAEC, April 1967.
13. R. M. Bergman, Investigations of Some Methods for Preparing Thorium Chloride, USAEC Report IS-T-150, Ames Laboratory, February 1967.
14. S. Takeuchi and T. Honma, Studies of the Reduction of Thoria by Calcium, *Nippon Kinzoki Gakkaishi*, 31: 42-48 (January 1967).
15. J. Knighton, Chemical Engineering Division, Argonne National Laboratory, personal communication, September 1967.

Correction: In Table 3 on page 58 of *Reactor and Fuel-Processing Technology*, Vol. 11, No. 1, decimal points were inadvertently omitted in the column for constant *A*. The corrected table is presented at the right.

Table 3 THERMAL-DISSOCIATION PRESSURE OF FLUORONIOBATES AND FLUORORUTHENATES AS A FUNCTION OF TEMPERATURE†

[$\log P(\text{torr}) = A - B/T\ (°K)$]

System	Temperature interval, °C	*A*	*B*
$LiF-NbF_5$	210–290	5.228	2456
$NaF-NbF_5$	330–480	4.410	2437
MgF_2-NbF_5	120–218	4.881	1659
CaF_2-NbF_5	87–223	3.039	864
BaF_2-NbF_5	88–247	1.995	464
$LiF-RuF_5$	229–360	5.992	2878
$NaF-RuF_5$	313–490	7.015	4004
MgF_2-RuF_5	165–301	3.821	1445
CaF_2-RuF_5	196–375	2.265	845
BaF_2-RuF_5	238–415	3.994	2312

Volatility Processes

By G. J. Vogel and J. J. Barghusen

Fluid-Bed Fluoride-Volatility Process

The development of a fluid-bed fluoride-volatility process for the recovery of uranium and plutonium values from low-enriched ^{235}U, irradiated UO_2 elements clad in either Zircaloy or stainless steel has been a joint effort of Argonne National Laboratory (ANL), which is responsible for flow-sheet development studies, Oak Ridge Gaseous Diffusion Plant (ORGDP), which is responsible for semiworks scale equipment testing, and Oak Ridge National Laboratory (ORNL), which is responsible for the design and operation of a radioactive pilot plant. Workers at all sites have published general papers describing the process and related experimental work.[1-3] Data pertinent to fluoride-volatility processing have also been published by Russian workers.[4]

The current fluoride-volatility-process flow sheet as reviewed in the ANL paper[1] entails the following discrete steps:

1. Removal of the Zircaloy cladding by reaction of the zirconium with HCl to form volatile $ZrCl_4$, while the unreacted UO_2-PuO_2 pellets remain in the reactor, or, in the case of stainless-steel cladding, disintegration of the cladding and pulverization of the pellets by an $HF-O_2$ treatment at 550°C.
2. Oxidation of the unreacted UO_2-PuO_2 pellets from the Zircaloy decladding step to form U_3O_8 powder and thereby increase the reaction rate in the subsequent fluorination steps.
3. Separation of uranium from plutonium by reacting the uranium with BrF_5 to form volatile UF_6, which leaves the reactor accompanied by bromine halides and fission products that must be separated later.
4. Removal of plutonium from the reactor by reacting it with fluorine to form volatile PuF_6, which leaves the reactor accompanied by a small amount of fission products from which the PuF_6 must be subsequently separated.

The ANL effort is divided into three parts: (1) laboratory-scale experiments to define the effect of process variables on the BrF_5 and fluorine fluorinations and to develop methods of separating uranium and plutonium from fission-product fluorides, (2) laboratory-scale experiments with radioactive material to determine the fate of fission products, and (3) engineering-scale experiments in the plutonium-handling facility to investigate the transport and the accountability of plutonium.

The ORGDP is responsible for equipment testing on a semiworks scale using nonirradiated uranium materials to confirm design assumptions and to evaluate scale-up problems.[2] The semiworks fluid-bed reactor, Fig. 1, which has been used for pellet oxidation tests, has an upper section 10 in. in diameter and 11 ft long and a smaller, lower section 5 in. in diameter and $3\frac{1}{3}$ ft long. Corrosion tests have shown that Nickel 201 would be the most satisfactory construction material for this reactor considering the variety of gases handled (HCl, O_2, HF, BrF_5, F_2) and the temperatures encountered (400 to 550°C).

Calculations have been made to assess problems associated with radioactive decay heat and criticality in a commercial-scale reactor. Fuel to be processed will be added to the reactor through a fuel charging device which may be a vertical pipe with valves at either end. During charging, some method of cooling of the fuel will be necessary because of the fission-product decay heat. Decay heat will also be a problem during the processing of the fuel if fluidization should be stopped or if caking should occur. Under these conditions, temperature rises of 50 to 100°C/hr could be expected in the reactor. Criticality calculations have indicated that 24 kg of plutonium could be processed, which is twice the amount that will probably be processed per batch in the 24-in.-diameter commercial-scale reactor.

Filter media, flanges and connectors, and gas-circulating compressors have been tested in the development program. From a corrosion standpoint the available porous nickel filter medium is satisfactory for use in the $HCl-O_2-F_2$ atmospheres. A sealing system for flanges and connectors consisting of double gaskets with a pressurized buffer gas

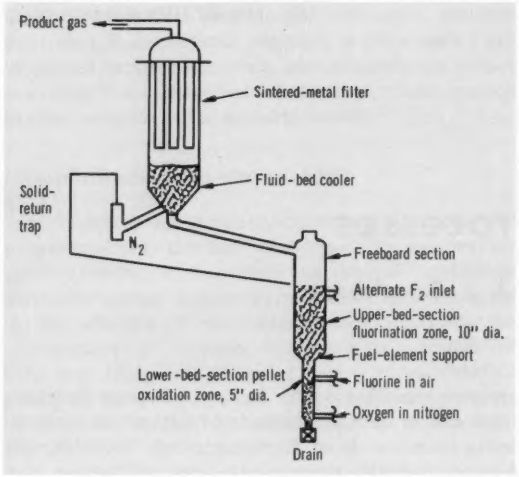

Fig. 1 Semiworks fluid-bed reactor.[2]

between the gaskets should suffice to keep any radioactivity from leaving the system. Two compressors for cycling the process gases are being compared, a nominal 30-in.-diameter, 12-scfm diaphragm compressor and a two-stage peripheral compressor having a 10-in.-diameter impeller.

A continuous sorber–desorber unit has also been tested. Uranium hexafluoride can be partially decontaminated from fission products IF_7 and TeF_6 by passing the gas mixture through a bed of NaF at about 125°C where the UF_6 is sorbed. The UF_6 is later desorbed at 400°C. This method of decontaminating the UF_6 is not currently a step in the process flow sheet but may have potential application. The sorption is conducted in a fluidized bed of NaF powder and the desorption in a screw-type unit. The NaF moves continuously between the two units. A diagram of the sorber–desorber was presented in a previous issue of *Reactor Fuel Processing*.[5]

The ORNL responsibility[3] includes design and operation of a pilot plant for radioactive materials using semiworks-scale equipment of a size similar to that tested at ORGDP. The fabrication and installation of nearly all the equipment required in the decladding, oxidation, and fluorination of "cold" uranium fuel has been fabricated. Structural steel and much of the shielding have been installed in the cell, and installation of process equipment has begun. Purchasing and fabrication are progressing on mechanical handling equipment and instrumentation.

ORNL reported[3] the following results from small-scale tests on possible process steps:

1. In the current process flow sheet, the Zircaloy cladding of the fuel is reacted with HCl. Plugging problems developed when the volatile $ZrCl_4$ was filtered through porous metal filters. The high-temperature, $HF-O_2$ treatment, which is being used to remove stainless-steel cladding from fuel elements, was tried on the Zircaloy-clad elements. Massive shards of ZrO_2 remained in the bed after the treatment, but the UO_2 pellets were oxidized successfully. The effect of zirconium in the alumina bed on plutonium retention during the fluorination step remains to be evaluated before the utility of the method can be assessed.

2. Tests using hydrogen to fracture the Zircaloy cladding and a subsequent treatment with $HF-O_2$ to pulverize the oxide were successful.

3. In a statistically designed experiment, the following variables had little effect on the final uranium concentration in the alumina bed when UF_4 was reacted with fluorine: temperature, fluorine concentration, alumina-particle diameter, reaction time, and initial concentration of uranium in the bed.

4. Neptunium hexafluoride (NpF_6) was satisfactorily sorbed and desorbed on NaF. Lithium, calcium, and barium fluorides were unsuitable for sorption of NpF_6. Magnesium fluoride was found to sorb NpF_6, but desorption was found to be a problem.

5. An aqueous KOH scrubber was tested for removal and disposal of fluorine from the process off-gas. Later, the effectiveness of adding KI to the KOH solution was demonstrated.

The following equipment and instruments were designed or tested:

1. A gas-powered jet for withdrawing solids from the fluid bed for sampling purposes.

2. A fluorine calorimeter for determining the concentration of bromine and BrF_3 in the reactor off-gas by mixing the off-gas with fluorine and measuring the temperature rise.

3. In-line instruments for measuring the hydrogen content of the pyrohydrolyzer off-gas stream, the oxygen in the process off-gas from the reactor in the oxidation step, and the fluorine concentration in the recycle gas in the plutonium fluorination step have been developed.

A review article on current Russian experiments, many of which parallel those made in this country, is presented by Prusakov et al.[4] The reaction of UO_2 with oxygen to form U_3O_8 and the immediate reaction of the U_3O_8 with fluorine were studied, as well as the batch oxidation of UO_2 followed by batch fluorination of the U_3O_8. Decontamination of the product UF_6 by sorption methods was also studied. Since these topics have been discussed in previous issues of this review,[6,7] they will not, therefore, be discussed in further detail here.

Fluorination of Oxide Fuels with ClF_3

A fluid-bed process for recovering uranium and plutonium from oxide fuels is being developed at Centre d'Étude de l'Énergie Nucléaire (CEN), Mol,

Belgium. The process is based on the use of ClF_3 as a selective fluorinating agent for separating the uranium from the plutonium. The plutonium is recovered by reaction with fluorine. The status of the work at CEN up to 1966 is presented in two recently published papers.[8,9] The laboratory and engineering experiments have been reviewed in recent issues of *Power Reactor Technology and Reactor Fuel Processing*[6,10] and *Reactor and Fuel-Processing Technology*.[11,12]

Radiochemical Pilot Plant for Volatility Processing—Attila Cell

Large-scale equipment installed in the Attila cell of Centre d'Études Nucléaires, Fontenay-aux-Roses, France, will be devoted to the study of fluoride-volatility methods using MTR-type fuel elements.[13] These are highly enriched alloy fuels either aluminum-clad U–Al alloys or Zircaloy-clad Zr–U alloys.

Details of the volatility process have been reviewed in *Reactor and Fuel-Processing Technology*.[14] First, the alloy is reacted with hydrogen chloride at 300 to 400°C in a fluidized bed of alumina forming volatile $ZrCl_4$ and nonvolatile UCl_3. The $ZrCl_4$ enters a pyrohydrolysis reactor where it is converted to the oxide by reaction with steam at 400°C in a fluid bed of silica. Second, the UCl_3 is reacted with fluorine at temperatures up to 500°C to form the volatile UF_6 that is later purified by sorption–desorption techniques using NaF. An equipment flow diagram for the process is shown in Fig. 2.

The alpha containment box, 10 m long, 4 m wide, and 5 m high, is fabricated from stainless-steel plates that are held externally by a framework of ordinary steel sections, fixed by means of pins welded to the outside of the plate.

Both the alpha containment box and the space between the box and the gamma shielding are ventilated. In the alpha box, 3 to 15 volume changes per hour of air pass through inlet air filters located in the ceiling of the cell and exit through filters on one side of the cell. Ten volume changes per hour of air are passed through the spacing between the box and the gamma containment wall. Reduced pressures are maintained in the alpha box and the space, 0.8 and 0.2 in. water negative, respectively. All ventilation air is passed through a washing tower to eliminate traces of corrosive gas, if present, before joining the air in the building ventilation system.

The cell is equipped with two Argonne Model 8 master–slave telemanipulators, a General Mills Model 150 manipulator, a robot manipulator, and a traveling hoist. Manipulations can be viewed through

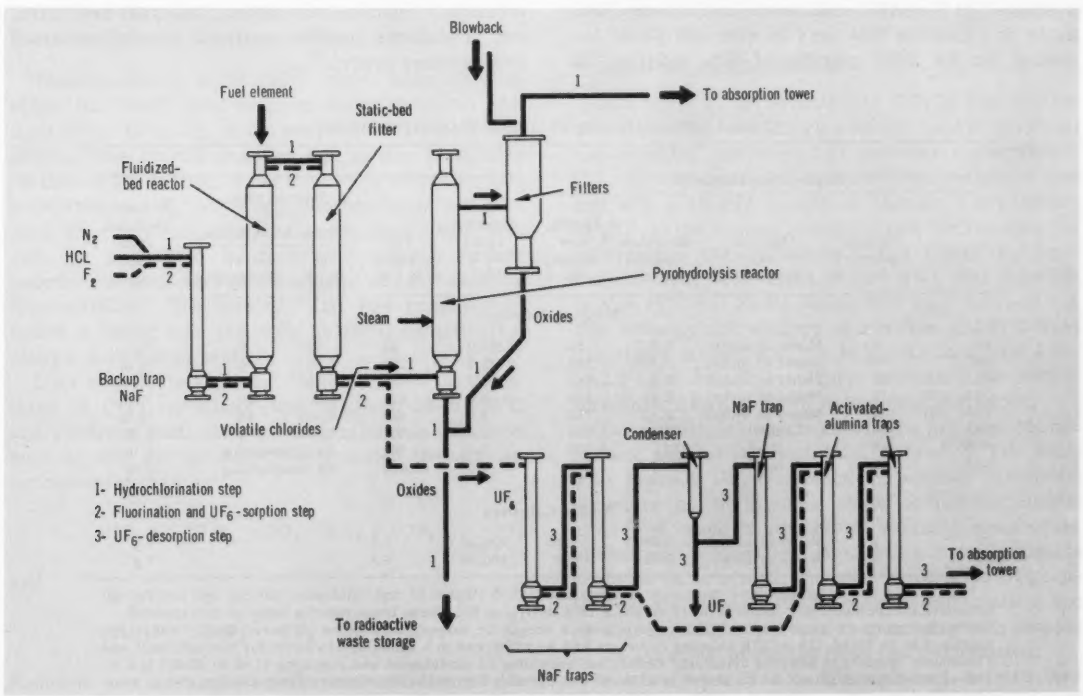

Fig. 2 Attila cell.[13]

seven lead-glass windows fitted into the gamma shielding blocks. Corresponding windows in the alpha box are of cerium-stabilized glass, 12 mm thick, and are sealed with a synthetic rubber polymer. For additional viewing there are two observation ports for use with bent binocular periscopes and a closed television circuit.

Before processing, radioactive fuel elements are cut into small plates and transported in a lead castle ("Ragueneau" type) to the cell. Noncontaminated materials are added, and slightly contaminated materials are removed from the cell through an opening in the roof of the cell. The transfer takes place under a polyvinyl chloride plastic envelope. Contaminated materials are dropped through a trapdoor in the floor into a lead castle. Radioactive samples are pneumatically transferred to the laboratory located just below the processing cell.

UF_6 Handling Procedures and Container Criteria

An excellent summary report has been prepared on UF_6 handling and container criteria based on 20 years of experience at AEC facilities.[15] In addition, reports have been published on the testing of a thin-walled cylinder[16] and on the testing of shipping packages, the outer protective case into which a cylinder is placed prior to shipment.[17,18] Uranium hexafluoride is shipped to non-AEC customers and between AEC plants in cylinders that vary in size and shape depending on the total quantity of UF_6 and the ^{235}U enrichment. In the summary report, procedures are listed for cleaning, testing, and repairing cylinders, for emptying and filling the cylinders, and for weighing and sampling the UF_6. Dimensioned drawings of cylinders are included. Physical and chemical properties of UF_6 are presented along with a list of analyses required before shipment. Safety considerations—hazards and precautions—complete the presentation.

Characteristics and packaging limits are given in Table 1 for six sizes of shipping cylinders and two sizes of sampling cylinders.[15] The shipping cylinders are generally filled by liquid transfer, although the smaller models (5A, 8A, and 12B) have two valves and a dip leg into which gaseous UF_6 can be passed and desublimed if the cylinder is in a cold bath. The UF_6 can be emptied from the cylinders as either a liquid or a gas. Smaller cylinders are weighed on equal-arm scales, and the larger ones are weighed on platform scales. Certification and control of standard weights and weighing devices are discussed.

A liquid sample of the bulk UF_6 in the shipping cylinders is preferred for chemical and isotopic analyses, and two liquid-sampling methods have been developed. For the smaller cylinders, up to size 12B, a calibrated sight gauge or pipette is used to visually determine the size of the sample; for the larger cylinders the liquid is drained directly to a sampling cylinder that is continuously weighed. The type and methods of chemical and isotopic analyses are listed, but procedures for the analyses must be obtained from another report.[19]

Table 1 STANDARD UF_6-CYLINDER PACKAGING LIMITS[15]

Cylinder characteristics					Packaging data				
							Routine size lot for† composite sampling		
Model No.	Nominal diameter, in.	Material of construction	Minimum volume, cu ft	Approx. tare weight, lb	Maximum assay, wt.% ^{235}U	Fill* limit, lb UF_6	lb UF_6	No. of cylinders	Maximum variation from reported weight
Shipping Cylinders									
5A	5	Monel or nickel	0.311	55	100.0	55	330	6	1 g
8A	8	Monel or nickel	1.359	120	12.5	250	1,500	6	¼ lb
12A, 12B	12	Monel or nickel	2.41	185	5.0	450	2,700	6	¼ lb
12A, 12B	12	Monel or nickel	2.41	185	5.0	450	4,500	10	¼ lb
12A, 12B	12	Monel or nickel	2.41	185	3.0	450	20,250	45	¼ lb
30A	30	Steel	25.64	1,600	4.5‡	4,800	24,000	5	1 lb
48A	48	Steel	111	4,500	3.0‡	21,000	No compositing		2 lb
48F	48	Steel	142.7	5,200	2.0‡	28,000	No compositing		2 lb
Sample Cylinders									
1S	1.5	Monel or nickel	0.0053	1.75	100.00	1.0			1 g
2S	3.5	Monel or nickel	0.026	4.2	100.00	4.8			1 g

*Fill limits are based on 300°F maximum temperature (190 lb UF_6/cu ft) and minimum internal volumes for all cylinders except Model 48F which is based on 250°F (204 lb UF_6/cu ft). These temperatures must not be exceeded.

†Routine sample compositing is limited to 6 cylinders except for large orders below 5% enrichment. Orders requiring 7 to 10 Model 12A or 12B shipping cylinders will be withdrawn in a Model 30A cylinder for measurement and subsequent transfer to shipping cylinders. Orders not exceeding 3% enrichment and requiring 11 to 45 Model 12A or 12B shipping cylinders will be withdrawn in a Model 48A cylinder for measurement and subsequent transfer to shipping cylinders.

‡Maximum assays indicated require moderation control equivalent to a UF_6 purity of 99.5%. Without moderation control the maximum permissible assay is 1.0 wt.% ^{235}U.

For shipment of cylinders up to and including Model 30A, an outer protective shipping package or case has been designed and tested in accordance with applicable AEC and Interstate Commerce Commission regulations. The shipping package consists of an inner and outer steel shell with the annulus filled with a high-temperature, foam plastic to which fiberglass has been added for structural strength.[17,18] Padding and stiffening devices complete the protective package. A phenolic-resin foam containing glass-fiber roving and foamed using a catalyst containing boron, which sorbs neutrons, has been developed.[20] The results of drop, puncture, thermal, and water immersion or water spray tests of the 8-, 12-, and 30-in.-diameter cylinder shipping packages have been described and the results illustrated photographically.[17,18]

Impact, puncture, and valve destruction tests have been made on a cylinder (without the shipping package) having the same capacity as a Model 48A cylinder but having only about half the tare weight because of thinner wall construction.[15] These cylinders are used currently for in-plant storage of UF_6 but not for interplant shipping. However, based on the results of these tests, a permit for use of this cylinder for shipping has been issued by the Bureau of Explosives. Further tests on this and other containers are contemplated.

Fluorination of Uranium Compounds

Thermobalance techniques[21] have been used to study the reaction of uranium dicarbide (UC_2) with fluorine to form UF_6 in the temperature range 220 to 300°C. The overall reaction mechanism is similar to that of UC in that, in the first step, UC_2 is rapidly converted to UF_4, polymeric fluorocarbons, and gaseous fluorocarbons, whereas in the second step, UF_4 and the polymeric fluorocarbons undergo further reaction at a lower rate to form UF_6 and gaseous fluorocarbons. The second step was observed to follow a linear rate law with an apparent activation energy of 19.5 kcal/mole.

Luce and Hartmanshenn[22,23] investigated the reactions of ClF_3 and ClO_2F with UO_2F_2 at 50 to 150°C and observed that, although intermediate compounds such as ClF are produced, the overall reactions can be represented as:

$$ClF_3 + 3UO_2F_2 \rightarrow 3O_2 + 2Cl_2 + 3UF_6 \qquad (1)$$

and

$$4ClO_2F + UO_2F_2 \rightarrow UF_6 + 2Cl_2 + 5O_2 \qquad (2)$$

Reaction 1 is in complete agreement with the results of Shrewsberry and Williamson which have been discussed in detail in previous reviews.[24–26]

Otey and LeDoux[27] have reported the existence of a uranium oxyfluoride, $U_3O_5F_8$, prepared by the reaction of UF_6 with a small quantity of water at 160 to 170°C. This material is thermally stable up to 408°C and reacts rapidly with water to yield UO_2F_2. The reaction of $U_3O_5F_8$ with ClF_3 proceeds in the same manner as the reaction of UO_2F_2 with ClF_3 and gives the same reaction products.

The kinetics of the gas–solid reactions between BrF_5 and UF_4 and UO_2F_2 have been studied in the temperature range 175 to 300°C and in the BrF_5 partial pressure range of 130 to 370 torrs.[28] Both these reactions produce UF_6 and elemental bromine as the main products, and, in the case of the UF_4–BrF_5 reaction, the intermediate uranium fluorides (U_2F_9, U_4F_{17}, and UF_5) are produced as minor products. The following equations were derived to represent the temperature and BrF_5 partial dependence of the reactions:

UF_4–BrF_5 reaction: $\log k$

$$= 0.38 \log P_{BrF_5}\ (\text{torr}) - 3690/T(°\text{K}) + 4.286$$

UO_2F_2–BrF_5 reaction: $\log k$

$$= 0.71 \log P_{BrF_5}\ (\text{torr}) - 1810/T(°\text{K})$$

Values of the activation energy of 16.9 and 8.3 kcal/mole were calculated for the reactions with UF_4 and UO_2F_2, respectively.

Properties of Fluorides

In a study of the synthesis of ClF_5 by reaction between chlorine and fluorine at 211 to 271°C, Bauer and Sheehan[29] observed that complete conversion to ClF_5 did not occur even over extended periods of time and with a 10-fold excess of fluorine. The presence of ClF_3 in the system suggested that the reaction was governed by the equilibrium $ClF_3 + F_2 \rightleftharpoons ClF_5$. Equilibrium data were fitted to the van't Hoff equation, $\ln K_p = 9175/T - 21.30$, where $K_p = P_{ClF_5}/(P_{ClF_3})(P_{F_2})$. The enthalpy and entropy of reaction at 240°C were calculated to be: $\Delta H_r = -18.2 \pm 0.9$ kcal and $\Delta S_r = -42.3 \pm 1.8$ eu. The authors estimated the heat of formation $\Delta H_{f500}[ClF_5(g)]$ to be −56.0 kcal/mole.

The vibrational spectrum of UF_6 has been studied in both the gaseous and solid states.[30,31] The study with gaseous UF_6 confirmed the regular octahedral structure of the fluorine atoms around the central atom and made it possible to evaluate some of the vibrational frequencies from which force constants could be determined. The spectra of solid UF_6 confirmed the essentially tetragonal deformation and revealed a slight decrease in symmetry with respect to the D_{4h} group predicted from this deformation.

In other work Blanchard[32] explained the structure of AsF_5 in terms of C_{3v} molecular symmetry, with the As–F bond stretching lying at 786 cm^{-1} and 811

cm^{-1}. Several methods of preparing pure AsF_5 are presented.

The standard enthalpy of formation of AlF_3 has been measured by direct combination of the elements in a bomb calorimeter.[33] The value obtained was -360.7 ± 0.3 kcal/mole.

One method being considered for purification of plutonium involves selective reduction of plutonium in liquid BrF_3. Therefore the chemistry of fluorides in BrF_3 is pertinent to the development of fluoride-volatility processes. Martin[34] has published the results of a comprehensive investigation of the reactions between sodium, potassium, rubidium, or cesium fluoride and UF_4 in BrF_3. Several complex fluoride salts, previously uncharacterized, were isolated and identified. Several compounds soluble in BrF_3 were disclosed: $RbUF_5$, $CsUF_5$, and $Cs_2U_5F_{22}$. In other work, Brown, Dixon, and Sharp[35] have investigated the system GeF_4-BrF_3 and have isolated three adduct species.

Meinert[36] has prepared a comprehensive survey of the physical and chemical properties of the interhalogen compounds, including a bibliography of over 250 references.

References

1. M. J. Steindler, N. M. Levitz, and A. A. Jonke, Development of Fluoride-Volatility Methods for Reprocessing Reactor Fuels, *Compt. Rend. Congr. Intern. Chim. Ind., 36th Conference, Brussels, 1966*, 1: 730-733 (1967).
2. S. H. Smiley, J. H. Pashley, and D. C. Brater, Fluid-Bed Volatility Component, Engineering Feasibility, and Scale-Up Studies at the Oak Ridge Gaseous Diffusion Plant, *Compt. Rend. Congr. Intern. Chim. Ind., 36th Conference, Brussels, 1966*, 1: 781-786 (1967).
3. Oak Ridge National Laboratory, Chemical Technology Division Annual Progress Report for Period Ending May 31, 1967, USAEC Report ORNL-4145, October 1967.
4. V. N. Prusakov, V. K. Ezhov, O. G. Lebedev, and V. K. Popov, Some aspects of Nuclear Fuel Reprocessing by Fluorination Method, *Compt. Rend. Congr. Intern. Chim. Ind., 36th Conference, Brussels, 1966*, 1: 787-792 (1967).
5. *Reactor Fuel Process.*, 9(2): 91 (Spring 1966).
6. *Power Reactor Technol. Reactor Fuel Process.*, 10(1): 72 (Winter 1966-1967).
7. *Reactor Fuel-Process. Technol.*, 11(1): 56 (Spring 1968).
8. J. Schmets, G. Camozzo, R. Heremans, and G. Pierini, Progress et Problemes en Matiere de Retraitement des Ceramiques par Volatilisation sous Forme de Fluorures, *Compt. Rend. Congr. Intern. Chim. Ind., 36th Conference, Brussels, 1966*, 1: 757-762 (1967).
9. G. Pierini, J. Schmets, and A. Francesconi, Une Nouvelle Voie pour le Retraitement des Combustibles Ceramiques: La Fluorination par le Trifluorure de Chlore Gazeux, *Compt. Rend. Congr. Intern. Chim. Ind., 36th Conference, Brussels, 1966*, 1: 752-756 (1967).
10. *Power Reactor Technol. Reactor Fuel Process.*, 10(2): 161 (Spring 1967).
11. *Reactor Fuel-Process. Technol.*, 10(3): 227 (Summer 1967).
12. *Reactor Fuel-Process. Technol.*, 10(4): 145 (Winter 1967-1968).
13. M. Bourgeois, G. Lefort, G. Manevy, and Y. Rochedereux, Attila—A Hot Facility for Reprocessing Studies on Irradiated Fuels by Fluoride Volatility Techniques, in *Proc. Conf. Remote Systems Technol., 15th, Chicago, November 6-9, 1967*, pp. 68-74, 1967.
14. *Reactor Fuel-Process. Technol.*, 10(3): 226 (Summer 1967).
15. E. L. Keller (Comp. and Ed.), Uranium Hexafluoride Handling Procedures and Container Criteria, USAEC Report ORO-651 (Rev. 1), Union Carbide Corporation, Nuclear Division, 1967.
16. W. R. Pedigo, V. A. Smith, S. Bernstein, W. J. Hamer, and J. L. Meyers, Testing of Ten-Ton Uranium Hexafluoride Cylinders, USAEC Report KY-500, Union Carbide Corporation, Nuclear Division, Paducah Gaseous Diffusion Plant, Oct. 22, 1965.
17. A. J. Mallett and C. E. Newlon, Protective Shipping Packages for 8- and 12-inch Diameter UF_6 Cylinders, USAEC Report K-1714, Union Carbide Corporation, Nuclear Division, Oak Ridge Gaseous Diffusion Plant, Apr. 20, 1967.
18. A. J. Mallett and C. E. Newlon, Protective Shipping Packages for 30-inch Diameter UF_6 Cylinders, USAEC Report K-1686, Union Carbide Corporation, Nuclear Division, Oak Ridge Gaseous Diffusion Plant, Apr. 13, 1967.
19. R. J. Jones (Comp. and Ed.), Selected Measurement Methods for Plutonium and Uranium in the Nuclear Fuel Cycle, USAEC Report TID-7029, 1963.
20. *Chem. Eng. News*, 44(24): 79 (June 13, 1966).
21. M. Iwasaki, T. Sakurai, and N. Ishikawa, Kinetic Studies of Fluorination of Uranium Carbides by Fluorine, II. Fluorination of Uranium Dicarbide, *J. Nucl. Sci. Technol. (Tokyo)*, 4(5): 249-253 (May 1967).
22. M. Luce and O. Hartmanshenn, Study of the Reactions $ClF_3-UO_2F_2$ and $ClO_2F-UO_2F_2$ (in French), French Report CEA-R-3210, March 1967.
23. M. Luce and O. Hartmanshenn, Reaction du Trifluoure de Chlore sur le Fluorure d'Uranyle, *J. Inorg. Nucl. Chem.*, 29(11): 2823-2824 (November 1967).
24. *Reactor Fuel Process.*, 7(4): 247-248 (Fall 1964).
25. *Reactor Fuel Process.*, 8(1): 26 (Winter 1964-1965).
26. *Power Reactor Technol. Reactor Fuel Process.*, 10(2): 162 (Spring 1967).
27. M. G. Otey and R. A. LeDoux, $U_3O_5F_8$—A New Compound in the U-O-F System, *J. Inorg. Nucl. Chem.*, 29(9): 2249-2256 (September 1967).
28. R. L. Jarry and M. J. Steindler, The Reaction of Gaseous Bromine Pentafluoride with Uranium Compounds. I. The Kinetics of the Reactions with UF_4 and UO_2F_2, *J. Inorg. Nucl. Chem.*, 29(7): 1591-1597 (July 1967).
29. H. F. Bauer and D. F. Sheehan, Equilibrium Studies of Chlorine Pentafluoride, *Inorg. Chem.*, 6(9): 1736-1737 (September 1967).
30. R. Bougon, Study of the Molecular Structure of Uranium Hexafluoride (in French), French Report CEA-R-3235, 1967.
31. R. Bougon and P. Rigny, Vibration Spectrum and Molecular Structure of Solid Uranium Hexafluoride, *Compt. Rend., Ser. C.*, 263: 1321-1324 (Nov. 28, 1966).
32. S. Blanchard, Infrared Spectrum of Arsenic Pentafluoride (in French), French Report CEA-R-3195, 1967.
33. E. Rudzitis, H. M. Feder, and W. N. Hubbard, Fluorine Bomb Calorimetry. XXII. The Enthalpy of Formation of Aluminum Trifluoride, *Inorg. Chem.*, 6(9): 1716-1717 (September 1967).
34. D. Martin, On the Alkaline Uranium Fluorides. Study of Bromine Trifluoride Solutions. Study of Some of the Solid Compounds, *Rev. Chem. Minerale*, 4(2): 367-397 (1967).
35. D. H. Brown, K. R. Dixon, and D. W. A. Sharp, The Structures of Bromine Trifluoride Adducts, *Chem. Commun.*, (No. 18): 654-655 (Sept. 21, 1966).
36. H. Meinert, Interhalogenverbindungen, *Z. Chem.*, 7(2): 41-57 (February 1967).

Progress in Waste-Disposal Research and Development

By Phillip Fineman

Conversion of High-Level-Activity Waste to Solids

ENGINEERING DEMONSTRATION OF SOLIDIFICATION PROCESSES

At Pacific Northwest Laboratory (PNL), a program is in progress to demonstrate on an engineering scale the technical, economic, and safety aspects of various solidification processes for converting high-level-activity wastes to solid form.[1] Three processes have been selected for testing in a multipurpose facility, known as the Waste-Solidification Engineering Prototypes (WSEP). They are (1) the PNL spray-solidification process, (2) the ORNL (Oak Ridge National Laboratory) pot-calcination and rising-level glass processes, and (3) the BNL (Brookhaven National Laboratory) phosphate-glass process. A schematic flow diagram of the WSEP was presented in a previous issue of *Reactor and Fuel-Processing Technology*.[2] Discussed below is recently reported PNL work on the spray-solidification[3] and phosphate-glass processes[4] and the storage of solidified wastes.[5] Also presented is BNL work performed in support of the phosphate-glass process.[6]

RADIANT-SPRAY CALCINER AND MELTER

The spray solidification of wastes is carried out by means of a radiant-heat spray calciner coupled to a continuous melter.[7] In this system, liquid waste is first converted in the spray calciner to a powder or calcine that is then discharged to the melter where it is melted. The molten calcine or glassy solid flows from the melter into a final receiver where the molten material is solidified for storage.

At PNL the first spray-solidification runs made with radioactive feeds (runs SS-1 and SS-2) have been carried out.[3] The first of the two runs (SS-1) was terminated when poor air atomization of the feed caused internal deposition (scaling) of calcine in the spray calciner. An external-mix nozzle was used to spray the feed.

The second run (SS-2), which was of 58 hr duration, was successfully completed. A simulated PW-1* feed containing added melt-glass formers (lithium, sodium, and phosphate ions) and 419,000 curies of mixed fission-product activity was tested. In this run an internal-mix nozzle was utilized to spray the feed into the calciner. Sugar, as a reductant chemical, was fed to the condensate evaporator and fractionator (Fig. 1) to determine its effectiveness for suppressing the volatilization of ruthenium. (In run SS-1, sugar was fed only to the condensate evaporator).

Some operating difficulties were encountered during the run, but these were handled successfully. An average feed rate of 13.4 liters/hr was maintained for the run. The feed spray nozzle became plugged twice very early in the run and was mechanically unplugged on both occasions. It then performed very satisfactorily to the end of the run. The plugging was believed to be caused by calcination of the feed within the nozzle. After the run, the calciner was found to be free of calcine deposits on the calciner wall.

Because the weir furnace for the melter was inoperable during run SS-2, the melt was discharged batchwise to the product receiver (pot). The pot was filled to a depth of 5 ft (melt volume of 48 liters) without stalagmite formation or wall deposition. A more even filling of the pot was obtained with batch discharge of the melt than with the continuous discharge that had been used in previous tests. (In the latter case, the melt trickles continuously over the weir.) The self-generating heat density of the melt

*The PW-1 waste is a first-cycle Purex-process waste. It is high in nitric acid (~5*M*), free of sulfate ion, and contains added iron from the dissolvable container used to transport chopped fuel.

was not measured, but it was estimated to be 44 watts/liter. This is equivalent to processing the waste from 1.7 metric tons of 20,000-Mwd power-reactor fuel that had been allowed to cool 3.8 years. At equilibrium, with the pot in a cool furnace, the maximum centerline temperature of the pot was 315°C, and the temperature of the pot wall was 255°C.

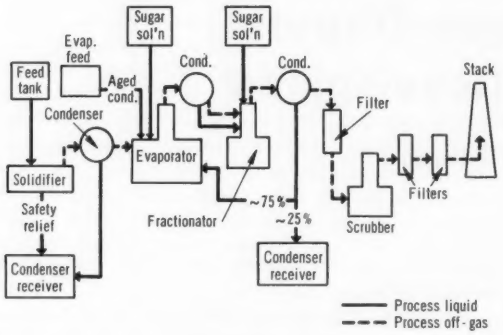

Fig. 1 Equipment arrangement[3] for spray-solidification run SS-2.

As in previous spray-solidification runs, about 75% of ruthenium in the feed volatilized to the waste evaporator (see Fig. 1). The amounts of ruthenium appearing in the condensates from the condensate evaporator and the acid fractionator increased about fivefold and tenfold, respectively, over that found in the same condensates in run SS-1; the addition of sugar to the acid fractionator apparently did not suppress ruthenium volatility from this unit. The causes for these increases are being determined.

In other PNL developmental spray-solidification work, laboratory process technology studies and nonradioactive engineering-scale runs were conducted to test flow sheets and improve the operation of the spray calciner. A flow sheet being considered involves carrying out the melting of the powder from the calciner directly in the product receiver (pot), thus bypassing the need for the continuous melter. Laboratory work has been carried out to evaluate low-temperature melts produced from PW-2* wastes for the in-pot melting flow sheet. Melts with sulfate and lithium as additives appear promising for PW-2 wastes (which already contain some sulfate ions). Compositions melting at less than 700°C were produced for a wide range of sulfate and lithium additive concentrations. Minimum concentrations of these additives required to produce a low-temperature (700°C) melt appear to be about 0.2*M* lithium and 0.4*M* sulfate. At these concentrations a viscous melt with an oxide slag was produced.

Engineering-scale runs with a PW-2 flow sheet have shown that it is feasible to melt the calcine directly in the final storage container and that a solids feeder employing a vibrating trough is a satisfactory method of controlling the addition of solid-melt formers for an in-pot melting method of operation.

PHOSPHATE-GLASS PROCESS

The phosphate-glass process produces a glass directly and continuously from an aqueous-process waste without a separate intermediate drying step.[8] For a wide range of waste compositions, phosphoric acid is the only necessary additive, although metal ions may be added to improve the glass characteristics. There are three main process steps: (1) admixing phosphoric acid in the waste, (2) evaporating the resulting solution to reduce its volume, and (3) heating the concentrated solution in the melter to 1200°C to form the glass, which is then discharged to a storage pot.

WSEP Prototype Equipment Tests. Preparatory to using the prototype equipment in the WSEP, a series of equipment design and verifications tests was conducted at PNL.[3] Operating parameters and run data obtained for the final two runs (CPG-6 and CPG-7) in this series were as follows. Both runs employed nonradioactive feeds and 12-in.-OD product receivers fabricated of 304L stainless steel. In run CPG-6 the feed composition was based on a modified PW-2 flow sheet and contained a high concentration (0.12*M*) of aluminum.† Phosphoric acid (75%) was the only additive introduced to the feed. The adjusted feed had a ratio of metallic cation (M) to phosphorus (P) of 1.0. Flow-sheet operability was good throughout the run. The quantity of sulfate retained in the condensate from the melter was increased from 85% to 95% of that fed to the melter when a steam spray was used to increase the scrubbing effect of the melter condenser. The Pt–5% Ir off-gas line from the melter showed signs of mild corrosion. Except for process startup and shutdown that employed manual control, operation of both the evaporator and the melter during the run was accomplished by automatic control. Process shutdown procedures were successfully tested. Filling of the product receiver with 71 liters of product was uniform. The solid product was glassy and had a bulk density of 2.62 g/cm^3.

In run CPG-7 the feed was a simulated PW-1 waste in which the "ruthenium" consisted of nonradioactive ruthenium (0.0032*M*) and manganese‡

*PW-2 waste is a combined first- and second-cycle Purex-process waste. It is high in nitric acid (~5*M*) and contains iron and sulfate ions from the ferrous sulfamate reductant.

†In PW-1 and PW-2 wastes, the aluminum concentration is usually 0.001*M*.

‡In the formulation of simulated PW-1 and PW-2 solutions, manganese was used as a stand-in for ruthenium.

(0.0288*M*). Sodium nitrate and 75% phosphoric acid were introduced as the glass formers. The adjusted feed had a M-to-P ratio of 1.00. Plugging difficulties were experienced with this flow sheet, particularly plugging of the dip tube in the denitrator evaporator. Periodic steam blowback of these tubes kept them from becoming completely plugged. About 71 liters of product was prepared, which had a bulk density of 2.47 g/cm^3. Ruthenium retention in the product was good; it contained 88% of the ruthenium processed. The remaining ruthenium was lost to the melter condensate stream (9%) and to the evaporator–denitrator condensate stream (3%). Visual examination of the Pt–5% Ir melter off-gas line did not reveal any evidence of corrosion.

Treatment of Glass Melter Condensate. The condensate from the melter represents an intermediate-level-activity waste (ILW) that will require treatment before storage.[9] It contains appreciable amounts of sulfuric and nitric acids and a small amount of phosphoric acid. A number of methods have been proposed for the treatment of this waste. Solidification[4] and distillation[6] processes are currently being investigated at PNL and BNL, respectively. PNL[4] is evaluating an asphalt-immobilization flow sheet* (Fig. 2). It is based on the treatment (per metric ton of uranium processed; PW-2 flow sheet) of a melter condensate having a volume of 60 gal and containing 318 moles of sulfuric acid, 159 moles of nitric acid, 18 moles of phosphoric acid, and varying quantities of fission products (principally ruthenium, cesium, and strontium). The flow sheet incorporates head-end scavenging steps for the removal of cesium and strontium and their recycle to the phosphate-glass process. With this flow sheet, the final asphalt-product volume is 18 gal.

BNL is examining the suitability of fractional distillation of the condensate.[6] The process (Fig. 3) involves feeding the melter condensate continuously to the still pot of a fractionator column. Nitric acid and water are removed from the top of the frac-

*Plants for immobilizing ILW in asphalt are already in operation at Mol, Belgium, and Marcoule, France.[10] A plant similar to that in Belgium is being constructed at Harwell, England. A pilot plant was constructed at ORNL for incorporating their ILW in asphalt.[11,12]

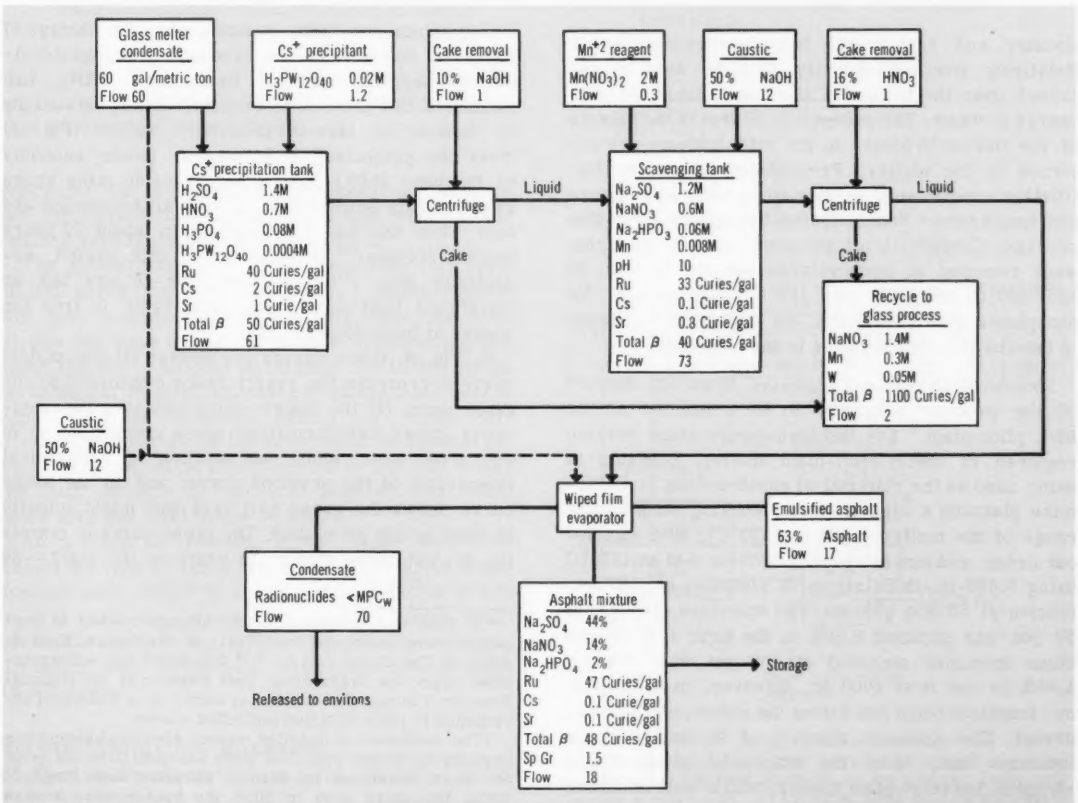

Fig. 2 Scavenging-asphalt incorporation flow sheet being developed at PNL for treating glass melter condensate.[4]

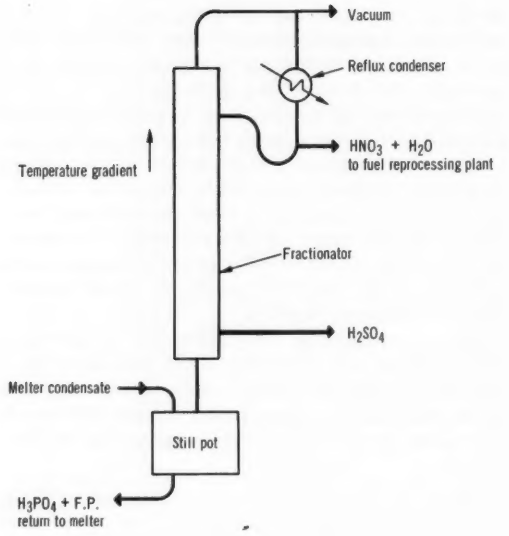

Fig. 3 Flow diagram of proposed BNL process for decontaminating melter off-gas products by fractional distillation.[6]

tionator and sent to the fuel-reprocessing plant. Relatively low-level-activity sulfuric acid is removed near the bottom of the fractionator for discharge to waste. The phosphoric acid plus the balance of the fission products in the still bottoms are returned to the melter. Preliminary laboratory distillation experiments performed at reduced pressure and temperature demonstrated the feasibility of this process. Essentially all the nitric and sulfuric acids were removed at temperatures ranging between 30 and 100°C and 100 and 185°C, respectively. No phosphoric acid volatilized. No ruthenium was found in the distillate fractions or in the cold trap.

Structural Strength of Platinum. Work in support of the process continues to be conducted at the BNL pilot plant.[6] For the high-temperature service required of their pilot-plant melter, platinum is being used as the material of construction. To determine platinum's strength in the working temperature range of the melter (1200 to 1250°C), BNL carried out creep measurements in a 6000-hr test at 1250°C using 0.060-in.-thick strips of platinum stressed in tension at 50 and 100 psi. The specimen stressed at 50 psi was strained 0.69% in the first 1800 hr; the other specimen stressed at 100 psi was strained 1.48% in the first 2000 hr. However, in each case, no elongation occurred during the subsequent 4000-hr period. The apparent absence of secondary creep indicates that, from the standpoint of structural strength, the pilot-plant melter, with a wall thickness of 0.080 in. and subjected to a maximum stess of 30 psi, is believed to be entirely adequate. To determine whether adverse effects would be expected as a result of migration of waste constituents into the platinum melter, BNL has initiated a program to ascertain the extent of any such migration.

SOLIDIFIED-PRODUCT STORAGE

One of the objectives of WSEP is to demonstrate the maximum heat content in packaged solidified waste that can be handled safely.[5] At PNL a theoretical study on the heat transfer within a product receiver (pot) was conducted. The results of this study indicated that the heat load in a pot can be increased by at least a factor of 2 if the pot is permitted to have a molten core. (The molten core is assumed to be surrounded by a 2-in.-thick layer of solidified material.) If molten-core operation can be achieved without adverse effects, 8- and 12-in.-diameter pots can be filled with molten product from wastes resulting from the reprocessing of 20,000 Mwd/metric ton fuel that had been out of the reactor less than 6 months. The filled pots would then be stored under water.

Calcined-Solids Storage in Salt Mines

Salt mines are being evaluated for the storage of packaged solids from the processing of high-level-activity aqueous wastes.* Bradshaw,[15] ORNL, has estimated the gross area required in salt formations to dispose of high-level-activity wastes (Fig. 4) from the projected U. S. nuclear power economy to the year 2065.† Previously reported mine space requirements showed that the overall economics are best when the waste is stored for about 30 years before disposal.[18] At the end of this period, essentially only $^{137}Cs-Ba$ and $^{90}Sr-Y$ are left as significant heat producers. (The same is true for wastes at least 10 years old.)

In Fig. 4, three curves are shown: (1) the middle curve represents the yearly space committed to any given year; (2) the upper curve indicates the cumulative gross salt-formation space committed up to any given year, which was obtained by a graphical integration of the previous curve; and (3) the lower curve shows the gross salt area that might actually be used by any given date. The lower curve is merely the second curve shifted 33 years to the right—30

*A field demonstration of this storage method is currently being conducted by ORNL at the Lyons, Kansas, mine of The Carey Salt Co.[13,14] Irradiated fuel subassemblies from the Engineering Test Reactor at the National Reactor Testing Station, Idaho, serve as a source of irradiation in place of actual solidified wastes.

†The estimates of installed nuclear electrical generating capacity up to the year 2000 were assumed to be the same as those developed by Blanco, Blomeke, and Boegly.[16] From the years 2000 to 2060, the figures were derived from the projections shown in Fig. 3, page 44, of the 1962 AEC report to the President on civilian nuclear power.[17]

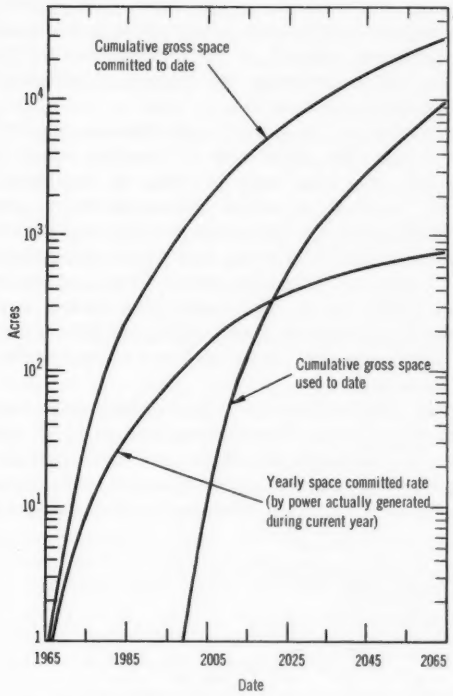

Fig. 4 Salt-formation space requirements for disposal of high-level wastes[15] to the year 2065.

years for the interim storage period and 3 years for the period from the time the fuel went into the reactor until the time it was processed.

The author notes that by the year 2065 only about 30,000 acres (an area less than 7 miles square) will have been committed, and only about one-third of this will have actually been used. Considering that about 250,000 to 500,000 sq miles of the United States is underlain by salt, no scarcity in available land is expected in the forseeable future, even though only a small percentage of the area might be suitable for waste disposal. Also, in some of the formations, where the salt deposits are several hundred feet thick, more than one level might be used.

As a point of interest, if the waste were to be stored for only 10 years instead of 30, the gross space commitments would be increased by a factor of 1.6. In that case, the "space-used-to-date" curve would be shifted back to the left by 20 years; for example, the space used to the year 2045 would then be about 16,000 acres.

Solvent Extraction Recovery of Fission Products

At ORNL, work is continuing on the development of processes, principally solvent extraction methods, that are applicable to large-scale recovery and purification of fission products from reactor fuel-processing wastes.[19,20]

Recent studies have included the small-scale demonstration at tracer-level activity of a new simplified flow sheet (Fig. 5) for isolating mixed rare earths, strontium, and cesium from each other and from

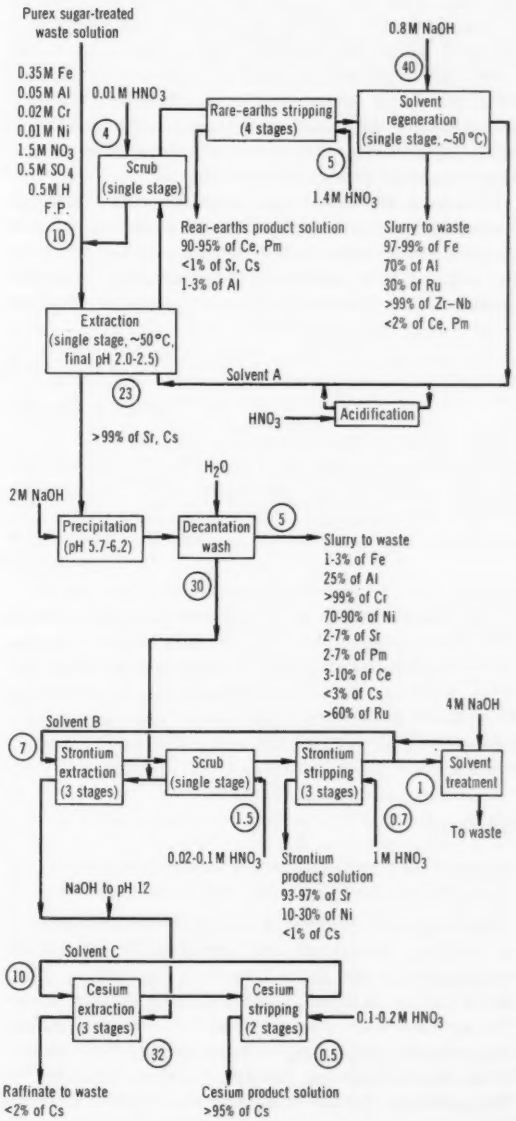

Fig. 5 The ORNL fission-product-recovery flow sheet.[20] Organic solvents: A—0.75M D2EHPA (80 to 100% in sodium salt form)—0.3M TBP–NPH; B—0.3M D2EHPA (10 to 20% in sodium salt form)—0.15M TBP–NPH; C—1M BAMBP in NPH. Numbers in circles show the relative solution flow rates.

other fission products and bulk contaminants.[20] The proposed process provides less pure rare earths and strontium concentrates than processes developed earlier; however, the proposed process requires less equipment and does not use large amounts of aqueous-phase complexing agents (e.g., tartrate or citrate). In this flow sheet the rare earths and bulk metal contaminants are extracted from unadjusted waste solution with the sodium salt of di(2-ethyl hexyl)-phosphoric acid, and the rare earths are selectively stripped from the extract. The raffinate from this operation is adjusted to a *p*H of about 6 to precipitate residual metal contaminants; the resulting solution is contacted first with di(2-ethyl hexyl)-phosphoric acid to recover strontium and then with a substituted phenol to recover cesium.

In Fig. 5 are given the estimates of the distribution of the more important fission products and bulk metal contaminants in the various process streams. In Table 1 are presented the estimates of the decontamination factors obtainable by the process.

Table 1 ESTIMATED DECONTAMINATION FACTORS FOR ORNL FISSION-PRODUCT-RECOVERY PROCESS[20]

(Based on Flow-Sheet Conditions Shown in Fig. 5)

Product	Estimated decontamination factors from								
	Fe	Al	Cr	Ni	Sr	Cs	RE	Nb–Zr	Ru
Mixed rare earths	>1,000	>30	>100	>100	>100	>100		>1,000	>50
Strontium	>5,000	>500	>100	3 to 10		>100	>200	>5,000	>100
Cesium	>10,000	>1000	>1000	>1000	>1000		>1000	>10,000	>100

These values should be considered as tentative since they were made on the basis of very limited process testing with simulated Purex wastes containing tracer-level amounts of activity. Recoveries of more than 90% of the rare earths, strontium, and cesium are indicated, with each of the concentrates being relatively free of contaminants.

General

STORAGE AND TREATMENT OF WASTE SOLUTIONS FROM REPROCESSING OF ZIRCONIUM-ALLOY FUELS

Nuclear fuels containing aluminum or zirconium as an alloying constituent are reprocessed in separate campaigns at the Idaho Chemical Processing Plant (ICPP) at the National Reactor Testing Station, Idaho. The aqueous wastes for the aluminum-containing fuels are presently being processed in the fluid-bed calciner in the Waste Calcining Facility (WCF) at the ICPP.[21,22] The aqueous wastes from the zirconium-containing fuels are being stored in the tanks that previously held wastes from the reprocessing of aluminum-alloy fuels, while a fluid-bed calcination process[23,24] is being developed to handle them. Since complete emptying of these storage tanks can never be accomplished without extensive rinsing, some blending of these two wastes* is inevitable. Also, blending may be used deliberately to reduce the total fluoride concentration present in the zirconium-alloy fuel wastes and to increase the degree of complexing of fluoride by aluminum.

Two areas of work were undertaken at the ICPP to evaluate the suitability of blending these two wastes.[25] One area was the study of the stability of the blending solutions to precipitation, since precipitation of the hydrolysis products of zirconium fluoride occurs. The other was the obtaining of corrosion data to determine which blend composition would result in minimum corrosive attack on two stainless steels of interest—304L and 347. Stability and corrosion data were obtained at temperatures of 35 and 55°C.

Blend compositions were found which were stable to precipitation of 1 year when held at 35°C; these were compositions in which the zirconium-alloy reprocessing wastes amounted to 20 vol.% or less and 90 vol.% or more. The range of stable compositions was even more limited at 55°C. The corrosion data showed that, at 35°C and for the stable-blend compositions, the corrosion of 304L and 347 stainless steel was acceptable for long-term use. The corrosion that did occur appeared to be directly related to the total fluoride concentration and was significantly higher at 55°C than at 35°C. Although all the corrosion rates measured by weight loss were very small and were equivalent to the rates observed for long-term exposure of specimens in actual storage tanks, the evidences of localized corrosion attack experienced at 55°C suggested that, for actual service conditions, an upper limit of 35°C should be placed on the temperature of the storage solution.

Pilot-plant work investigating the fluid-bed calcination of zirconium-alloy fuel wastes is in progress at the ICPP.[23,24] A 212-hr run was completed in the 12-in.-diameter calciner in which a nonradioactive waste containing principally zirconium, aluminum, and fluoride ions plus added calcium nitrate (to complex fluoride ion), was calcined. Steady-state operation

*Both wastes contain aluminum nitrate as a major component. In addition, the wastes from the aluminum-alloy fuels have high concentrations of nitric acid, sodium ion, or ammonium ion; those from the zirconium-alloy fuels are high in fluoride ion and nitric acid.

was achieved. The results indicate that this waste can be successfully calcined at 400°C and a fluidizing velocity of 1.0 ft/sec if a Ca/F mole ratio of at least 0.55 is maintained in the waste feed. The resulting product had a bulk density of 1.4 g/cm^3, a mass median particle of about 0.62 mm, and a satisfactory attrition resistance. In the off-gas, analysis for fluoride showed 10 μg of fluoride per liter of gas at an off-gas flow rate of 44 scfm.

Other pilot-plant studies performed in a corrosion–erosion test loop[23] indicate that the WCF scrubbing system should satisfactorily withstand the corrosion–erosion characteristics of fines present in the system from the calcining of zirconium-alloy fuel wastes.[26]

It is planned to store the zirconia calcine in storage bins similar in design to those used for storing the calcined solids from Al–U fuel wastes.[27] Long-term corrosion tests with various materials of construction have been initiated to evaluate how corrosive the stored zirconia calcine may be.[28] The materials being examined include the following: various stainless steels [304 (of which the present storage facilities are constructed), 304L, 316ELC, 347, and 405], carbon steel, and 6061 aluminum alloy.

GENERAL ELECTRIC'S MIDWEST FUEL-RECOVERY PLANT: TREATMENT OF PROCESS WASTES

The General Electric Company has applied to the USAEC for a permit to build a reprocessing plant that would be known as the Midwest Fuel Recovery Plant (MFRP) and located near Morris, Ill.[29] The plant would recover uranium, plutonium, and neptunium utilizing the Aquafluor* process. (This process has been described in the preceding issue of *Reactor and Fuel-Processing Technology.*[30]) In their design and analysis report submitted in support of the application for a construction permit and operating license for the MFRP, the General Electric Company describes their proposed method of handling process wastes. All process waste streams except gaseous effluents are converted to solid form and retained within the main process building for surveillance and possible retrieval in the various on-site storage facilities. Their capacity is sufficient for a minimum of 10 years of plant operation, and provision is made for future expansion, if required. The handling of the various types of wastes is described below.

High-Level-Activity Aqueous Wastes. These wastes are first concentrated in an evaporator, then fluid-bed calcined to a solid form, and the resulting calcined solids placed in a corrosion-resistant steel container.[31] The packaged solids are submerged in a water-filled basin to provide cooling and shielding.

Low-Level-Activity Aqueous Wastes. These wastes are concentrated and then immobilized in an asphalt matrix.[32] The solidified waste is stored in a concrete vault.

Process Scrap, Equipment, and Chemicals Disposition. Cladding hulls from the sheared fuel elements, discarded process equipment, and other wastes of low specific activity and negligible leachability are held in a water-filled vault that is ventilated to prevent hydrogen accumulation from radiolytic decomposition of water.[33] Storage of solid dry chemical wastes, such as the sodium fluoride sorption bed, used in the UF_6 purification system, is being provided by a concrete vault.

Process Off-Gases. Process radioactive gases and vapors are exhausted to off-gas treatment facilities and then discharged into the building ventilation system.[34] Treatment includes filtration of particulates and iodine removal by scrubbing with sodium hydroxide solution and reaction with silver nitrate. All gaseous effluents (including xenon, krypton, and tritium) are discharged through a sand filter and a 300-ft-high stack under conditions that assure protection of plant personnel and the public.

SELECTED CURRENT LITERATURE

The International Atomic Energy Agency held a symposium on the disposal of radioactive wastes into the ground.[35] The meeting was held in Vienna, May 29 to June 2, 1967. There were three sessions, each of which covered different aspects of this method of treatment:

Session 1. Operational experience in the release of radioactive liquid wastes into the soil; the injection of wastes into deep formations; the shallow land burial of solid or solidified radioactive storage. The economics of these operations.

Session 2. The hydrology of the movement of groundwater and the geochemistry of mineral reactions that control the migration rate of radionuclides in the ground. Techniques for monitoring the migrations and methods for site investigation or evaluation.

Session 3. Current research and development on mines or cavities for waste disposal. The exploitation of salt formations and deep cavities, hydrofracturing, and the use of porous formations for radioactive gas disposal.

The proceedings of this meeting will be published. Three papers presented at this meeting have become available.[36–38]

Tamura,[39] ORNL, has reported on the development of cement mixes for use in the ORNL disposal of their ILW by the hydraulic fracturing[13] method. This paper is another one in the series of five that are being published to describe the work on this technique conducted at ORNL.[40]

Hill, Savannah River Laboratory, describes equipment and techniques that were developed for removal of sludge that has accumulated at the bottom of

*Service trademark for the General Electric Company.

radioactive-waste storage tanks.[41] Sludge removal is accomplished by using high-velocity jets of water to disperse the sludge into a slurry that can be removed with centrifugal pumps. The developmental program culminated in the successful removal of sludge from two plant waste tanks.

Clark, Bradshaw, and Empson, ORNL, have issued a report summarizing the results of corrosion studies evaluating various candidate materials of construction in support of the ORNL program for developing methods of disposal of high-level-activity wastes by fixation in insoluble glassy solids.[42] The data show that, depending upon service requirements of the process of the materials evaluated, two satisfactory ones are titanium and 304L stainless steel.

The Japan Atomic Energy Research Institute has compiled a bibliography (in English) of references concerned with the shipping, handling, and storage of irradiated fuel, and the design and fabrication of fuel shipping casks.[43] The references, which are divided into 12 categories, are to literature published after 1959.

A standard has been issued which assigns definite meanings to terms used to describe broad categories of radioactive wastes.[44] The standard, sponsored by the American Institute of Chemical Engineers and accepted by the United States of America Standards Institute, should be useful to both the environmentalist and the engineer engaged in nuclear operations. The proposed categorization, consisting of five major categories, is presented in Table 2. The categories are defined in terms of the maximum permissible concentration (MPC), maximum permissible exposure (MPE), and the maximum permissible quarterly intake (MPQI) as established by the International Commission on Radiological Protection (ICRP). As changes occur in the ICRP values, the numerical values for the categories would change, but the basic definitions would remain unchanged. The ICRP values that would be used in conjunction with Table 2 for

Table 2 RADIOACTIVE WASTE CATEGORIZATION[44]
(Not Intended for Regulatory Use)

Class A (population level)	
Liquid and gas	≤Maximum permissible concentration (MPC)* for members of the population at large (including persons living in the neighborhood of controlled areas)
Solid	≤Maximum permissible quarterly intake (MPQI) for members of the population at large (including persons living in the neighborhood of controlled areas)/kg solid
Surface radiation†	≤Maximum permissible whole-body exposure (MPE)* for members of the population at large‡ (including persons living in the neighborhood of controlled areas)
Class B (occupational level)	
Liquid and gas	>Class A but ≤ (MPC)* occupational exposure (40-hr week)
Solid	>Class A but ≤ (MPQI)§ for occupational exposure/kg solid
Surface radiation†	>Class A but ≤ (MPE)¶ for occupational exposure‡ (40-hr week)
Class C (low level)	
Liquid and gas	>Class B but ≤ 10^4 × Class B
Solid	>Class B but ≤ 10^4 × Class B
Surface radiation	
Class C-1	≤(MPE)¶ (occupational) at surface‡
Class C-2	>(MPE)¶ (occupational) at surface‡
Class D (intermediate level)	
Liquid, gas, or solid	>Class C but ≤ 10^4 × Class C
Solid	>Class C but ≤ 10^4 × Class C
Surface radiation	
Class D-1	≤(MPE)¶ (occupational) at surface‡
Class D-2	>(MPE)¶ (occupational) at surface‡
Class E (high level)	
Liquid, gas, or solid	>Class D
Surface radiation†	
Class E-1	≤(MPE)¶ (occupational) at surface‡
Class E-2	>(MPE)¶ (occupational) at surface‡

*See Refs. 45–47.
†Applies to surface of container, object, or pool of liquid.
‡The recommended MPE to the gonads or the whole body is 5 rems/year for occupational exposure. For the population at large, it is assumed to be 1/1000 of 5, or 0.05 rem/year, for the whole-body genetic effect (see Refs. 47 and 48).
§MPQI = (MPC_w for 168-hr occupational exposure) (2200 ml/day) (91 days/quarter) = (MPC_w) (2×10^5); MPC_w applies to water.
¶See Ref. 49.

Table 3 MAXIMUM LIMITING RADIATION VALUES FOR WASTE CLASSES[44]

(Based on Unidentified Radionuclides)

	Class	$\mu c/cm^3$ air MPC_a	$\mu c/cm^3$ liquid MPC_w	$\mu c/kg$ MPQI*	rem/year† MPE
A	Population at large‡	1×10^{-11}	1×10^{-7}	0.02	0.05
B	Occupational (40 hr)	1×10^{-9}	1×10^{-5}	0.7	5
C	Low level	1×10^{-5}	1×10^{-1} (0.1 mg/liter)	0.7×10^{4}	5
D	Intermediate level	0.1	1×10^{3} (1 curie/liter)	0.7×10^{8} (70 curie/kg)	5
E	High level	0.1	$>1 \times 10^{3}$ >(1 curie/liter)	$>0.7 \times 10^{8}$ (70 curie/liter)	5

*Calculation of MPQI (MPQI values reduced to one significant place):

Population at large
Air—1×10^{-11} $\mu c/cm^3 \times 2 \times 10^{7}$ cm^3/day × 7 days/week × 13 weeks/quarter = 0.02 μc/quarter
Water—1×10^{-7} $\mu c/cm^3 \times 2200$ cm^3/day × 7 days/week × 13 weeks/quarter = 0.02 μc/quarter

Occupational
Air—1×10^{-9} $\mu c/cm^3 \times 1 \times 10^{7}$ cm^3/day × 5 days/week × 13 weeks per quarter = 0.65 ≈ 0.7 μc/quarter
Water—1×10^{-5} $\mu c/cm^3 \times 1100$ cm^3/day × 5 days/week × 13 weeks/quarter = 0.71 ≈ 0.7 μc/quarter

†The recommended MPE to the gonads or the whole body is 5 rems/year for occupational exposure. For the population at large, it is assumed to be 1/100 of 5, or 0.05 rem/year, for whole-body genetic effect (see Refs. 47 and 48).

‡1/30 of MPC or MPE for 168 hr occupational for somatic effect: $1/30 \times 4 \times 10^{-6} = 1.3 \times 10^{-7}$ $\mu c/cm^3$; 1.3×10^{-7} is considered equal to 1.0×10^{-7} for purposes of waste categorization.

determining the waste classification for unidentified radionuclides are shown in Table 3. The values are based on ^{90}Sr. Since, at most atomic energy installations, ^{226}Ra, ^{228}Ra, and ^{210}Pb are known to be absent, the unknown activity is assumed to be ^{90}Sr, the next most limiting radionuclide. If ^{226}Ra, ^{228}Ra, and ^{210}Pb could be present, the values in Table 3 must be decreased by a factor of approximately 30.

Of interest are the following articles published in *Nuclear Safety*, one of four Technical Progress Reviews issued by the USAEC. Parker discusses the status and effects of the disposal of low-level-activity wastes into the oceans.[50] Brooksbank and McDuffie review the current practices employed by typical commercial nuclear fuel-fabrication firms in the United States in the storing and handling of their process wastes.[51] Thompson and Morgan survey the nuclear transportation research being conducted under USAEC sponsorship.[52]

References

1. *Reactor Fuel-Process. Technol.*, 10(4): 319 (Fall 1967).
2. *Reactor Fuel-Process. Technol.*, 10(3): 255 (Summer 1967).
3. A. M. Platt (Ed.), Fixation of Radioactive Residues, Quarterly Progress Report Research and Development Activities, April–June 1967, USAEC Report BNWL-507, pp. 8-22, Pacific Northwest Laboratory, August 1967.
4. *Ibid.*, pp. 4-8 and 30-31.
5. *Ibid.*, pp. 23-28.
6. Brookhaven National Laboratory, Nuclear Engineering Department Annual Report, December 31, 1966, USAEC Report BNL-50023 (S-69), pp. 45-47, May 1967.
7. *Reactor Fuel-Process. Technol.*, 10(3): 253 (Summer 1967).
8. *Reactor Fuel-Process. Technol.*, 10(3): 255-256 (Summer 1967).
9. *Reactor Fuel Process.*, 9(4): 229-230 (Fall 1966).
10. Oak Ridge National Laboratory, Chemical Technology Division Annual Progress Report for Period Ending May 31, 1967, USAEC Report ORNL-4145, pp. 111-122, October 1967.
11. *Reactor Fuel-Process. Technol.*, 10(3): 253 and 254 (Summer 1967).
12. R. E. Blanco and F. L. Parker, Waste Treatment and Disposal Semiannual Progress Report, July–December 1966, USAEC Report ORNL-TM-1887, pp. 16-38, November 1967.
13. *Power Reactor Technol. Reactor Fuel Process.*, 10(2): 177 (Spring 1967).
14. R. E. Blanco and F. L. Parker, Waste Treatment and Disposal Semiannual Progress Report, July–December 1966, USAEC Report ORNL-TM-1887, pp. 59-72, Oak Ridge National Laboratory, November 1967.
15. *Ibid.*, p. 72-76.
16. R. E. Blanco et al., Survey of a Site for a Nuclear Fuel-Processing Plant and Waste-Disposal Area at Oak Ridge, USAEC Report ORNL-TM-1748, Oak Ridge National Laboratory, Jan. 13, 1967.
17. U. S. Atomic Energy Commission, *Civilian Nuclear Power ... a Report to the President—1962.*
18. R. L. Bradshaw et al., Disposal of High-Activity Power-Reactor Wastes in Salt Mines: A Concept and Field Scale Demonstration, *Nucl. Struct. Eng.*, 2: 438-446 (1965).
19. *Reactor Fuel Process.*, 9(2): 117-118 (Spring 1966).
20. Oak Ridge National Laboratory, Chemical Technology Division Annual Progress Report for Period Ending May 31, 1967, USAEC Report ORNL-4145, pp. 240-242, October 1967.
21. *Reactor Fuel-Process. Technol.*, 11(1): 65 (Winter 1967–1968).
22. J. R. Bower (Ed.), Chemical Technology Branch Annual Report, Fiscal Year 1967, USAEC Report IN-1087, pp. 32-42, Idaho Nuclear Corporation, October 1967.
23. *Reactor Fuel-Process. Technol.*, 11(1): 65 (Winter 1967–1968).
24. J. R. Bower (Ed.), Chemical Technology Branch Annual Report, Fiscal Year 1967, USAEC Report IN-1087, pp. 42-45, Idaho Nuclear Corporation, October 1967.
25. B. J. Newby and T. L. Hoffman, Blending Raffinates from Zirconium and Aluminum Processes, USAEC Report IN-1114, Idaho Nuclear Corporation, September 1967.

26. J. R. Bower (Ed.), Chemical Technology Branch Annual Report, Fiscal Year 1967, USAEC Report IN-1087, pp. 50-52, Idaho Nuclear Corporation, October 1967.
27. *Reactor Fuel Process.*, 9(4): 232 (Fall 1966).
28. J. R. Bower (Ed.), Chemical Technology Branch Annual Report, Fiscal Year 1967, USAEC Report IN-1087, p. 57, Idaho Nuclear Corporation, October 1967.
29. Design and Analysis, Midwest Fuel Recovery Plant, Docket 50-268, General Electric Company, Fuel Recovery Operation, Nuclear Energy Division.
30. *Reactor Fuel-Process. Technol.*, 11(1): 54-56 (Winter 1967–1968).
31. Design and Analysis, Midwest Fuel Recovery Plant, Docket 50-268, General Electric Company, Fuel Recovery Operation, Nuclear Energy Division, I-4-2 and I-4-3; V-14-1 through V-15-4; X-2-1.
32. *Ibid.*, I-4-2 and 1-4-3; V-16-1 and V-16-2; X-2-1.
33. *Ibid.*, I-4-3; V-5-1 and V-5-2; V-12-1.
34. *Ibid.*, I-4-2 and I-4-4; VI-1-1 through VI-3-3.
35. International Atomic Energy Agency, Program of Symposium on Disposal of Radioactive Wastes into the Ground, Vienna, 29 May–2 June 1967.
36. W. C. McClain, R. L. Bradshaw, and F. M. Empson, Disposal of High-Level Solidified Wastes in Salt Mines, USAEC Report ORNL-P-3053, Oak Ridge National Laboratory, 1967.
37. W. C. McClain, Hydraulic Fracturing as a Waste-Disposal Method, USAEC Report ORNL-P-3054, Oak Ridge National Laboratory, 1967.
38. J. W. Enders, Solid Radioactive Waste Disposal at the Los Alamos Scientific Laboratory, USAEC Report LA-DC-8347, Los Alamos Scientific Laboratory, 1967.
39. T. Tamura, Disposal of Radioactive Wastes by Hydraulic Fracturing. Part IV. Chemical Development of Waste–Cement Mixes, *Nucl. Eng. Design*, 5: 477-485 (1967).
40. *Power Reactor Technol. Reactor Fuel Process.*, 10(1): 91 (Winter 1966–1967).
41. A. J. Hill, Jr., Removal of Sludge from High-Activity Waste Tanks, USAEC Report DP-1093, Savannah River Laboratory, July 1967.
42. W. E. Clark, D. N. Hess, P. D. Neumann, L. Rice, and J. L. English, Laboratory Development of Processes for Fixation of High-Level Radioactive Wastes in Glassy Solids. (4) Corrosion Studies on Candidate Materials of Construction, USAEC Report ORNL-3816, Oak Ridge National Laboratory, August 1967.
43. S. Sawai and D. Shichi, Bibliography on Irradiated Fuel Shipping and Its Shipping Casks (in English), Japanese Report JAERI-4039, October 1966.
44. USA Standards, *Proposed Definition of Radioactive Waste Categories*, American Institute of Chemical Engineers, 1967.
45. *Recommendations of the International Commission on Radiological Protection, as Amended 1959 and Revised 1962*, ICRP Publication 6, Pergamon Press, London, 1964.
46. *Ibid.*, Chap. 5, 1962 Supplement to Report of Committee II on Permissible Dose for Internal Radiation (see Ref. 47).
47. *Recommendations of the International Commission on Radiological Protection*, Report of Committee II on Permissible Dose for Internal Radiation, ICRP Publication 2, Pergamon Press, London, 1959; and *Health Physics*, Vol. 3 (June 1960).
48. *Radiation Protection—Recommendations of the International Commission on Radiological Protection (adopted Sept. 9, 1958)*, ICRP Publication 1, Pergamon Press, London, 1959.
49. *Ibid.*, Sec. C.
50. F. L. Parker, Disposal of Low-Level Radioactive Wastes into the Oceans, *Nucl. Safety*, 8(4): 376 (Summer 1967).
51. R. E. Brooksbank and W. T. McDuffie, Current Practices in the Disposal of Radioactive Wastes from Fuel-Fabrication Facilities, *Nucl. Safety*, 8(4): 385 (Summer 1967).
52. J. Trueman Thompson and J. M. Morgan, Jr., Nuclear Transportation, *Nucl. Safety*, 8(5): 443 (Sept.–Oct. 1967).

LEGAL NOTICE

This journal was prepared under the sponsorship of the U. S. Atomic Energy Commission. Neither the United States, nor the Commission, nor any person acting on behalf of the Commission:

A. Makes any warranty or representation, expressed or implied, with respect to the accuracy, completeness, or usefulness of the information contained in this journal, or that the use of any information, apparatus, method, or process disclosed in this journal may not infringe privately owned rights; or

B. Assumes any liabilities with respect to the use of, or for damages resulting from the use of any information, apparatus, method, or process disclosed in this journal.

As used in the above, "person acting on behalf of the Commission" includes any employee or contractor of the Commission, or employee of such contractor, to the extent that such employee or contractor of the Commission, or employee of such contractor prepares, disseminates, or provides access to, any information pursuant to his employment or contract with the Commission, or his employment with such contractor.

NUCLEAR SCIENCE ABSTRACTS

The U. S. Atomic Energy Commission, Division of Technical Information, publishes *Nuclear Science Abstracts* (*NSA*), a semimonthly journal containing abstracts of the literature of nuclear science and engineering.

NSA covers (1) research reports of the U. S. Atomic Energy Commission and its contractors; (2) research reports of government agencies, universities, and industrial research organizations on a worldwide basis; and (3) translations, patents, books, and articles appearing in technical and scientific journals.

Complete indexes covering subject, author, source, and report number are included in each issue. These are cumulated quarterly, semiannually, and annually providing a detailed and convenient key to the literature.

Availability of *NSA*

SALE *NSA* is available on subscription from the Superintendent of Documents, U. S. Government Printing Office, Washington, D. C., 20402, at $30.00 per year for the semimonthly abstract issues and $22.00 per year for the four cumulated-index issues. Subscriptions are postpaid within the United States, Canada, Mexico, and all Central and South American countries, except Argentina, Brazil, Guyana, French Guiana, Surinam, and British Honduras. Subscribers in these Central and South American countries, and in all other countries throughout the world, should remit $37.00 per year for subscriptions to semimonthly abstract issues and $25.00 per year for the four cumulated-index issues.

EXCHANGE *NSA* is also available on an exchange basis to universities, research institutions, industrial firms, and publishers of scientific information. Inquiries should be directed to the Division of Technical Information Extension, U. S. Atomic Energy Commission, P. O. Box 62, Oak Ridge, Tennessee, 37830.

TECHNICAL PROGRESS REVIEWS may be purchased from Superintendent of Documents, U. S. Government Printing Office, Washington, D. C., 20402. *Nuclear Safety* at $3.50 per year (six issues) for each subscription or $0.60 per issue; each of the other journals at $2.50 per year (four issues) or $0.70 per issue. The use of the coupon below will facilitate the handling of your order.

POSTAGE AND REMITTANCE: Postpaid within the United States, Canada, Mexico, and all Central and South American countries except Argentina, Brazil, Guyana, French Guiana, Surinam, and British Honduras. For these Central and South American countries and all other countries: add, for each annual subscription, $1.00 for *Nuclear Safety* and $0.75 for each of the other journals; for single issues, add one-fourth of the single-issue price. Payment should be by check, money order, or document coupons, and MUST accompany order. Remittances from foreign countries should be made by international money order or draft on an American bank payable to the Superintendent of Documents or by UNESCO book coupons.

order form

SUPERINTENDENT OF DOCUMENTS
U. S. GOVERNMENT PRINTING OFFICE
WASHINGTON, D. C., 20402

Enclosed:

document coupons ☐ check ☐ money order ☐

Charge to Superintendent of Documents No. _____

Please send a one-year subscription to

☐ ISOTOPES AND RADIATION TECHNOLOGY
☐ NUCLEAR SAFETY
☐ REACTOR AND FUEL-PROCESSING TECHNOLOGY
☐ REACTOR MATERIALS

SUPERINTENDENT OF DOCUMENTS
U. S. GOVERNMENT PRINTING OFFICE
WASHINGTON, D. C., 20402

(Print clearly)

_____
Name

_____
Street

_____
City, State, ZIP Code